

NIST Technical Note 2229

Tensile Tests at 77 K and 4 K on 316L Stainless Steel Welded Plates

Timothy Weeks
Nicholas Derimow
Jake Benzing

This publication is available free of charge from:
<https://doi.org/10.6028/NIST.TN.2229>

NIST Technical Note 2229

Tensile Tests at 77 K and 4 K on 316L Stainless Steel Welded Plates

Timothy Weeks

Nicholas Derimow

Jake Benzing

Applied Chemicals and Materials Division

Material Measurement Laboratory

This publication is available free of charge from:
<https://doi.org/10.6028/NIST.TN.2229>

July 2022



U.S. Department of Commerce

Gina M. Raimondo, Secretary

National Institute of Standards and Technology

Laurie E. Locascio, NIST Director and Undersecretary of Commerce for Standards and Technology

Certain commercial entities, equipment, or materials may be identified in this document in order to describe an experimental procedure or concept adequately. Such identification is not intended to imply recommendation or endorsement by the National Institute of Standards and Technology, nor is it intended to imply that the entities, materials, or equipment are necessarily the best available for the purpose.

National Institute of Standards and Technology Technical Note 2229
Natl. Inst. Stand. Technol. Tech. Note 2229, 84 pages (July 2022)
CODEN: NTNOEF

This publication is available free of charge from:
<https://doi.org/10.6028/NIST.TN.2229>

Abstract

Based on the collaborative framework established between ASME, NASA, and NIST, quasi-static tensile tests were performed in liquid nitrogen (77 K) and liquid helium (4 K) on tensile specimens extracted from the centers of four welded 316L stainless steel plates, each produced by a different vendor. Relatively large differences in strength, elongation, and reduction in area were observed between the welds with the strongest two welds (W4 and W2) demonstrating a difference of almost 20 % in ultimate tensile strength at 4 K when compared to the welds with the lowest 4 K tensile strength (W1 and W3). As the testing temperature decreases from 77 K to 4 K, all welds exhibit a rise in yield strength, plus a decrease of total elongation and reduction in area. As expected, serrated yielding was observed in every test conducted at 4 K. The tensile properties reported in this work will be used during the analysis of fracture toughness (single edge notch bending) tests conducted at 77 K and 4 K on the same four sets of welded plates.

Key words

316L stainless steel, welding, tensile properties, liquid nitrogen, liquid helium.

Table of Contents

Abstract.....	1
Key words	1
1. Introduction	5
2. Materials.....	5
3. Experimental procedure	8
3.1 Tests in liquid nitrogen (77 K)	8
3.2 Tests in liquid helium (4 K)	9
4. Analytical procedure	9
4.1 Generalized Procedure	9
4.2 Peak finding for LHe tensile data.....	12
5. Tensile properties	12
5.1 Tests in liquid nitrogen.....	12
5.2 Tests in liquid helium.....	13
5.3 Summary of tensile properties.....	14
6. Fractography.....	17
6.1 Summary of fractography of welds 1 – 4	17
6.2 Tests in liquid nitrogen (77 K)	19
6.3 Tests in liquid helium (4 K)	20
7. Discussion	21
8. Conclusions	22
Acknowledgements	23
References.....	24
Appendix A: Technical drawing.....	26
Appendix B: Supplemental information for each weld	26
Appendix C: Tensile results	28
Appendix D: Digital images used to measure total elongation	48
Appendix E: Additional fractography: Optical images	59
Appendix F: Additional fractography: SEM images.....	79

List of Tables

Table 1: Processing information gleaned from welding process specification reports.	6
Table 2: Base plate composition (average of 3 measurements) in % mass fraction provided by NASA MSFC.	7
Table 3: Weld composition (average of 3 measurements) in % mass fraction provided by NASA MSFC.	8
Table 4: Ferrite percentage in welds, based on the average of 24 measurements per weld.	8
Table 5: Summary of tensile properties (engineering stress-strain) for all welds and temperatures investigated.	15
Table 6: Summary of elongation and reduction of area for all welds and temperatures.	16
Table 7: Summary of the fractography in Welds 1 – 4 at 4 K and 77 K. Green text indicates that SEM fractography was performed in addition to the light optical fractography.	18

List of Figures

Figure 1: Depiction of tensile specimen orientation with respect to a welded 316L stainless steel plate.	5
Figure 2: Representative view of the top of each weld (weld cap / final cover pass). W1 used a single final pass, W2 used four final passes, W3 used three final passes, and W4 used two final passes.	7
Figure 3: (Left) Tensile load train assembly with pull rods, fixtures and a tensile specimen screwed into both fixtures with clip gages attached to (middle) two C-shaped rings where the initial separation distance between the spring-loaded pins holding the C-shaped rings to the specimen is 25.4 mm (initial gage length). (Right) The cryo-stat assembly which is being lowered into a dewar filled with liquid nitrogen.....	9
Figure 4: Example data header for each specimen from the data record associated with the machine controller DAQ.....	10
Figure 5: (Top) characteristic engineering stress-strain tensile properties in liquid nitrogen for W1T1 and (bottom) yield transition behavior	13
Figure 6: (Top) characteristic full stress-strain tensile properties in liquid helium for W1T5 and (bottom) yield transition behavior.....	14
Figure 7: Typical cup-and-cone fracture morphology of a tensile specimen tested at 77 K (W1-T2 pictured, cup morphology). a) flattened image, b) cone morphology.....	19
Figure 8: Typical MVC features in specimens tested at 77 K.	19
Figure 9: a) Wormhole pore, b) Particles adhering to the surface cavity of the pore.	20
Figure 10: High angle shear fracture morphology in a tensile specimen brought to fracture at 4 K. a) flattened image, b) High angle shear morphology.....	20
Figure 11: a) SE image of the entire fracture surface of a tensile specimen brought to fracture in 4K, b) cracks at the surface with adjacent cleavage fractures.	21

1. Introduction

Currently, ASME Boiler and Pressure Vessel Code (BPVC) Section VIII [1] and ASME Piping Code B31.12 Hydrogen Piping and Pipelines [2] both require that Charpy impact tests be performed at liquid nitrogen (LN2) temperature, *i.e.*, 77 K (-196 °C), to assess the fracture toughness of austenitic stainless steels at liquid helium (LHe) temperature, *i.e.*, 4 K (-269 °C). The same procedure was also proposed for ASME Piping Code B31.3 Process Piping [3]. Charpy testing provides a relatively inexpensive measurement of the impact toughness of a material, quantified by absorbed energy and lateral expansion [4]. Due to adiabatic heating that occurs at high strain rates during Charpy impact testing [5], conducting Charpy tests at temperatures below 77 K is not technically viable and calls into question the technical basis of using Charpy impact toughness values measured at LN2 temperature to assess the reliability of quasi-static fracture toughness tests conducted on single-edge bend (Charpy-type) specimens at LHe temperature.

The framework of this study is a joint project between the American Society of Mechanical Engineers (ASME), the National Aeronautics and Space Administration (NASA), and the National Institute for Standards and Technology (NIST). The analysis of compliance-based fracture toughness tests requires values of modulus, yield strength, and ultimate tensile strength [6]. The objective of this report is to provide quasi-static tensile properties at 77 K and 4 K for all materials of interest. Fracture toughness measurements will have been conducted and compared to Charpy impact tests of the same four welded lots of material, the latter of which has already been completed [7]. These four unique lots of material are welded 316L stainless steel plate with differences in welding process, chemical content, and delta ferrite fraction.

2. Materials

Tensile specimens were extracted from the center of welds (see Figure 1) in four lots of welded 316L stainless steel plates, identified as W1, W2, W3, and W4. The technical drawing of the tensile specimen is provided in Appendix A: Technical drawing.

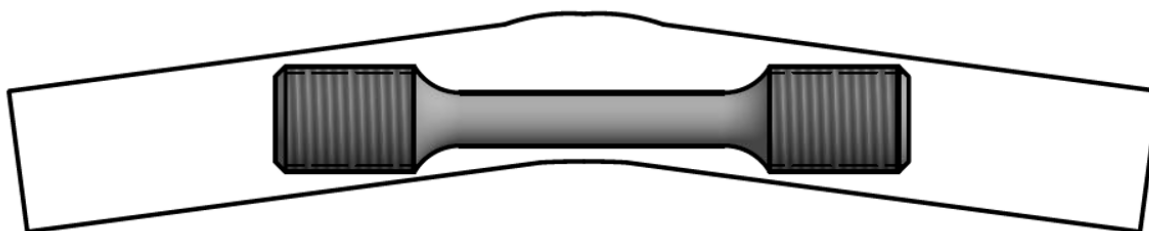


Figure 1: Depiction of tensile specimen orientation with respect to a welded 316L stainless steel plate.

The plates were welded by four vendors in accordance with ASME Boiler and Pressure Vessel Code requirements using 316L plates and weld material individually procured by each vendor. The welds were made following each vendor's standard in-house welding procedure. A summary of the welding processing specifications provided by each welding vendor, as well as other pertinent information, is provided in Table 1. Gas tungsten arc welding (GTAW) does not use flux, but instead uses frequency to clean the surfaces and an inert gas shield to protect

the weld pool from oxidation. Flux core arc welding (FCAW) is an automated process involving a spool of flux-cored wire (filler metal). The flux is released when the filler metal melts allowing it to clean the surfaces and “float” to the surface along with impurities. The purpose of the flux is to clean the surfaces, so the process usually includes a cover gas to reduce oxidation. The flux can absorb moisture from the air if not properly stored.

Generally, GTAW is used to join smaller pipes since the deposition rate is slower than FCAW. All GTAW processes used to weld flat plates in this work were performed using straight polarity direct current, whereas the FCAW processes used reverse polarity. Notably, all suppliers used GTAW to perform the first few root passes, but only the vendor that produced W2 used GTAW to complete the rest of the weld passes. Figure 2 provides a top view of the final passes (weld cap) used by each welding vendor, which range from one final pass (W1) to four final passes (W2). Additional information about each weld is provided in Appendix B: Supplemental information for each weld.

Table 1: Processing information gleaned from welding process specification reports.

Welded plate	W1		W2		W3		W4	
Process	Root	Cover	Root	Cover	Root	Cover	Root	Cover
	GTAW	FCAW	GTAW, manual	GTAW, manual	GTAW	FCAW	GTAW	FCAW
Tungsten electrode dimensions and composition	0.125", 2% Thoriated		0.094", 2% Thoriated	0.125", 2% Thoriated	0.125", 2% Thoriated		0.125", 2% Thoriated	
Stringer or weave	stringer	stringer	either	either	stringer	either	either	either
Shielding gas	GTAW: Ar, backing Ar	CO2	GTAW: Ar, backing: Ar	GTAW: Ar, backing: Ar	GTAW: Ar, backing: Ar	Ar/CO2 75%/25%	Ar	Ar/CO2 75%/25%, backing: Ar
Root filler diameter	0.094"		0.094"		0.125"		.0625" and .094"	
Cover filler diameter		0.045"		0.125"		0.045"		0.045"
Interpass temperature	50 °F to 350 °F	50 °F to 350 °F	50 °F to 300 °F	50 °F to 300 °F	70 °F to 350 °F	70 °F to 350 °F	50 °F to 350 °F	50 °F to 350 °F



Figure 2: Representative view of the top of each weld (weld cap / final cover pass). W1 used a single final pass, W2 used four final passes, W3 used three final passes, and W4 used two final passes.

Chemical composition measurements were performed by NASA MSFC upon receiving the welded plates and are provided in Table 2 (base plate) and Table 3 (weld). As delta ferrite can form upon cooling, ferrite content measurements were performed on the welds since fracture toughness measurements are centered in each weld. The ferrite measurements were performed using a contact-based Fisher Feritscope FMP30, which was verified using a sample of known ferrite content. The results are provided in Table 4.

Table 2: Base plate composition (average of 3 measurements) in % mass fraction provided by NASA MSFC.

Welded plate	C	Si	Mn	P	S	Cr	Mo	Ni	Al	Co	Cu	Nb	Ti	V	W	Pb	Sn	As	Zr	Ca	B	Fe
W1	0.045	0.28	1.19	0.047	0.01	15	2.13	10.22	0.007	0.4	0.47	0.039	0.022	0.076	0.058	0.011	0.01	0.005	0.003	0.001	0.0005	70
W2	0.039	0.24	1.14	0.054	0.007	15.2	2.11	10.17	0.008	0.31	0.49	0.005	0.018	0.083	0.05	0.013	0.011	0.005	0.003	0.001	0.0005	70.1
W3	0.033	0.31	1.28	0.048	0.008	14.88	2.14	10.24	0.006	0.36	0.33	0.028	0.017	0.058	0.065	0.011	0.007	0.005	0.003	0.0007	0.0005	70.2
W4	0.053	0.29	1.13	0.046	0.006	15.25	2.14	10.15	0.008	0.33	0.35	0.0009	0.02	0.13	0.089	0.011	0.008	0.005	0.003	0.001	0.0005	70

Table 3: Weld composition (average of 3 measurements) in % mass fraction provided by NASA MSFC.

Welded plate	C	Si	Mn	P	S	Cr	Mo	Ni	Al	Co	Cu	Nb	Ti	V	W	Pb	Sn	As	Zr	Ca	B	Fe
W1	0.049	0.47	1.07	0.049	0.012	16.84	2.71	12.41	0.009	0.1	0.22	0.01	0.044	0.071	0.04	0.011	0.008	0.005	0.004	0.0009	0.0005	65.9
W2	0.07	0.41	1.88	0.031	0.039	16.69	2.94	13.23	0.018	0.053	0.12	0.013	0.016	0.032	0.04	0.016	0.006	0.005	0.003	0.002	0.0008	64.4
W3	0.064	0.52	0.82	0.046	0.011	15.89	2.23	12.87	0.007	0.11	0.22	0.027	0.039	0.078	0.04	0.01	0.008	0.005	0.003	0.001	0.0005	67
W4	0.074	0.64	1.4	0.038	0.026	16.71	2.96	11.96	0.04	0.19	0.12	0.005	0.084	0.092	0.04	0.013	0.003	0.005	0.003	0.002	0.0005	65.6

Table 4: Ferrite percentage in welds, based on the average of 24 measurements per weld.

Weld	W1		W2		W3		W4	
	Root	Cover	Root	Cover	Root	Cover	Root	Cover
Ferrite (%)	5.64	8.19	4.00	4.25	3.02	2.29	8.04	9.83

3. Experimental procedure

3.1 Tests in liquid nitrogen (77 K)

Six tensile specimens were sectioned from each weld. Three tensile tests per weld were performed in liquid nitrogen (77 K). A 55-kip (222 kN) servo-hydraulic load frame, equipped with a 25-kip (100 kN) load cell and three clip gages (calibrated in LN2 and verified before testing) were used during tensile testing. A thermocouple was also attached to the fixture well above the specimen to verify that the specimen was constantly submerged in LN2 during testing. Below is a general description of the experimental procedure, which is based on the methods described in ASTM E8 [8].

Firstly, C-shaped rings (clip gage mounts) were attached to the specimen using an alignment jig to set the offset distance between the spring-loaded pins to 25.4 mm. Then the specimen was screwed into the upper fixture. The lower fixture was then threaded onto the bottom of the specimen. Next, the hemispherical ends of the clip gages were seated in the hemispherical divots of the C-shaped rings. Then, a reaction tube was placed over the fixtures and locked into place. The threaded rod of the bottom fixture protruded out of the bottom of the reaction tube. A spherical nut was threaded onto the bottom rod of the lower fixture and hand tightened against the seating face of the reaction tube. A more precise pre-load (50 lb) was applied using servo-hydraulic force control. The entire setup (cryo-stat) was then slowly lowered into a double-walled vacuum cylinder (dewar) filled with liquid nitrogen. Images showing the cryo-state assembly (pull rod, upper fixture, specimen, c-shaped rings, clip gages, lower fixture, and reaction tube) and the dewar are provided in Figure 3. If the thermocouple (placed well above the specimen) did not produce a reading consistent with LN2 temperatures (77 K = -196 °C), the cylinder was filled with more LN2. A custom-written procedure was used to measure the cryogenic tensile properties by recording force, displacement, and clip gage extension at a rate of 2 Hz. Once the specimen and fixtures had been submerged in liquid nitrogen for at least 5 minutes, the procedure was initiated in displacement control at 0.076 mm/min until fracture was detected by a significant force drop of 50% or more. The displacement-controlled test resulted in an elastic strain rate of 0.015 mm/mm/min.

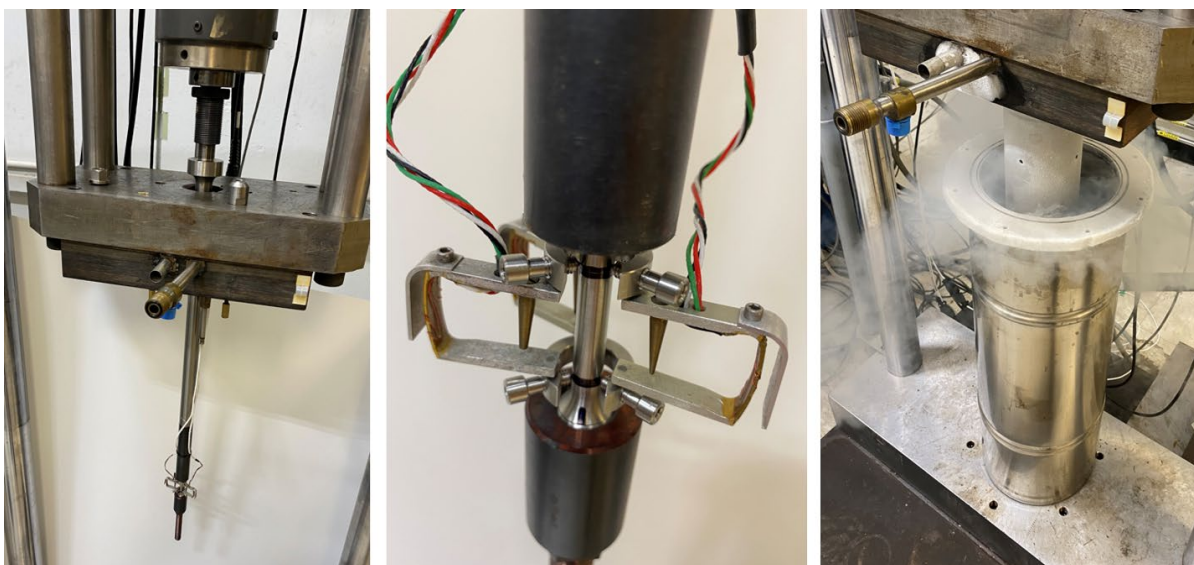


Figure 3: (Left) Tensile load train assembly with pull rods, fixtures and a tensile specimen screwed into both fixtures with clip gages attached to (middle) two C-shaped rings where the initial separation distance between the spring-loaded pins holding the C-shaped rings to the specimen is 25.4 mm (initial gage length). (Right) The cryo-stat assembly which is being lowered into a dewar filled with liquid nitrogen.

3.2 Tests in liquid helium (4 K)

Two tensile tests per weld were performed in liquid helium (4 K). Tensile testing in liquid helium used similar equipment and software procedures as described for testing in LN₂. However, some key equipment-related differences existed. First, the clip gages were re-calibrated and verified in liquid helium. Also, a rod-like liquid level indicator was placed near the specimen/fixtures (as opposed to the thermocouple used in LN₂ tests) to monitor the liquid level during testing. To minimize boil-off, a smaller dewar was used and placed in contact with the reaction frame using a silicone seal. The dewar was tightened into place with threaded nuts. Once the specimen and fixtures had been submerged in liquid helium for at least 5 minutes, the same testing procedure as for LN₂ tests was initiated.

4. Analytical procedure

4.1 Generalized Procedure

This section describes the general procedure for analyzing the data acquired for each test specimen. Each specimen has a data set from two different data acquisition (DAQ) systems. One system is associated with the machine controller and key specimen data are captured in the header of this record. An example of this header is shown in Figure 4 and these key data are later used in the calculations and report setup. The second data record contains raw data from an external DAQ associated with the excitation and signal processing of the multiple clip gages. The machine displacement and force are part of that data record since they were output from the machine controller as hi-level outputs (± 10 V), and input into the external DAQ.

Operator Information

Operator	Dash Weeks	
Project	ASME-NASA	
Material/Condition	316L Weld	
Test Temperature	4K	
Target Test Rate	0.015	mm/mm/min
Control Mode	Displacement	
Specimen ID	W4T5	
Diameter	6.361	mm
OAL	76.15	mm
Test Frame	MTS 55KIP Cryo	
Frame Last Calibrated	2/3/2021	
Extensometer	Shepic - Avg of 3 Ball End Clip Gauges - DAQ = System 7000	
Extensometer Last Calibrated	8/19/2021	
Extensometer Gauge Length	25.4	mm

Figure 4: Example data header for each specimen from the data record associated with the machine controller DAQ.

The list of steps used to analyze the tensile data are provided below; details of each step will follow in this section.

1. Data Validation
2. Time Offset
3. Stress Calculation
4. Strain Calculation
5. Displacement Slack Compensation
6. Strain Slack Compensation
7. Extrapolated Strain (77 K tests)
8. Reduced Data
9. Interpolations
10. Peak Finding (4 K tests)
11. Check-Sum Validations
12. Visual Review

The data records frequently have erroneous/spurious data at the beginning and end of the record that do not reflect actual specimen response. These rows of data are not included in subsequent data arrays for calculations. These spurious data points are different than slack, as described below.

The time stamp from the DAQ was converted to seconds and was offset so that the first row of valid data was at time = 0 s. The force data was converted to an array with the same start and end as the “time” array with units of N. The specimen diameter, which was saved in the specimen data header, was used to calculate the initial specimen cross-sectional area. The force array was divided by the area to calculate engineering stress in units of MPa. The

machine displacement array was fetched directly from the original data. The clip gage data was averaged, and divided by the gage length (from the specimen header) to calculate the engineering strain in mm/mm.

The next step was to calculate the slack compensation for both machine displacement and strain. Slack is typically associated with fixture seating and specimen misalignment at the beginning of the test. The data record will have two features that the slack compensation will eliminate. Firstly, to eliminate the non-linear data in the beginning since it does not represent a material response, and this involves replacing non-linear data with linear data in the range where the non-linear data was removed. The second feature is to shift the new linear data and the rest of the data array so that the linear data goes through the origin.

Knowing the post-test plastic elongation, an elastic elongation was added to this number as an estimate of the total expected strain at failure. The extrapolated strain data up to this final estimated value was calculated from the slope of the time-strain data prior to the maximum of strain rate. The slope and intercept were found using an optimization solver such that the total elongation value was obtained while the extrapolated data immediately after the maximum strain rate did not exhibit a significant shift in the curve, since a smooth curve is expected.

Displacement data are not typically used in tensile analysis; however, these tensile tests were conducted in displacement control and to reduce the data it was easiest to do a time-stepped reduction which required a time-dependent data record. An imaginary displacement data array was generated with consistent increments all the way up to the maximum slack compensated displacement for the test; hypothetically from 0.01 mm to 12.5 mm in 0.01 mm increments would yield a new array with 1251 rows (reduced from 10k-20k+ rows). For each increment of hypothetical displacement, that value is found in the original displacement data array and the row is determined. The stress and strain data associated with each increment are then taken as the average of the stress and strain data respectively around that row (between rows associated with ± 0.005 mm displacement). This averaging method is like multi-point smoothing but instead of a pre-defined number of points to average, all of the data associated with the increment are used.

The stress at 0.5 % strain is determined by interpolation between the two data points closest to 0.5 % strain (slack compensated). It is important to note that using slack compensated strain data is very important when determining the stress at 0.5 % strain, whereas a yield definition like 0.2 % offset yield is less sensitive to slack compensation.

All specimens tested in LHe at 4 K had serrated stress-strain curves. These serrations are legitimate material responses, yet the data can be simplified with good accuracy by finding the peaks of the serrations and reducing the number of data points that are used in the data record to describe the overall stress-strain response. The serrations are typically associated with small specimens and not structures, so to model a structure it is appropriate to use the “peak” data set.

Each data record analyzed had several validation checks to ensure that the calculations are appropriate for the specific test record, these validations ensure that the array data has been transferred and used appropriately. One example check is to ensure that the maximum stress of the raw data matches the maximum stress of the reduced data. Another is to ensure that the number of rows of raw data match the number of rows of transferred data.

The final review is a visual review of the data and associated plots for each test.

4.2 Peak finding for LHe tensile data

A number of algorithms are practical for finding the peaks of serrated data sets. However, some data sets presented unique issues that required individualized solutions. The goal in this project was to reduce the number of individual “engineering” solutions by making the algorithm(s) tolerant enough of these special cases thus decreasing the time to complete the analysis while increasing the confidence that the solution was based on sound logic. A simple slope reversal algorithm fails to find the peak or maximum associated with each serration. The following logic was used to determine the peak of each serration.

```
For i = 2 to end (i = row #, end is the end of the array)
    If AND(Stress(i) = Average (Stress(i-1): Stress(i+1), Stress(i)>Stress(i+1),
    Stress(i)>Stress(i-1), Stress(i)>Yield Stress
    Then RESULT(i) = “Peak”
    End If
```

Find the row numbers in the RESULT array that contain the result “Peak”

Build a new strain array from row 1 to the first peak row.

Build a new stress array from row 1 to the first peak row.

Append the strain array with each strain associated with the row #'s in the RESULT array.

Append the stress array with each stress associated with the row #'s in the RESULT array.

5. Tensile properties

The sections below provide selected engineering stress-strain responses of selected tests. The engineering stress-strain curves and properties of every test (encompassing all four weld types and both test temperatures) can be found in Appendix C: Tensile . Similarly, all images of every tested specimen can be found in Appendix D: Digital images used to measure total elongation. All specimens fractured within the gage section of each specimen and more specifically within the weld material portion of the gage section.

5.1 Tests in liquid nitrogen

All specimen tests performed in liquid nitrogen demonstrated smooth transitions from elastic to elastic-plastic response. Fully plastic response was not captured due to the range of the clip gages used. The full stress-strain curve for specimen W1T1 is shown in Figure 5 (top), the extrapolated strain is also shown in that plot representing the estimated stress-strain response of the specimen up to failure. The yield transition is better shown in Figure 5 (bottom), along with the line representing the modulus, the associated 0.2 % offset line as well as a vertical line marking 0.5 % strain. The intersection between the curve and the vertical line at 0.5 % strain is shown with a data marker (×). This marker is only coincidentally the same as the intersection of the 0.2 % offset line with the curve for this specimen and is not a characteristic of all specimens.

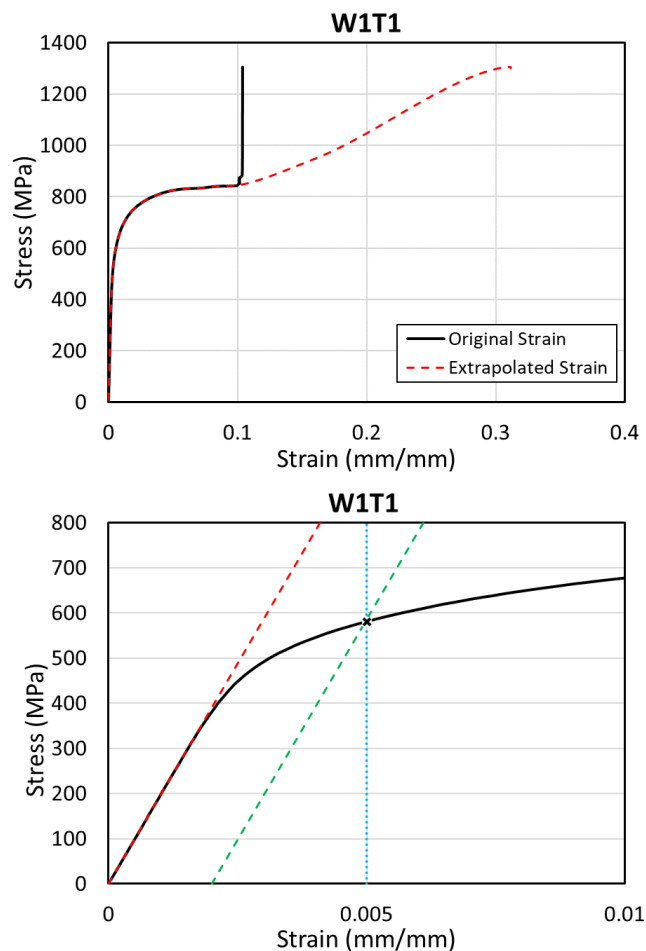


Figure 5: (Top) characteristic engineering stress-strain tensile properties in liquid nitrogen for W1T1 and (bottom) yield transition behavior

5.2 Tests in liquid helium

All specimen tests performed in liquid helium demonstrated a reasonably smooth transition from elastic to elastic-plastic response. Offset corrections or special algorithms to determine the appropriate intersection between the curve representing the data and the 0.5 % designation (see Figure 6 (bottom)) were not required. The full stress-strain curve for specimen W1T5 is shown in Figure 6 (top), and data representing the specimen response without serrations is also presented as red data markers. Extrapolated strain was calculated on serrated data and an estimated strain at failure is available in the specimen reports (see Appendix C: Tensile). However, the plot of that extrapolated data is not particularly useful, and the extrapolated strain based on the non-serrated (peak) data was not calculated. All specimens demonstrated a discontinuous stress-strain response after yield with varying shapes in the flow region of the specimen response.

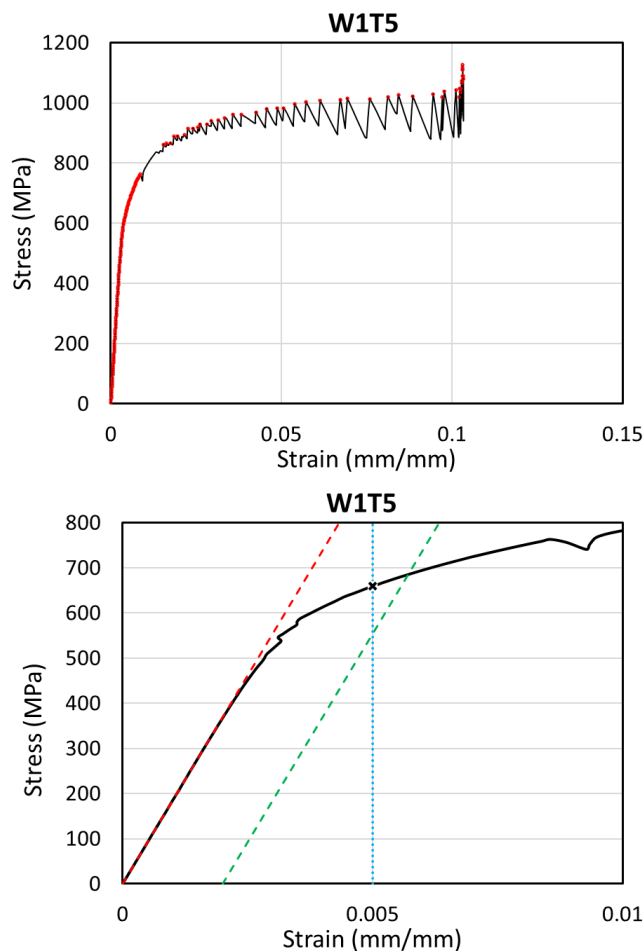


Figure 6: (Top) characteristic full stress-strain tensile properties in liquid helium for W1T5 and (bottom) yield transition behavior

5.3 Summary of tensile properties

This program included tests in liquid nitrogen and liquid helium to document the change in properties and to qualify welds for use at low service temperatures. Open literature has adequately documented the change in properties as a function of temperature for base metal, but welds can have significant differences between them, therefore each weld must be compared for selection and then qualified for service. The key tensile parameters for each specimen tested are given in Table 5, these include the elastic modulus, yield strength (defined as the stress at 0.5 % strain), and the tensile strength. Post-test measurements were used to determine the plastic elongation at failure as well as the plastic area reduction at failure and are given for each specimen in Table 6. Averages are provided in the tables for each temperature and each weld in addition to the difference between temperature averages for each weld. However, the data represent a very small sampling, therefore trends based on averages are likely to be mis-leading as they are based on limited data.

Table 5: Summary of tensile properties (engineering stress-strain) for all welds and temperatures investigated.

Weld	Test	T (K)	Elastic modulus (GPa)	Yield Strength (MPa)	Tensile Strength (MPa)
1	T1	77	195	581	1306
	T2	77	197	579	1289
	T3	77	184	587	1067
	Avg	77	192	582	1221
	T5	4	185	659	1126
	T6	4	188	667	1216
	Avg	4	187	663	1171
	Δ	4-77	-5	81	-50
2	T1	77	169	585	1221
	T2	77	169	579	1218
	T3	77	180	578	1220
	Avg	77	173	581	1220
	T4	4	169	634	1422
	T5	4	191	657	1453
	Avg	4	180	646	1438
	Δ	4-77	7	65	218
3	T1	77	185	549	1238
	T2	77	169	542	1251
	T3	77	164	541	1242
	Avg	77	173	544	1244
	T4	4	176	627	1103
	T5	4	178	625	1290
	Avg	4	177	626	1197
	Δ	4-77	4	82	-47
4	T1	77	162	552	1272
	T2	77	163	568	1288
	T3	77	163	575	1286
	Avg	77	163	565	1282
	T4	4	177	651	1517
	T5	4	155	645	1550
	Avg	4	166	648	1534
	Δ	4-77	3	83	252

Table 6: Summary of elongation and reduction of area for all welds and temperatures.

Weld	Test	T (K)	Total elongation (%)	Reduction of Area (%)
1	T1	77	30.5	19.2
	T2	77	30.5	21.3
	T3	77	19.5	12.7
	Avg	77	26.8	17.7
	T5	4	15.2	9.9
	T6	4	18.1	11.6
	Avg	4	16.7	10.8
	Δ	4 to 77	-10.1	-6.9
2	T1	77	29.9	22.1
	T2	77	31.7	27.5
	T3	77	33	30.9
	Avg	77	31.5	26.8
	T4	4	26.8	16.9
	T5	4	31	21.6
	Avg	4	28.9	19.3
	Δ	4 to 77	-2.6	-7.5
3	T1	77	36.4	28.6
	T2	77	36.1	29.2
	T3	77	28.1	21.1
	Avg	77	33.5	26.3
	T4	4	15.2	13.1
	T5	4	21	15.2
	Avg	4	18.1	14.2
	Δ	4 to 77	-15.4	-12.1
4	T1	77	34.2	29.2
	T2	77	34	29.7
	T3	77	36	35.1
	Avg	77	34.7	31.3
	T4	4	18.4	21.1
	T5	4	31.2	27.4
	Avg	4	24.8	24.3
	Δ	4 to 77	-9.9	-7

6. Fractography

6.1 Summary of fractography of welds 1 – 4

Both light optical and SEM-based fractography were performed on all the weld/temperature conditions investigated herein. Optical images of every weld condition are presented in Appendix E: Additional fractography: Optical images. Note that the “Dot” designation for the optical images represents the top half of the fractured specimen. Table 7 summarizes the macroscopic features and mechanisms of fracture in the tensile specimens, where MVC stands for microvoid coalescence. In the summary tables, green text indicates that SEM fractography was performed in addition to the light optical fractography. All SEM conducted on the specimens can be found in Appendix F: Additional fractography: SEM images.

Table 7: Summary of the fractography in Welds 1 – 4 at 4 K and 77 K. Green text indicates that SEM fractography was performed in addition to the light optical fractography.

Weld	Test	T (K)	Macroscopic Features	Mechanism of Fracture
1	T1	77	Cup and cone, sign of wormhole pore, no tail, 100 um diameter or less	MVC, wormhole pore
	T2	77	Cup and cone, lack of fusion porosity, 100 um diameter or less	MVC
	T3	77	Cup and cone, wormhole pore contacting edge of specimen, head \approx 200 um diameter	MVC
	T4	4	Cup and cone, wormhole pore head and lack of fusion porosity = 200 um diameter or less, large cracks	MVC
	T5	4	Cup and cone, wormhole pore contacting edge of specimen, head = 200 um diameter	MVC
	T6	4	Partial high angle shear/cup cone, wormhole pore, head = 200 um diameter	MVC, signs of brittle fracture at partial shear
2	T1	77	Cup and cone, remnant spherical pores 100 um diameter or less	MVC
	T2	77	Cup and cone, cracks present	MVC
	T3	77	Cup and cone	MVC
	T4	4	Cup and cone	MVC
	T5	4	High angle shear, cracks present	Mixed MVC + brittle fracture (cleavage)
3	T1	77	Cup and cone, crack present, remnant spherical pore 100 um diameter	MVC
	T2	77	Cup and cone	MVC
	T3	77	Cup and cone	MVC
	T4	4	Flat shear	Mixed MVC + brittle fracture (cleavage)
	T5	4	Cup and cone	Mixed MVC + brittle fracture
4	T1	77	Cup and cone	MVC
	T2	77	Partial cup and cone/partial high angle shear, lack of fusion porosity 200 um diameter	MVC, signs of brittle fracture at partial shear
	T3	77	Cup and cone	MVC
	T4	4	Shear	MVC
	T5	4	Cup and cone, cracks present	Mixed MVC + brittle fracture (cleavage)

6.2 Tests in liquid nitrogen (77 K)

The macroscopic features of the tensile specimens tested at 77 K consisted mostly of cup-and-cone fracture morphology. Figure 7a displays the entire fracture surface of a specimen tested at 77 K with a small lack of fusion pore highlighted by a white arrow. Note that the image has been flattened. Figure 7b displays a three-dimensional depth profile of the fracture surface displaying cone morphology. The predominant fracture mechanism in these specimens tested at 77 K was observed to be microvoid coalescence (MVC) and is shown in Figure 8. Along with lack of fusion porosity, several of these specimens contained wormhole pores, shown in Figure 9a. There were observed particles on the surface of the wormhole pore cavity, shown in Figure 9b.

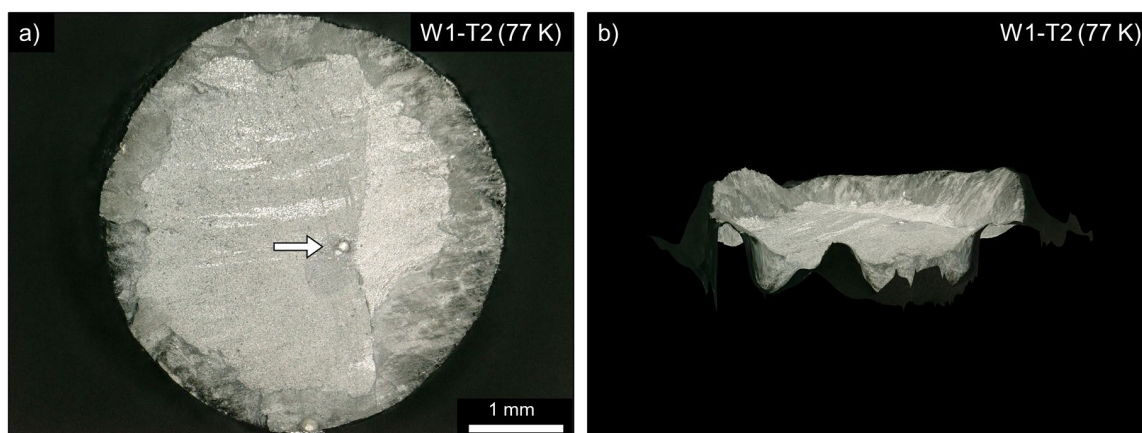


Figure 7: Typical cup-and-cone fracture morphology of a tensile specimen tested at 77 K (W1-T2 pictured, cup morphology). a) flattened image, b) cone morphology.

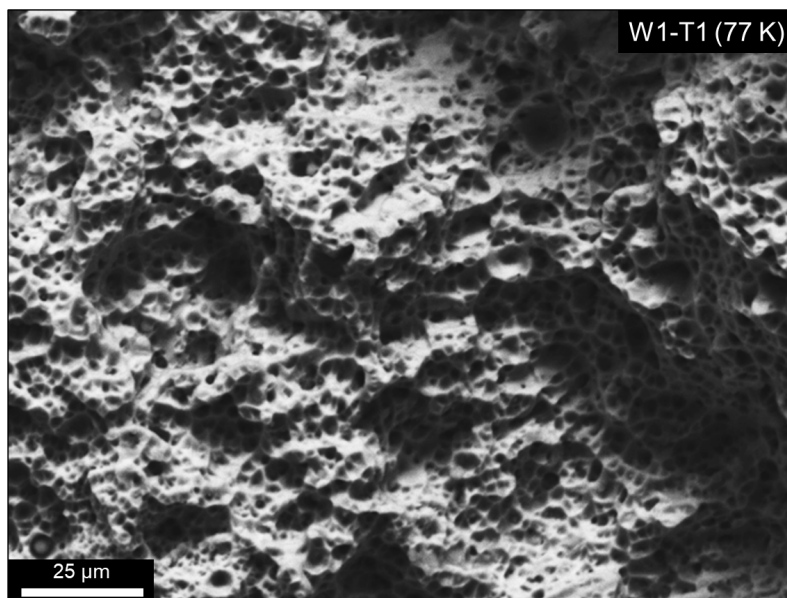


Figure 8: Typical MVC features in specimens tested at 77 K.

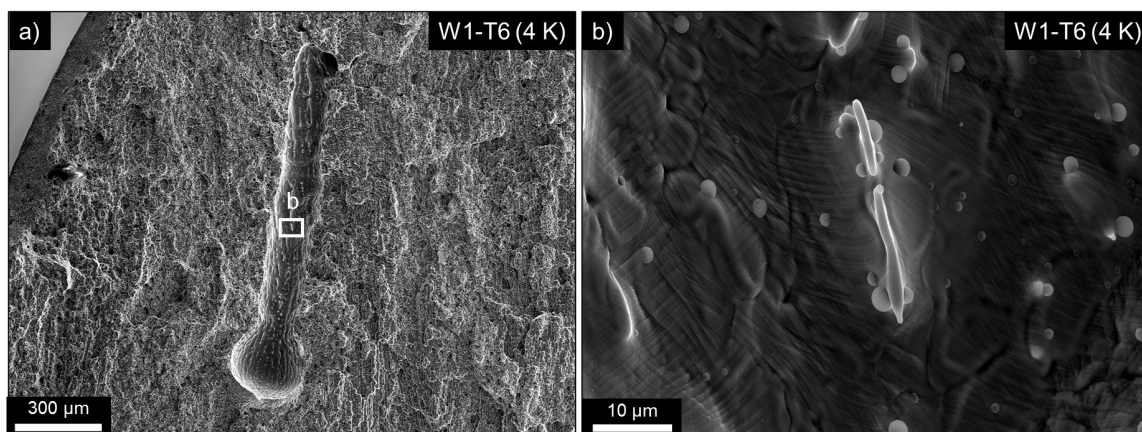


Figure 9: a) Wormhole pore, b) Particles adhering to the surface cavity of the pore.

6.3 Tests in liquid helium (4 K)

Tests conducted at 4 K showed a mix of both macroscopic cup-and-cone along with flat and high angle shear fracture morphology. Figure 10a depicts a flattened optical image of the high angle shear, whereas Figure 10b shows a three-dimensional depth profile of the fracture surface detailing the high angle. Additional SE images of the same specimen are presented in Figure 11. Figure 11a shows the entire fracture surface with higher resolution which showed less overall plastic deformation than the specimens tested at 77 K. Figure 11b depicts a higher magnification image displaying cracking and cleavage-like fracture features.

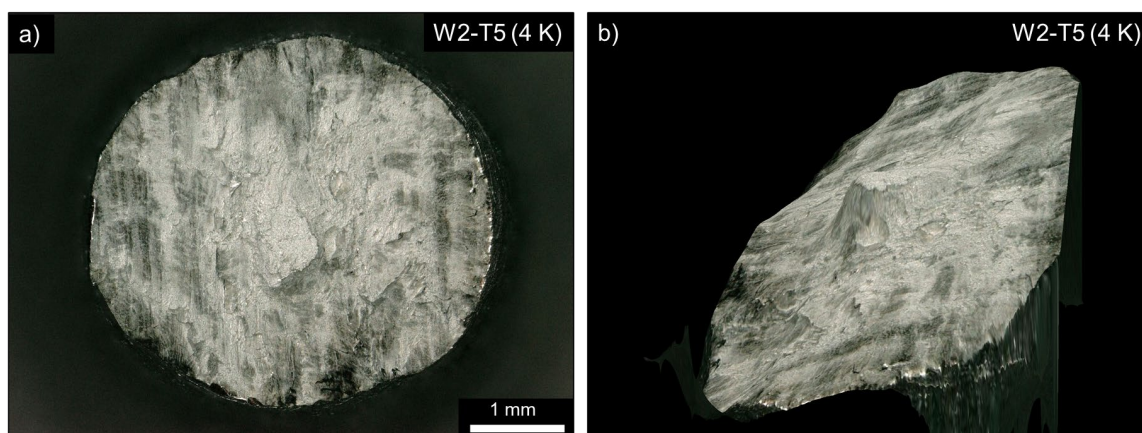


Figure 10: High angle shear fracture morphology in a tensile specimen brought to fracture at 4 K. a) flattened image, b) High angle shear morphology.

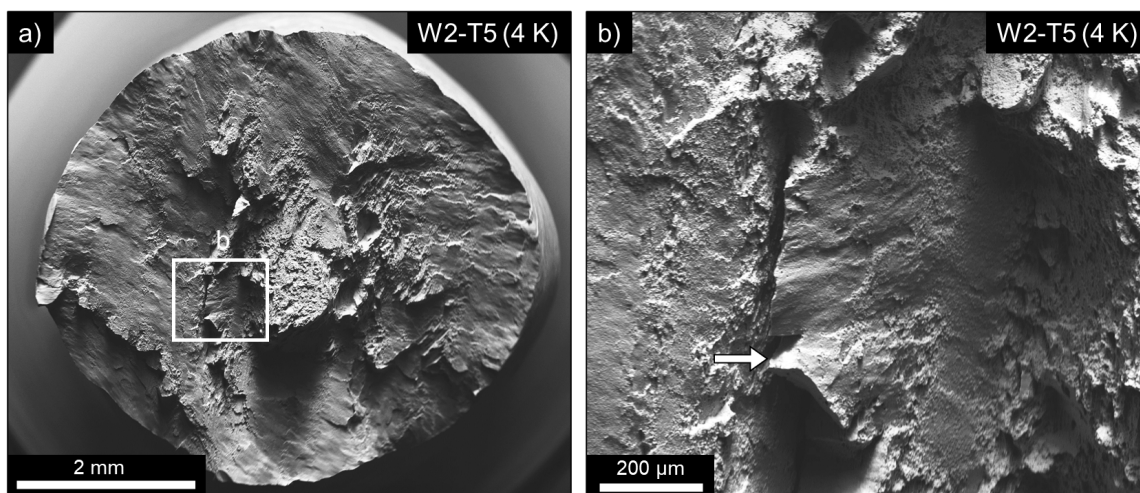


Figure 11: a) SE image of the entire fracture surface of a tensile specimen brought to fracture in 4K, b) cracks at the surface with adjacent cleavage fractures.

7. Discussion

As the test temperature decreased from 77 K to 4 K, all welds exhibited an increase in yield strength. This trend is consistent with previous studies on AISI 316L steel (base metal) [9]. In addition, serrated yielding and serrated flow stresses were observed in tests conducted at 4 K, which is consistent with previous studies on AISI 316L [10] and is a result of changes in dislocation character, sometimes referred to as low temperature plastic instabilities [11]. As temperature decreased, all welds showed a diminution in total elongation and reduction of area, which is consistent with work by Tobler *et al.* [12]. However, only two of the welds (W2 and W4) showed an increase in UTS with decreasing temperature but given the low number of test replicates it is likely that outliers in W1 and W3 exist. While most W1 tensile samples contained some type of porosity, it should be noted that wormhole porosity extending from the interior and all the way to the edge of the tensile specimen was observed in samples W1T3 and W1T5 (see Appendix E: Additional fractography: Optical images), which also coincided with lower UTS values when compared with other corresponding tests at the same temperature. These observations demonstrate the value of characterizing the fracture surface of every specimen to provide context in the case of a potential outlier. This also begs the question of whether nondestructive evaluation should be performed on welds prior to specimen extraction or on specimens prior to testing. Specimen W3T4 also produced a relatively low value of UTS, but it should be noted that parallel ledges were observed on the fracture surfaces (see Appendix F: Additional fractography: SEM images). These ledges indicate a type of cleavage fracture, which is a reasonable and likely reason given the low fraction of microvoid coalescence.

In rank order from strongest to weakest, based on 4 K tensile strength, the order is W4, W2, W3, W1. Composition and interstitial carbon content within a given range is known to increase tensile strength in steels [13,14], even in cryogenic environments [15], which translates well to strength trends observed in this work where carbon contents for W4, W2, W3, and W1 (strongest to weakest) are respectively 0.74 %, 0.7 %, 0.064 %, 0.049 %. The weakest weld, W1, also exhibited the least amount of total elongation and reduction of area, regardless of test temperature when compared to the other welds. Wormhole porosity and observed cleavage likely play a role in reduced ductility [16][17].

Ongoing work will involve microstructural analysis to determine the role of grain size, grain orientation, and phase fraction on tensile properties, plus an analysis on the effects of number of weld passes and microstructural changes. Also, it is suggested that for future projects of similar goals, more tensile tests are planned to ensure trends are confidently established. Finally, while the test apparatus allowed for efficient sample exchanges and measurement of force was conducted within a sufficient range of the cell capacity, new clip gages with greater measurement range should be utilized.

8. Conclusions

In this work, quasi-static tensile tests were performed in liquid nitrogen (77 K) and liquid helium (4 K) on specimens extracted from the centers of four welded 316L stainless steel plates. Differences in strength between the welds were directly correlated with carbon content. As carbon content increased, the ultimate tensile strength at 4 K also increased such that a 20% difference in strength was measured between the strongest (W4) and the weakest (W1) weld. Ferrite content did not correlate to tensile strength. When the environment temperature decreases from 77 K to 4 K, all welds exhibit an increase in yield strength, plus a decrease in total elongation and reduction of area. While a similar increase in ultimate tensile strength was expected for a decrease in temperature, this was not observed, perhaps because of the limited number of samples and observed weld defects. As expected, serrated yielding was observed in every sample deformed at 4 K. The tensile properties reported in this work will be used during analysis of planned fracture toughness (single edge notch bending) tests conducted at 77 K and 4 K on the same four sets of welded plates in the framework of the same collaborative project between ASME, NASA, and NIST.

Acknowledgements

We would like to acknowledge our colleagues who were instrumental in planning and facilitating nearly all aspects of this collaborative project.

National Institute of Standards and Technology:

- David McColskey for guidance on fixture design and proper implementation of ASTM standards.
- Ted Stauffer for guidance on dewar/transfer rod handling, experimental setup, and monitoring of liquid helium levels and pressures.
- Ross Rentz for producing technical drawings of all specimen geometries and swift implementation of necessary changes to the experimental setup.

NASA and NASA contractors:

- Levi Shelton for coordinating materials delivery and providing guidance on proper implementation of ASTM standards.
- Owen Greulich for guidance on interpretation of welding procedure specifications for each welding lot.

Swagelok Company:

- Shelly Tang for completing ferroscope measurements on welds and base plates, plus guidance on interpretation of welding procedure specifications for each welding lot.

Sperko Engineering Services:

- Walter Sperko for guidance on interpretation of welding procedure specifications for each welding lot.

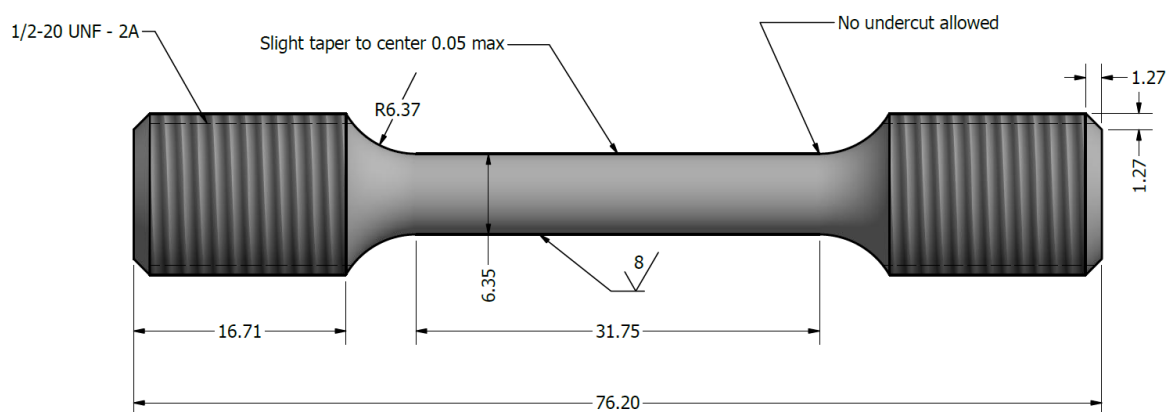
Finally, we would like to acknowledge the welding vendors, in no particular order, for providing their services: Nooter, Team Industries, Atlas, and Boardman.

References

- [1] The American Society of Mechanical Engineers Boiler and Pressure Vessel Code, BPVC Section VIII-Rules for Construction of Pressure Vessels, Division 1, BVPC-VIII-1, ASME, (2021).
- [2] The American Society of Mechanical Engineers, Hydrogen Piping and Pipelines, B31.12, ASME, (2019).
- [3] The American Society of Mechanical Engineers Process Piping, ASME Code for Pressure Piping, B31, ASME, (2020).
- [4] ASTM E23 Standard Test Methods for Notched Bar Impact Testing of Metallic Materials. American Society for Testing and Material International, West Conshohocken, PA, (2018).
- [5] N.I. Vazquez-Fernandez, G.C. Soares, J.L. Smith, J.D. Seidt, M. Isakov, A. Gilat, V.T. Kuokkala, M. Hokka, Adiabatic Heating of Austenitic Stainless Steels at Different Strain Rates, *J. Dyn. Behav. Mater.* 5 (2019) 221–229. <https://doi.org/10.1007/s40870-019-00204-z>.
- [6] ASTM E1820 Standard Test Method for Measurement of Fracture Toughness. American Society for Testing and Material International, West Conshohocken, PA, (2021).
- [7] E. Lucon, J.T. Benzing, Instrumented Charpy Tests at 77 K on 316L Stainless Steel Welded Plates, *Natl. Inst. Stand. Technol. NIST Tech. Note.* (2021). <https://doi.org/https://doi.org/10.6028/NIST.TN.2196>.
- [8] ASTM E8 Standard Test Methods for Tension Testing of Metallic Materials. American Society for Testing and Material International, West Conshohocken, PA., (2016).
- [9] O. Umezawa, Review of the mechanical properties of high-strength alloys at cryogenic temperatures, *Mater. Perform. Charact.* 10 (2021) 3–15. <https://doi.org/10.1520/MPC20200138>.
- [10] P. Fernández-Pisón, J.A. Rodríguez-Martínez, E. García-Tabarés, I. Avilés-Santillana, S. Sgobba, Flow and fracture of austenitic stainless steels at cryogenic temperatures, *Eng. Fract. Mech.* 258 (2021) 108042. <https://doi.org/https://doi.org/10.1016/j.engfracmech.2021.108042>.
- [11] B. Obst, A. Nyilas, Experimental evidence on the dislocation mechanism of serrated yielding in f.c.c. metals and alloys at low temperatures, *Mater. Sci. Eng. A.* 137 (1991) 141–150. [https://doi.org/https://doi.org/10.1016/0921-5093\(91\)90328-K](https://doi.org/https://doi.org/10.1016/0921-5093(91)90328-K).
- [12] R.L. Tobler, R.P. Reed, Interstitial Carbon and Nitrogen Effects on the Cryogenic Fatigue Crack Growth of AISI 304 Type Stainless Steels, *J. Test. Eval.* 12 (1984) 364–370.
- [13] M. Ghasri-Khouzani, J.R. McDermid, Effect of carbon content on the mechanical properties and microstructural evolution of Fe-22Mn-C steels, *Mater. Sci. Eng. A.* 621 (2015) 118–127. <https://doi.org/10.1016/j.msea.2014.10.042>.
- [14] H. Berns, V.G. Gavriljuk, S. Riedner, A. Tyshchenko, High Strength Stainless Austenitic CrMnCN Steels – Part I: Alloy Design and Properties, *Mater. Technol. High.* 78 (2007) 714–.
- [15] D.T. Read, R.P. Reed, Fracture and strength properties of selected austenitic stainless steels at cryogenic temperatures, *Cryogenics (Guildf).* 21 (1981) 415–417.

- [https://doi.org/https://doi.org/10.1016/0011-2275\(81\)90175-2](https://doi.org/https://doi.org/10.1016/0011-2275(81)90175-2).
- [16] D.K. Matlock, J.G. Speer, Third generation of AHSS: microstructure design concepts, in: A. Haldar, S. Suwas, D. Bhattacharjee (Eds.), *Microstruct. Texture Steels*, Springer, London, 2009: pp. 185–205. https://doi.org/10.1007/978-1-84882-454-6_11.
- [17] D.-Y. Kim, I. Hwang, G. Jeong, M. Kang, D. Kim, J. Seo, Y.-M. Kim, Effect of Porosity on the Fatigue Behavior of Gas Metal Arc Welding Lap Fillet Joint in GA 590 MPa Steel Sheets, *Met. .* 8 (2018). <https://doi.org/10.3390/met8040241>.

Appendix A: Technical drawing

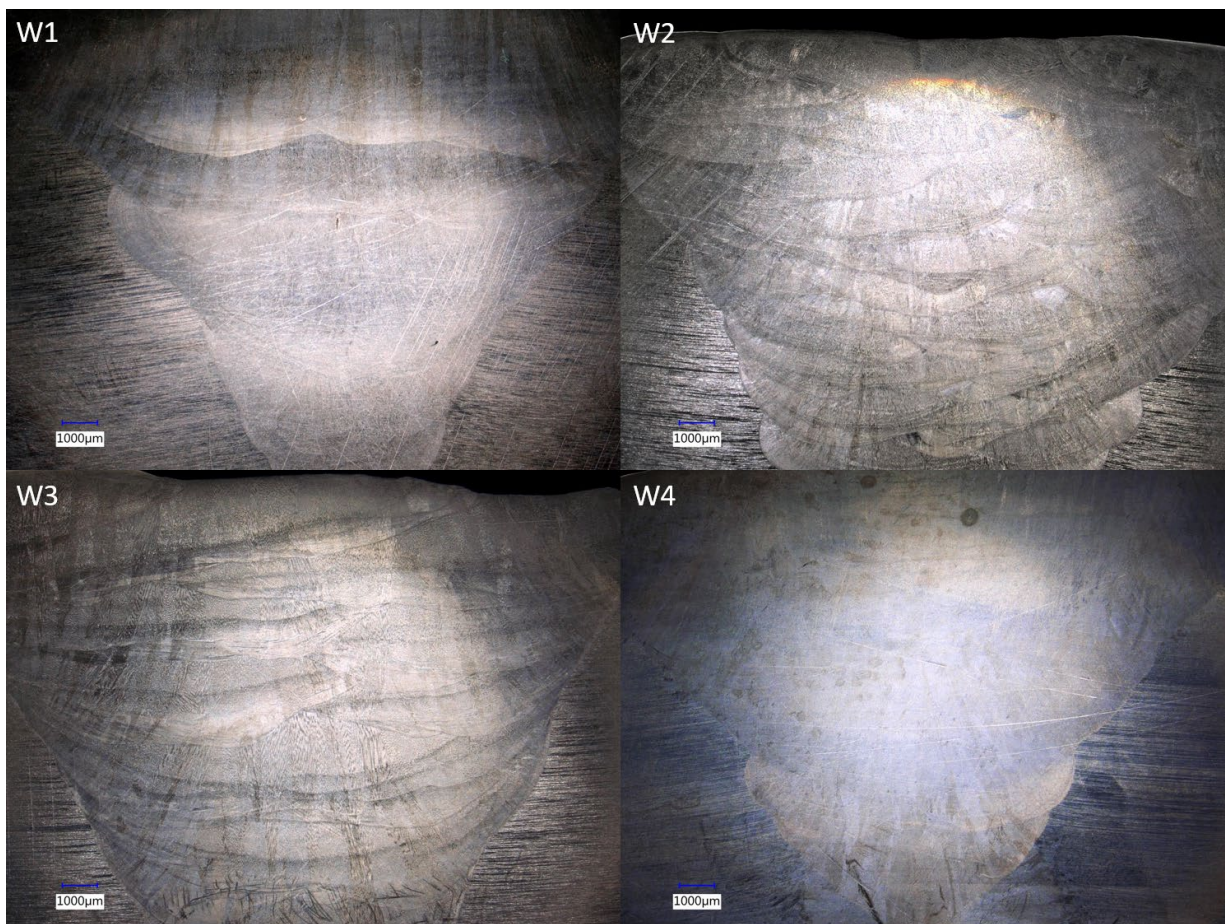


NOTES: all dimensions in millimeters. Default tolerances are ± 0.1 mm and $\pm 1^\circ$. Default surface finish, unless specified, is $< 1.6 \mu\text{m}$.

Appendix B: Supplemental information for each weld

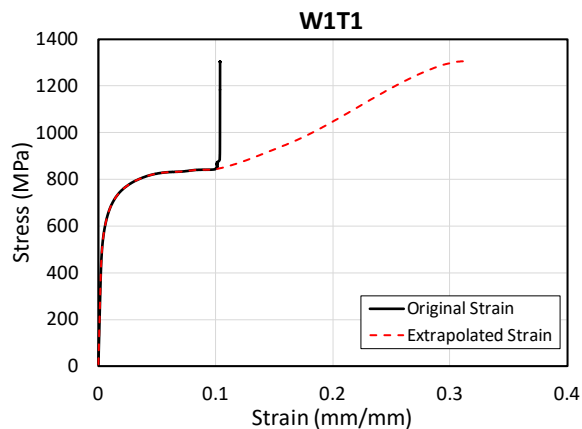
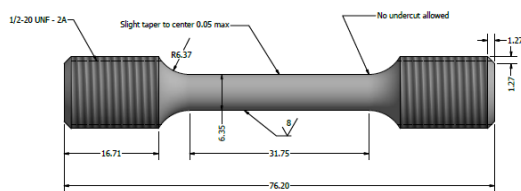
Wire composition (% mass fraction) provided by welding vendors

Welded plate	W1		W3		W4	
	AWS/SFA 5.9 (Root)	AWS/SFA 5.22 (Cover)	Root	Cover	Root/Hot pass	Cover
C	0.014	0.03	0.016	0.03	<0.01/<0.01	0.022
Cr	18.16	18.89	18.3	17.74	18.3/18.0	18.68
Ni	11.81	12.48	12.75	12.94	12.2/12.0	11.88
Mo	2.56	2.55	2.54	2.1	2.5/2.5	2.72
Mn	1.78	1.14	1.89	0.85	1.6/1.5	1.53
Si	0.36	0.7	0.35	0.56	0.35/0.37	0.72
P	0.014	0.26	0.015	0.025	0.021/0.023	0.024
S	0.012	0.005	0.012	0.004	0.012/0.01	0.008
Cu	0.08	0.21	0.1	0.2	0.18/0.16	0.12



Optical image of weld cross sections after mechanical polishing and etching (Kalling's No. 2: 5 g CuCl_2 , 40 ml HCl , 30 ml H_2O).

Tensile Test - Specimen Report



Specimen ID: W1T1
Material/Condition: 316L Weld
Test Temperature: 77K

Test Date: 8/23/2021
Operator: Dash Weeks
Analysis Performed on: 07/01/2022

Test Frame: MTS 55KIP Cryo
Last Calibration: 2/3/2021
Instrumentation: Avg of 3 Extensometers
Last Calibration: 8/19/2021

Specimen Type:	Round
Specimen Area:	31.76 mm ²
Overall Length:	76.24 mm
Gage Length:	25.4 mm

Target Strain Rate: 0.015 mm/mm/min
Displacement Rate: 0.763 mm/min

Total Plastic Elongation: 30.5 %
Reduction of Area: 19.2 %

Modulus of Elasticity: 195 GPa
*Modulus of Elasticity: 28.3 Msi

Yield Stress at 0.5% Strain:	581 MPa
*Yield Stress at 0.5% Strain:	84.3 ksi

Max Stress:	1306 MPa
*Max Stress:	189.4 ksi
Strain at Max Stress:	0.104 mm/mm
Extrapolated Strain at Max Stress:	0.311 mm/mm

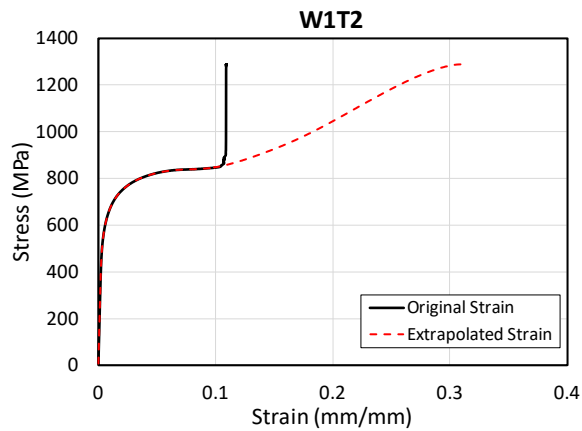
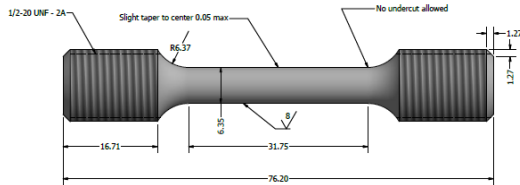
* Converted from results in SI Units

W1T1, tested at 77 K



U.S. Department of Commerce
National Institute of Standards and Technology
Materials Measurement Laboratory
Applied Chemicals and Materials Division
Fatigue and Fracture Group
Boulder, CO

Tensile Test - Specimen Report



* Converted from results in SI Units

Specimen ID: W1T2
Material/Condition: 316L Weld
Test Temperature: 77K

Test Date: 9/7/2021
Operator: Dash Weeks
Analysis Performed on: 06/30/2022

Test Frame: MTS 55KIP Cryo
Last Calibration: 2/3/2021
Instrumentation: Avg of 3 Extensometers
Last Calibration: 8/19/2021

Specimen Type: Round
Specimen Area: 31.78 mm²
Overall Length: 76.14 mm
Gage Length: 25.4 mm

Target Strain Rate: 0.015 mm/mm/min
Displacement Rate: 0.762 mm/min

Total Plastic Elongation: 30.5 %
Reduction of Area: 21.3 %

Modulus of Elasticity: 197 GPa
*Modulus of Elasticity: 28.6 Msi

Yield Stress at 0.5% Strain: 579 MPa
*Yield Stress at 0.5% Strain: 84 ksi

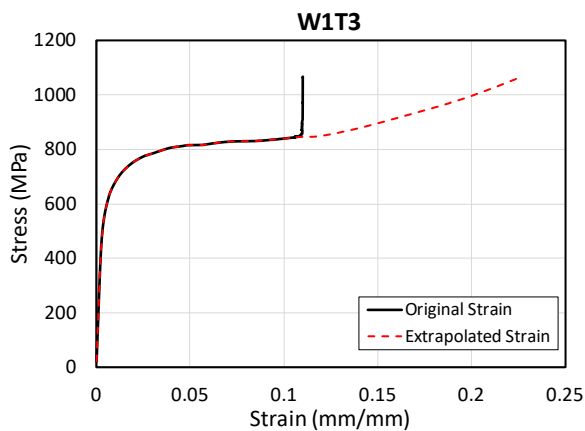
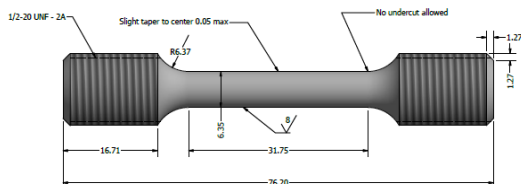
Max Stress: 1289 MPa
*Max Stress: 187 ksi
Strain at Max Stress: 0.109 mm/mm
Extrapolated Strain at Max Stress: 0.311 mm/mm

W1T2, tested at 77 K



U.S. Department of Commerce
National Institute of Standards and Technology
Materials Measurement Laboratory
Applied Chemicals and Materials Division
Fatigue and Fracture Group
Boulder, CO

Tensile Test - Specimen Report



* Converted from results in SI Units

Specimen ID: W1T3
Material/Condition: 316L Weld
Test Temperature: 77K

Test Date: 9/7/2021
Operator: Dash Weeks
Analysis Performed on: 06/30/2022

Test Frame: MTS 55KIP Cryo
Last Calibration: 2/3/2021
Instrumentation: Avg of 3 Extensometers
Last Calibration: 8/19/2021

Specimen Type: Round
Specimen Area: 31.79 mm²
Overall Length: 76.14 mm
Gage Length: 25.4 mm

Target Strain Rate: 0.015 mm/mm/min
Displacement Rate: 0.762 mm/min

Total Plastic Elongation: 19.5 %
Reduction of Area: 12.7 %

Modulus of Elasticity: 184 GPa
*Modulus of Elasticity: 26.7 Msi

Yield Stress at 0.5% Strain: 581 MPa
*Yield Stress at 0.5% Strain: 84.3 ksi

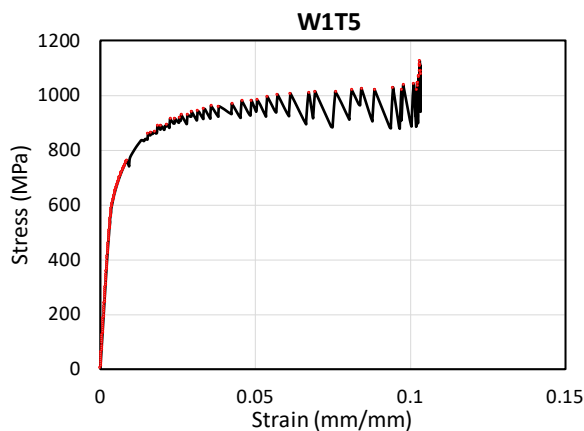
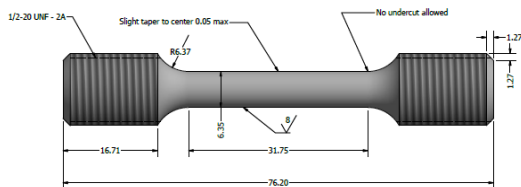
Max Stress: 1067 MPa
*Max Stress: 154.8 ksi
Strain at Max Stress: 0.11 mm/mm
Extrapolated Strain at Max Stress: 0.201 mm/mm

W1T3, tested at 77 K



U.S. Department of Commerce
National Institute of Standards and Technology
Materials Measurement Laboratory
Applied Chemicals and Materials Division
Fatigue and Fracture Group
Boulder, CO

Tensile Test - Specimen Report



* Converted from results in SI Units

Specimen ID: W1T5
Material/Condition: 316L Weld
Test Temperature: 4K

Test Date: 9/28/2021
Operator: Dash Weeks
Analysis Performed on: 07/01/2022

Test Frame: MTS 55KIP Cryo
Last Calibration: 2/3/2021
Instrumentation: Avg of 3 Extensometers
Last Calibration: 8/19/2021

Specimen Type: Round
Specimen Area: 31.8 mm²
Overall Length: 76.22 mm
Gage Length: 25.4 mm

Target Strain Rate: 0.015 mm/mm/min
Displacement Rate: 0.763 mm/min

Total Plastic Elongation: 15.2 %
Reduction of Area: 9.9 %

Modulus of Elasticity: 185 GPa
*Modulus of Elasticity: 26.8 Msi

Yield Stress at 0.5% Strain: 659 MPa
*Yield Stress at 0.5% Strain: 95.6 ksi

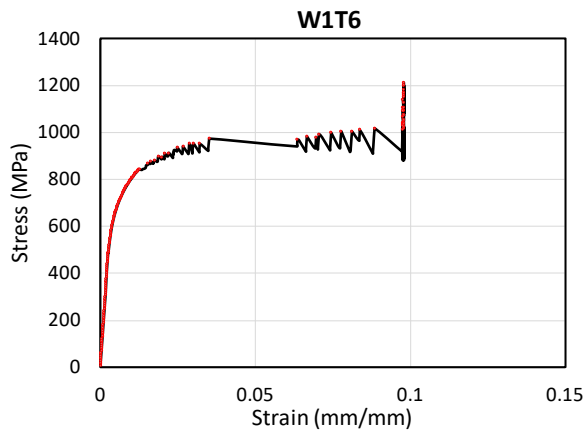
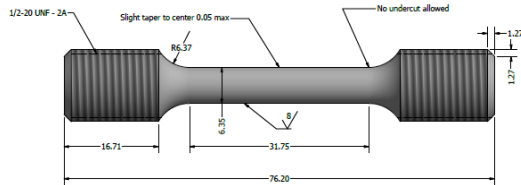
Max Stress: 1126 MPa
*Max Stress: 163.3 ksi
Strain at Max Stress: 0.103 mm/mm
Extrapolated Strain at Max Stress: 0.158 mm/mm

W1T5, tested at 4 K



U.S. Department of Commerce
National Institute of Standards and Technology
Materials Measurement Laboratory
Applied Chemicals and Materials Division
Fatigue and Fracture Group
Boulder, CO

Tensile Test - Specimen Report



* Converted from results in SI Units

Specimen ID: W1T6
Material/Condition: 316L Weld
Test Temperature: 4K

Test Date: 9/28/2021
Operator: Dash Weeks
Analysis Performed on: 06/27/2022

Test Frame: MTS 55KIP Cryo
Last Calibration: 2/3/2021
Instrumentation: Avg of 3 Extensometers
Last Calibration: 8/19/2021

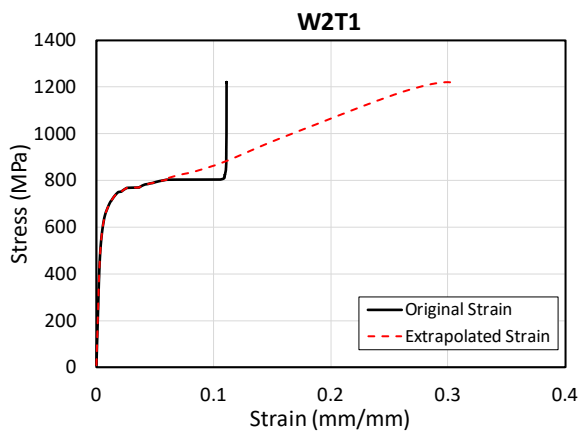
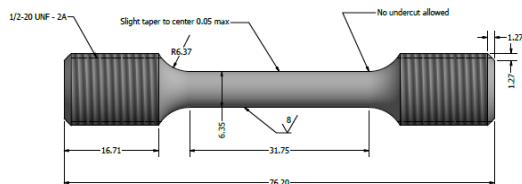
Specimen Type:	Round
Specimen Area:	31.77 mm ²
Overall Length:	76.12 mm
Gage Length:	25.4 mm
Target Strain Rate:	0.015 mm/mm/min
Displacement Rate:	0.763 mm/min
Total Plastic Elongation:	18.1 %
Reduction of Area:	11.6 %
Modulus of Elasticity:	184 GPa
*Modulus of Elasticity:	26.7 Msi
Yield Stress at 0.5% Strain:	666 MPa
*Yield Stress at 0.5% Strain:	96.6 ksi
Max Stress:	1213 MPa
*Max Stress:	175.9 ksi
Strain at Max Stress:	0.098 mm/mm
Extrapolated Strain at Max Stress:	0.188 mm/mm

W1T6, tested at 4 K



U.S. Department of Commerce
National Institute of Standards and Technology
Materials Measurement Laboratory
Applied Chemicals and Materials Division
Fatigue and Fracture Group
Boulder, CO

Tensile Test - Specimen Report



* Converted from results in SI Units

Specimen ID: W2T1
Material/Condition: 316L Weld
Test Temperature: 77K

Test Date: 9/7/2021
Operator: Dash Weeks
Analysis Performed on: 06/30/2022

Test Frame: MTS 55KIP Cryo
Last Calibration: 2/3/2021
Instrumentation: Avg of 3 Extensometers
Last Calibration: 8/19/2021

Specimen Type: Round
Specimen Area: 31.78 mm²
Overall Length: 76.16 mm
Gage Length: 25.4 mm

Target Strain Rate: 0.015 mm/mm/min
Displacement Rate: 0.762 mm/min

Total Plastic Elongation: 29.9 %
Reduction of Area: 22.1 %

Modulus of Elasticity: 169 GPa
*Modulus of Elasticity: 24.5 Msi

Yield Stress at 0.5% Strain: 585 MPa
*Yield Stress at 0.5% Strain: 84.8 ksi

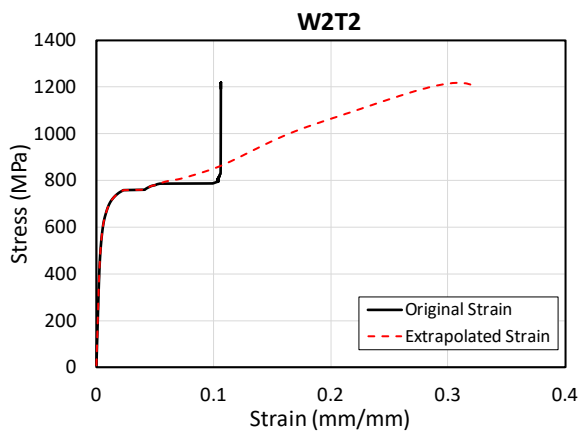
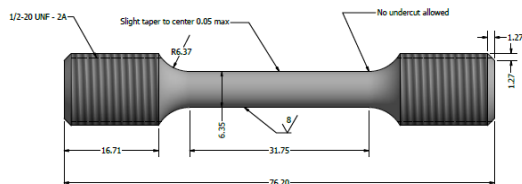
Max Stress: 1221 MPa
*Max Stress: 177.1 ksi
Strain at Max Stress: 0.111 mm/mm
Extrapolated Strain at Max Stress: 0.306 mm/mm

W2T1, tested at 77 K



U.S. Department of Commerce
National Institute of Standards and Technology
Materials Measurement Laboratory
Applied Chemicals and Materials Division
Fatigue and Fracture Group
Boulder, CO

Tensile Test - Specimen Report



* Converted from results in SI Units

Specimen ID: W2T2
Material/Condition: 316L Weld
Test Temperature: 77K

Test Date: 9/7/2021
Operator: Dash Weeks
Analysis Performed on: 06/30/2022

Test Frame: MTS 55KIP Cryo
Last Calibration: 2/3/2021
Instrumentation: Avg of 3 Extensometers
Last Calibration: 8/19/2021

Specimen Type: Round
Specimen Area: 31.88 mm²
Overall Length: 76.13 mm
Gage Length: 25.4 mm

Target Strain Rate: 0.015 mm/mm/min
Displacement Rate: 0.762 mm/min

Total Plastic Elongation: 31.7 %
Reduction of Area: 27.5 %

Modulus of Elasticity: 169 GPa
*Modulus of Elasticity: 24.5 Msi

Yield Stress at 0.5% Strain: 579 MPa
*Yield Stress at 0.5% Strain: 84 ksi

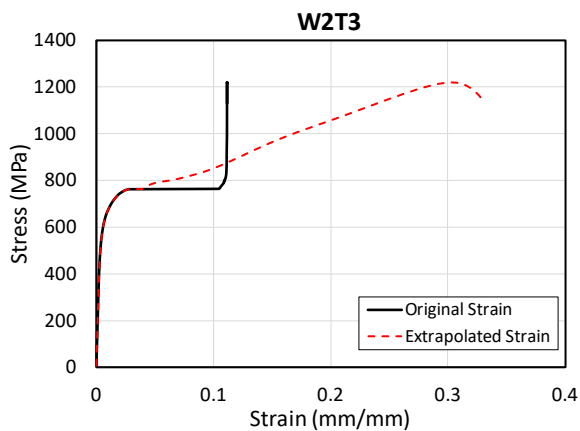
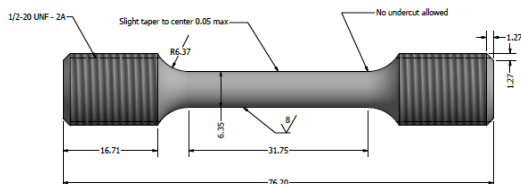
Max Stress: 1218 MPa
*Max Stress: 176.7 ksi
Strain at Max Stress: 0.106 mm/mm
Extrapolated Strain at Max Stress: 0.324 mm/mm

W2T2, tested at 77 K



U.S. Department of Commerce
National Institute of Standards and Technology
Materials Measurement Laboratory
Applied Chemicals and Materials Division
Fatigue and Fracture Group
Boulder, CO

Tensile Test - Specimen Report



* Converted from results in SI Units

Specimen ID: W2T3
Material/Condition: 316L Weld
Test Temperature: 77K

Test Date: 9/7/2021
Operator: Dash Weeks
Analysis Performed on: 06/30/2022

Test Frame: MTS 55KIP Cryo
Last Calibration: 2/3/2021
Instrumentation: Avg of 3 Extensometers
Last Calibration: 8/19/2021

Specimen Type: Round
Specimen Area: 31.74 mm²
Overall Length: 76.13 mm
Gage Length: 25.4 mm

Target Strain Rate: 0.015 mm/mm/min
Displacement Rate: 0.762 mm/min

Total Plastic Elongation: 33 %
Reduction of Area: 30.9 %

Modulus of Elasticity: 180 GPa
*Modulus of Elasticity: 26.1 Msi

Yield Stress at 0.5% Strain: 578 MPa
*Yield Stress at 0.5% Strain: 83.8 ksi

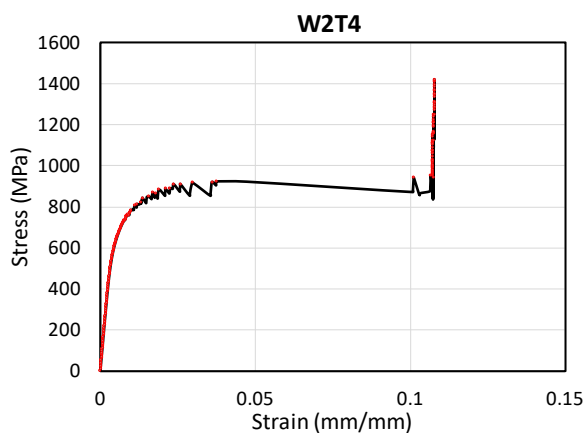
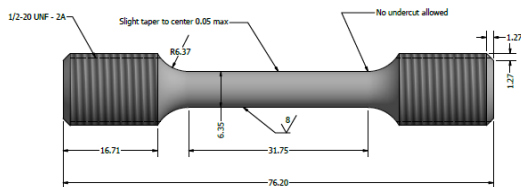
Max Stress: 1220 MPa
*Max Stress: 176.9 ksi
Strain at Max Stress: 0.112 mm/mm
Extrapolated Strain at Max Stress: 0.336 mm/mm

W2T3, tested at 77 K



U.S. Department of Commerce
National Institute of Standards and Technology
Materials Measurement Laboratory
Applied Chemicals and Materials Division
Fatigue and Fracture Group
Boulder, CO

Tensile Test - Specimen Report



* Converted from results in SI Units

Specimen ID: W2T4
Material/Condition: 316L Weld
Test Temperature: 4K

Test Date: 9/28/2021
Operator: Dash Weeks
Analysis Performed on: 06/27/2022

Test Frame: MTS 55KIP Cryo
Last Calibration: 2/3/2021
Instrumentation: Avg of 3 Extensometers
Last Calibration: 8/19/2021

Specimen Type: Round
Specimen Area: 31.84 mm²
Overall Length: 76.14 mm
Gage Length: 25.4 mm

Target Strain Rate: 0.015 mm/mm/min
Displacement Rate: 0.762 mm/min

Total Plastic Elongation: 26.8 %
Reduction of Area: 16.9 %

Modulus of Elasticity: 169 GPa
*Modulus of Elasticity: 24.5 Msi

Yield Stress at 0.5% Strain: 634 MPa
*Yield Stress at 0.5% Strain: 92 ksi

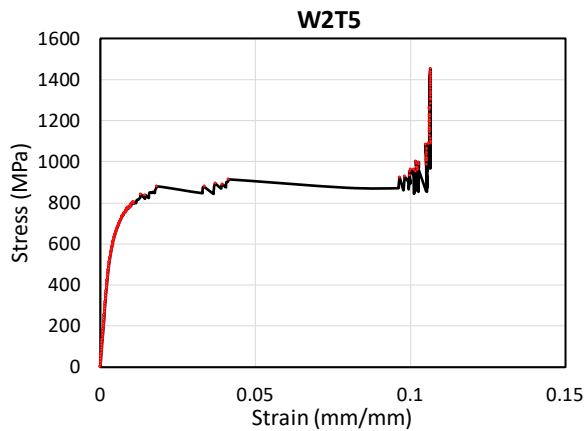
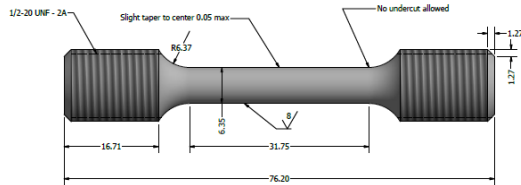
Max Stress: 1422 MPa
*Max Stress: 206.2 ksi
Strain at Max Stress: 0.108 mm/mm
Extrapolated Strain at Max Stress: 0.276 mm/mm

W2T4, tested at 4 K



U.S. Department of Commerce
National Institute of Standards and Technology
Materials Measurement Laboratory
Applied Chemicals and Materials Division
Fatigue and Fracture Group
Boulder, CO

Tensile Test - Specimen Report



* Converted from results in SI Units

Specimen ID: W2T5
Material/Condition: 316L Weld
Test Temperature: 4K

Test Date: 9/28/2021
Operator: Dash Weeks
Analysis Performed on: 06/27/2022

Test Frame: MTS 55KIP Cryo
Last Calibration: 2/3/2021
Instrumentation: Avg of 3 Extensometers
Last Calibration: 8/19/2021

Specimen Type: Round
Specimen Area: 31.78 mm²
Overall Length: 76.13 mm
Gage Length: 25.4 mm

Target Strain Rate: 0.015 mm/mm/min
Displacement Rate: 0.762 mm/min

Total Plastic Elongation: 31 %
Reduction of Area: 21.6 %

Modulus of Elasticity: 191 GPa
*Modulus of Elasticity: 27.7 Msi

Yield Stress at 0.5% Strain: 657 MPa
*Yield Stress at 0.5% Strain: 95.3 ksi

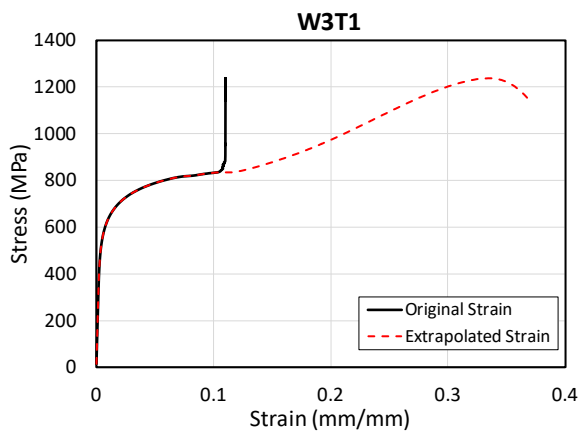
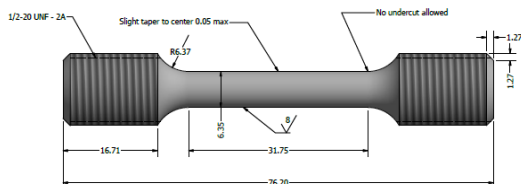
Max Stress: 1453 MPa
*Max Stress: 210.7 ksi
Strain at Max Stress: 0.106 mm/mm
Extrapolated Strain at Max Stress: 0.317 mm/mm

W2T5, tested at 4 K



U.S. Department of Commerce
National Institute of Standards and Technology
Materials Measurement Laboratory
Applied Chemicals and Materials Division
Fatigue and Fracture Group
Boulder, CO

Tensile Test - Specimen Report



* Converted from results in SI Units

Specimen ID: W3T1
Material/Condition: 316L Weld
Test Temperature: 77K

Test Date: 9/8/2021
Operator: Dash Weeks
Analysis Performed on: 07/01/2022

Test Frame: MTS 55KIP Cryo
Last Calibration: 2/3/2021
Instrumentation: Avg of 3 Extensometers
Last Calibration: 8/19/2021

Specimen Type: Round
Specimen Area: 31.7 mm²
Overall Length: 76.13 mm
Gage Length: 25.4 mm

Target Strain Rate: 0.015 mm/mm/min
Displacement Rate: 0.762 mm/min

Total Plastic Elongation: 36.4 %
Reduction of Area: 28.6 %

Modulus of Elasticity: 185 GPa
*Modulus of Elasticity: 26.8 Msi

Yield Stress at 0.5% Strain: 549 MPa
*Yield Stress at 0.5% Strain: 79.6 ksi

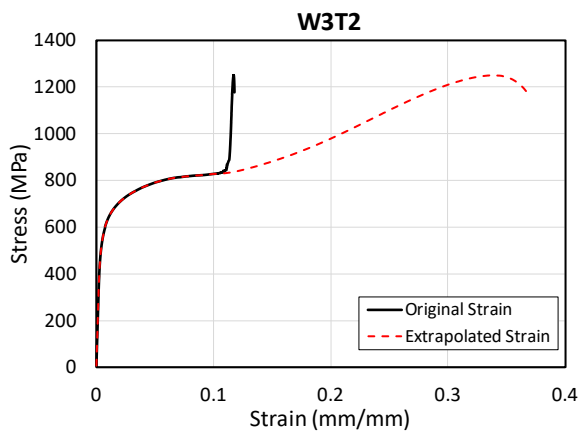
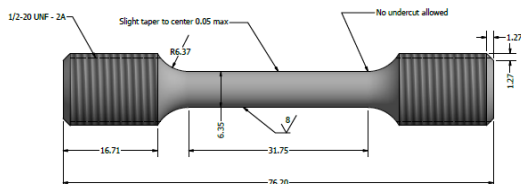
Max Stress: 1238 MPa
*Max Stress: 179.6 ksi
Strain at Max Stress: 0.11 mm/mm
Extrapolated Strain at Max Stress: 0.37 mm/mm

W3T1, tested at 77 K



U.S. Department of Commerce
National Institute of Standards and Technology
Materials Measurement Laboratory
Applied Chemicals and Materials Division
Fatigue and Fracture Group
Boulder, CO

Tensile Test - Specimen Report



* Converted from results in SI Units

Specimen ID: W3T2
Material/Condition: 316L Weld
Test Temperature: 77K

Test Date: 9/8/2021
Operator: Dash Weeks
Analysis Performed on: 06/30/2022

Test Frame: MTS 55KIP Cryo
Last Calibration: 2/3/2021
Instrumentation: Avg of 3 Extensometers
Last Calibration: 8/19/2021

Specimen Type: Round
Specimen Area: 31.76 mm²
Overall Length: 76.13 mm
Gage Length: 25.4 mm

Target Strain Rate: 0.015 mm/mm/min
Displacement Rate: 0.762 mm/min

Total Plastic Elongation: 36.1 %
Reduction of Area: 29.2 %

Modulus of Elasticity: 169 GPa
*Modulus of Elasticity: 24.5 Msi

Yield Stress at 0.5% Strain: 542 MPa
*Yield Stress at 0.5% Strain: 78.6 ksi

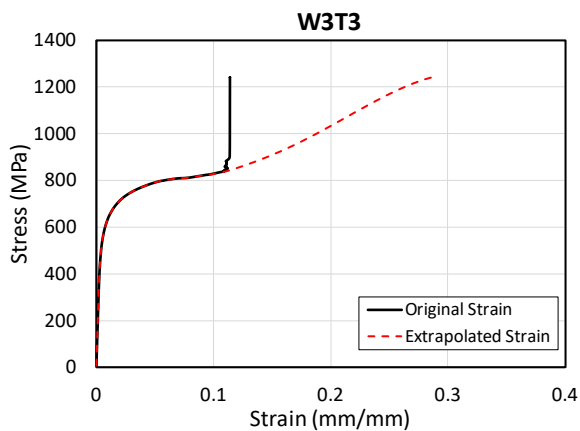
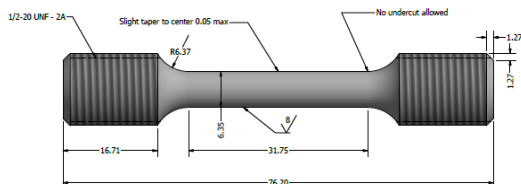
Max Stress: 1251 MPa
*Max Stress: 181.4 ksi
Strain at Max Stress: 0.117 mm/mm
Extrapolated Strain at Max Stress: 0.368 mm/mm

W3T2, tested at 77 K



U.S. Department of Commerce
National Institute of Standards and Technology
Materials Measurement Laboratory
Applied Chemicals and Materials Division
Fatigue and Fracture Group
Boulder, CO

Tensile Test - Specimen Report



* Converted from results in SI Units

Specimen ID: W3T3
Material/Condition: 316L Weld
Test Temperature: 77K

Test Date: 9/8/2021
Operator: Dash Weeks
Analysis Performed on: 06/30/2022

Test Frame: MTS 55KIP Cryo
Last Calibration: 2/3/2021
Instrumentation: Avg of 3 Extensometers
Last Calibration: 8/19/2021

Specimen Type: Round
Specimen Area: 31.76 mm²
Overall Length: 76.13 mm
Gage Length: 25.4 mm

Target Strain Rate: 0.015 mm/mm/min
Displacement Rate: 0.762 mm/min

Total Plastic Elongation: 28.1 %
Reduction of Area: 21.1 %

Modulus of Elasticity: 164 GPa
*Modulus of Elasticity: 23.8 Msi

Yield Stress at 0.5% Strain: 541 MPa
*Yield Stress at 0.5% Strain: 78.5 ksi

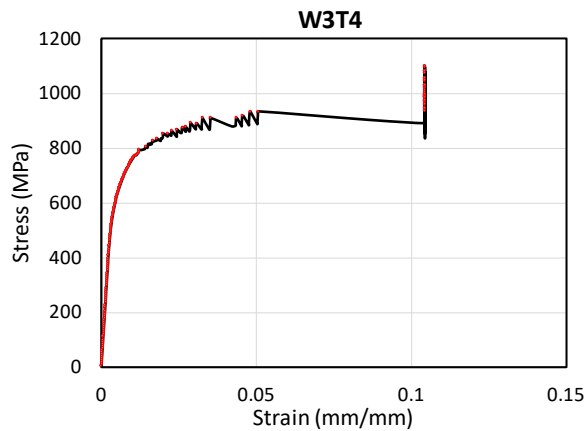
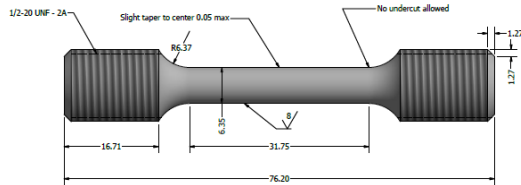
Max Stress: 1242 MPa
*Max Stress: 180.1 ksi
Strain at Max Stress: 0.114 mm/mm
Extrapolated Strain at Max Stress: 0.289 mm/mm

W3T3, tested at 77 K



U.S. Department of Commerce
National Institute of Standards and Technology
Materials Measurement Laboratory
Applied Chemicals and Materials Division
Fatigue and Fracture Group
Boulder, CO

Tensile Test - Specimen Report



* Converted from results in SI Units

Specimen ID: W3T4
Material/Condition: 316L Weld
Test Temperature: 4K

Test Date: 9/28/2021
Operator: Dash Weeks
Analysis Performed on: 06/27/2022

Test Frame: MTS 55KIP Cryo
Last Calibration: 2/3/2021
Instrumentation: Avg of 3 Extensometers
Last Calibration: 8/19/2021

Specimen Type: Round
Specimen Area: 31.79 mm²
Overall Length: 76.12 mm
Gage Length: 25.4 mm

Target Strain Rate: 0.015 mm/mm/min
Displacement Rate: 0.761 mm/min

Total Plastic Elongation: 15.2 %
Reduction of Area: 13.1 %

Modulus of Elasticity: 176 GPa
*Modulus of Elasticity: 25.5 Msi

Yield Stress at 0.5% Strain: 627 MPa
*Yield Stress at 0.5% Strain: 90.9 ksi

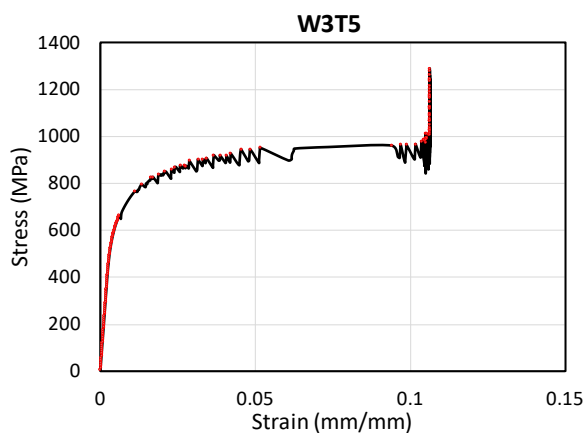
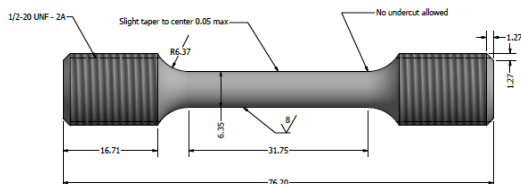
Max Stress: 1101 MPa
*Max Stress: 159.7 ksi
Strain at Max Stress: 0.104 mm/mm
Extrapolated Strain at Max Stress: 0.158 mm/mm

W3T4, tested at 4 K



U.S. Department of Commerce
National Institute of Standards and Technology
Materials Measurement Laboratory
Applied Chemicals and Materials Division
Fatigue and Fracture Group
Boulder, CO

Tensile Test - Specimen Report



* Converted from results in SI Units

Specimen ID: W3T5
Material/Condition: 316L Weld
Test Temperature: 4K

Test Date: 9/28/2021
Operator: Dash Weeks
Analysis Performed on: 06/27/2022

Test Frame: MTS 55KIP Cryo
Last Calibration: 2/3/2021
Instrumentation: Avg of 3 Extensometers
Last Calibration: 8/19/2021

Specimen Type: Round
Specimen Area: 31.84 mm²
Overall Length: 76.14 mm
Gage Length: 25.4 mm

Target Strain Rate: 0.015 mm/mm/min
Displacement Rate: 0.761 mm/min

Total Plastic Elongation: 21 %
Reduction of Area: 15.2 %

Modulus of Elasticity: 178 GPa
*Modulus of Elasticity: 25.8 Msi

Yield Stress at 0.5% Strain: 625 MPa
*Yield Stress at 0.5% Strain: 90.6 ksi

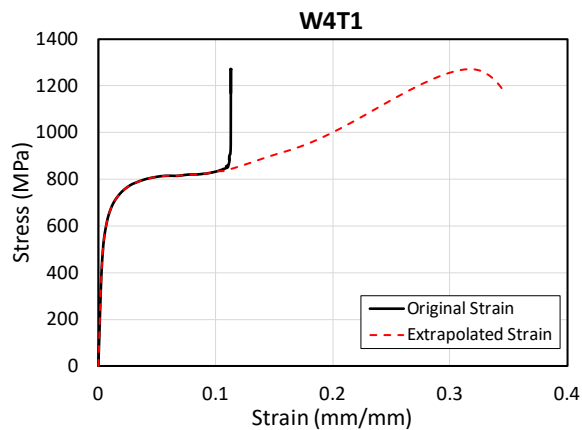
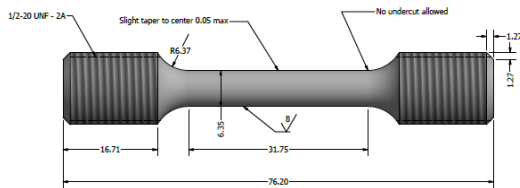
Max Stress: 1290 MPa
*Max Stress: 187.1 ksi
Strain at Max Stress: 0.106 mm/mm
Extrapolated Strain at Max Stress: 0.217 mm/mm

W3T5, tested at 4 K



U.S. Department of Commerce
National Institute of Standards and Technology
Materials Measurement Laboratory
Applied Chemicals and Materials Division
Fatigue and Fracture Group
Boulder, CO

Tensile Test - Specimen Report



* Converted from results in SI Units

Specimen ID: W4T1
Material/Condition: 316L Weld
Test Temperature: 77K

Test Date: 9/8/2021
Operator: Dash Weeks
Analysis Performed on: 06/30/2022

Test Frame: MTS 55KIP Cryo
Last Calibration: 2/3/2021
Instrumentation: Avg of 3 Extensometers
Last Calibration: 8/19/2021

Specimen Type: Round
Specimen Area: 31.7 mm²
Overall Length: 76.16 mm
Gage Length: 25.4 mm

Target Strain Rate: 0.015 mm/mm/min
Displacement Rate: 0.762 mm/min

Total Plastic Elongation: 34.2 %
Reduction of Area: 29.2 %

Modulus of Elasticity: 158 GPa
*Modulus of Elasticity: 22.9 Msi

Yield Stress at 0.5% Strain: 552 MPa
*Yield Stress at 0.5% Strain: 80.1 ksi

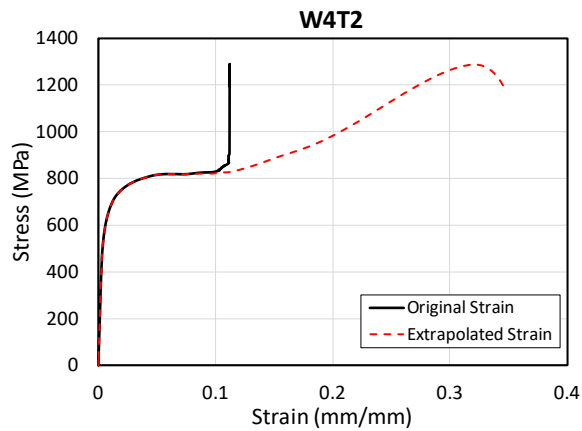
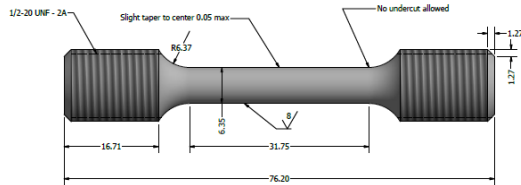
Max Stress: 1272 MPa
*Max Stress: 184.5 ksi
Strain at Max Stress: 0.113 mm/mm
Extrapolated Strain at Max Stress: 0.349 mm/mm

W4T1, tested at 77 K



U.S. Department of Commerce
National Institute of Standards and Technology
Materials Measurement Laboratory
Applied Chemicals and Materials Division
Fatigue and Fracture Group
Boulder, CO

Tensile Test - Specimen Report



* Converted from results in SI Units

Specimen ID: W4T2
Material/Condition: 316L Weld
Test Temperature: 77K

Test Date: 9/8/2021
Operator: Dash Weeks
Analysis Performed on: 06/30/2022

Test Frame: MTS 55KIP Cryo
Last Calibration: 2/3/2021
Instrumentation: Avg of 3 Extensometers
Last Calibration: 8/19/2021

Specimen Type: Round
Specimen Area: 31.76 mm²
Overall Length: 76.14 mm
Gage Length: 25.4 mm

Target Strain Rate: 0.015 mm/mm/min
Displacement Rate: 0.156 mm/min

Total Plastic Elongation: 34 %
Reduction of Area: 29.7 %

Modulus of Elasticity: 163 GPa
*Modulus of Elasticity: 23.6 Msi

Yield Stress at 0.5% Strain: 568 MPa
*Yield Stress at 0.5% Strain: 82.4 ksi

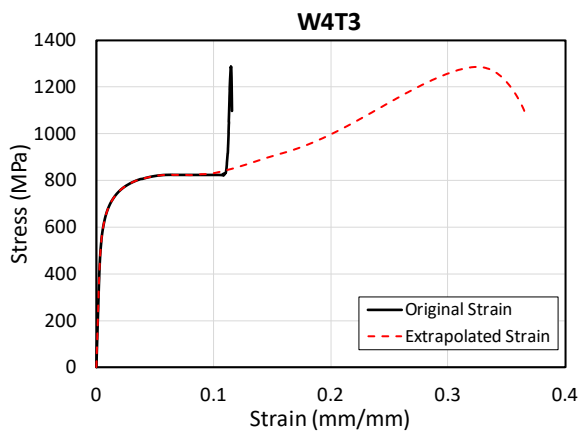
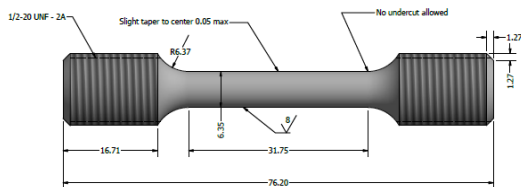
Max Stress: 1288 MPa
*Max Stress: 186.8 ksi
Strain at Max Stress: 0.112 mm/mm
Extrapolated Strain at Max Stress: 0.347 mm/mm

W4T2, tested at 77 K



U.S. Department of Commerce
National Institute of Standards and Technology
Materials Measurement Laboratory
Applied Chemicals and Materials Division
Fatigue and Fracture Group
Boulder, CO

Tensile Test - Specimen Report



* Converted from results in SI Units

Specimen ID: W4T3
Material/Condition: 316L Weld
Test Temperature: 77K

Test Date: 9/8/2021
Operator: Dash Weeks
Analysis Performed on: 06/30/2022

Test Frame: MTS 55KIP Cryo
Last Calibration: 2/3/2021
Instrumentation: Avg of 3 Extensometers
Last Calibration: 8/19/2021

Specimen Type: Round
Specimen Area: 31.71 mm²
Overall Length: 76.14 mm
Gage Length: 25.4 mm

Target Strain Rate: 0.015 mm/mm/min
Displacement Rate: 0.762 mm/min

Total Plastic Elongation: 36 %
Reduction of Area: 35.1 %

Modulus of Elasticity: 163 GPa
*Modulus of Elasticity: 23.6 Msi

Yield Stress at 0.5% Strain: 575 MPa
*Yield Stress at 0.5% Strain: 83.4 ksi

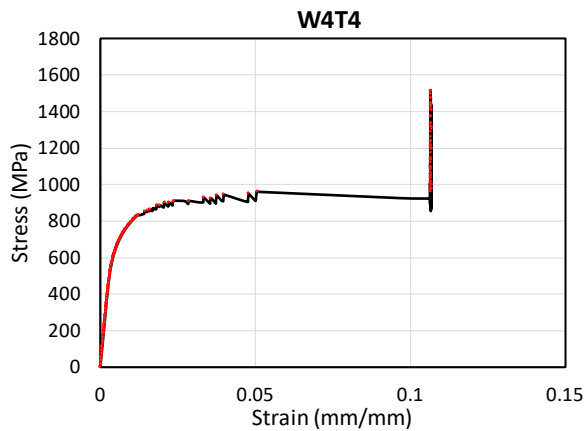
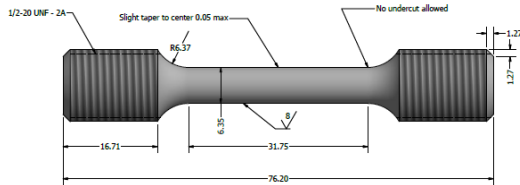
Max Stress: 1286 MPa
*Max Stress: 186.5 ksi
Strain at Max Stress: 0.115 mm/mm
Extrapolated Strain at Max Stress: 0.367 mm/mm

W4T3, tested at 77 K



U.S. Department of Commerce
National Institute of Standards and Technology
Materials Measurement Laboratory
Applied Chemicals and Materials Division
Fatigue and Fracture Group
Boulder, CO

Tensile Test - Specimen Report



* Converted from results in SI Units

Specimen ID: W4T4
Material/Condition: 316L Weld
Test Temperature: 4K

Test Date: 9/28/2021
Operator: Dash Weeks
Analysis Performed on: 07/01/2022

Test Frame: MTS 55KIP Cryo
Last Calibration: 2/3/2021
Instrumentation: Avg of 3 Extensometers
Last Calibration: 8/19/2021

Specimen Type: Round
Specimen Area: 31.69 mm²
Overall Length: 76.14 mm
Gage Length: 25.4 mm

Target Strain Rate: 0.015 mm/mm/min
Displacement Rate: 0.762 mm/min

Total Plastic Elongation: 18.4 %
Reduction of Area: 21.1 %

Modulus of Elasticity: 177 GPa
*Modulus of Elasticity: 25.7 Msi

Yield Stress at 0.5% Strain: 651 MPa
*Yield Stress at 0.5% Strain: 94.4 ksi

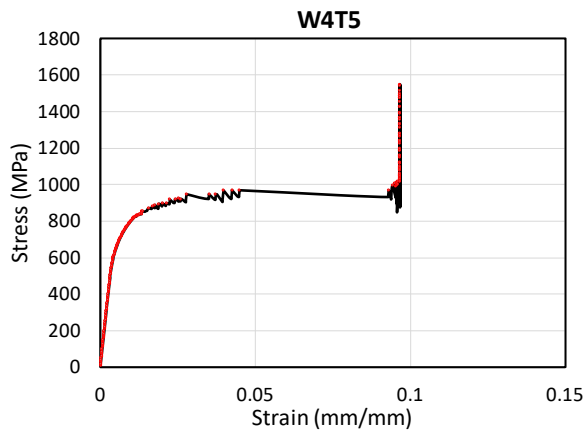
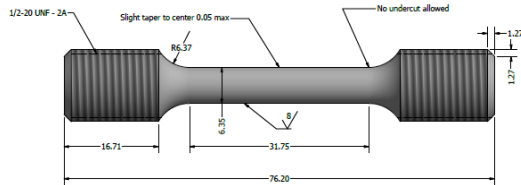
Max Stress: 1517 MPa
*Max Stress: 220 ksi
Strain at Max Stress: 0.107 mm/mm
Extrapolated Strain at Max Stress: 0.193 mm/mm

W4T4, tested at 4 K



U.S. Department of Commerce
National Institute of Standards and Technology
Materials Measurement Laboratory
Applied Chemicals and Materials Division
Fatigue and Fracture Group
Boulder, CO

Tensile Test - Specimen Report



* Converted from results in SI Units

Specimen ID: W4T5
Material/Condition: 316L Weld
Test Temperature: 4K

Test Date: 9/28/2021
Operator: Dash Weeks
Analysis Performed on: 06/27/2022

Test Frame: MTS 55KIP Cryo
Last Calibration: 2/3/2021
Instrumentation: Avg of 3 Extensometers
Last Calibration: 8/19/2021

Specimen Type: Round
Specimen Area: 31.78 mm²
Overall Length: 76.15 mm
Gage Length: 25.4 mm

Target Strain Rate: 0.015 mm/mm/min
Displacement Rate: 0.762 mm/min

Total Plastic Elongation: 31.2 %
Reduction of Area: 27.4 %

Modulus of Elasticity: 155 GPa
*Modulus of Elasticity: 22.5 Msi

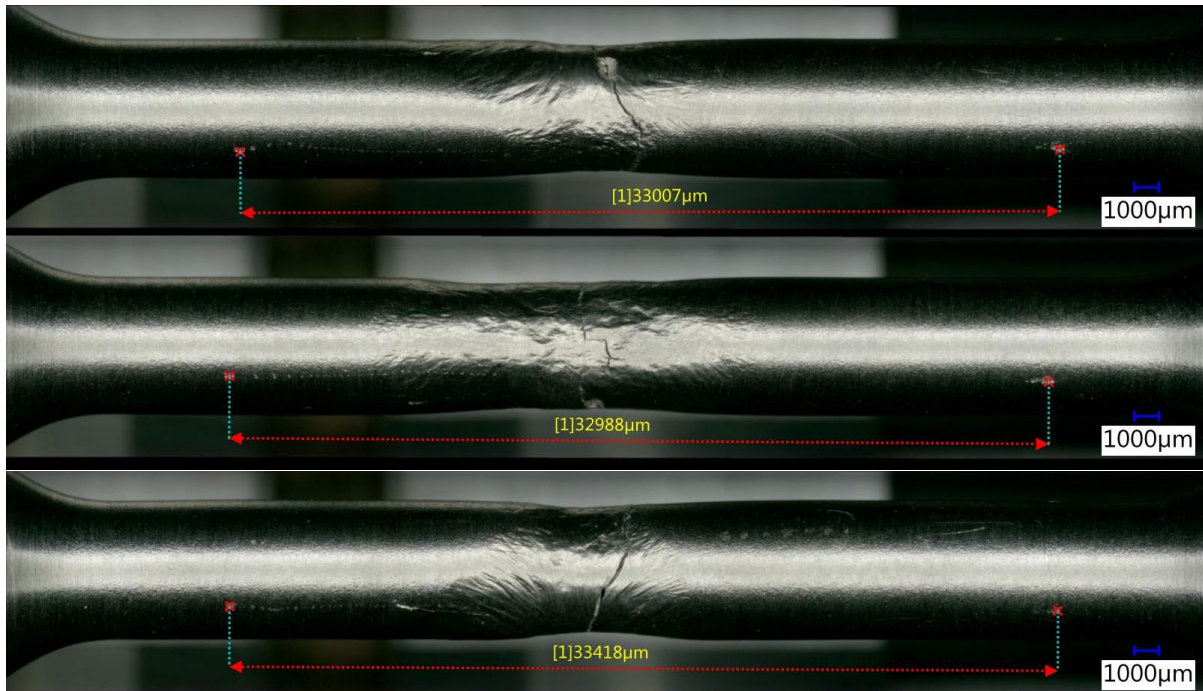
Yield Stress at 0.5% Strain: 645 MPa
*Yield Stress at 0.5% Strain: 93.5 ksi

Max Stress: 1550 MPa
*Max Stress: 224.8 ksi
Strain at Max Stress: 0.097 mm/mm
Extrapolated Strain at Max Stress: 0.322 mm/mm

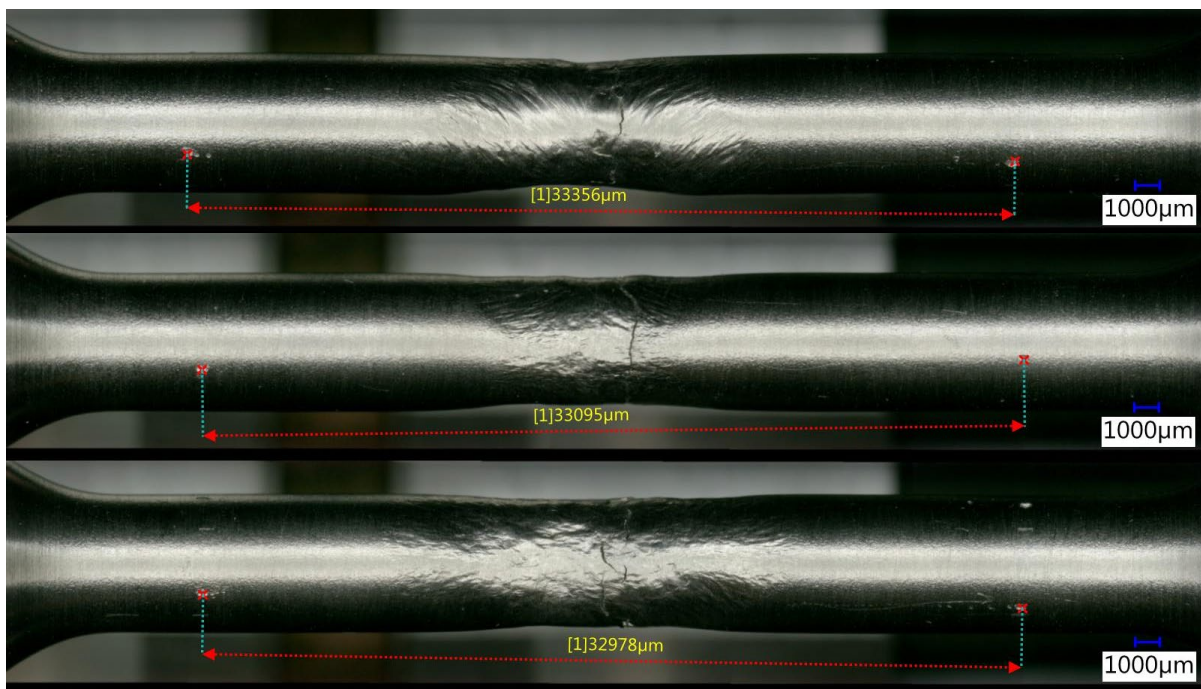
W4T5, tested at 4 K

Appendix D: Digital images used to measure total elongation

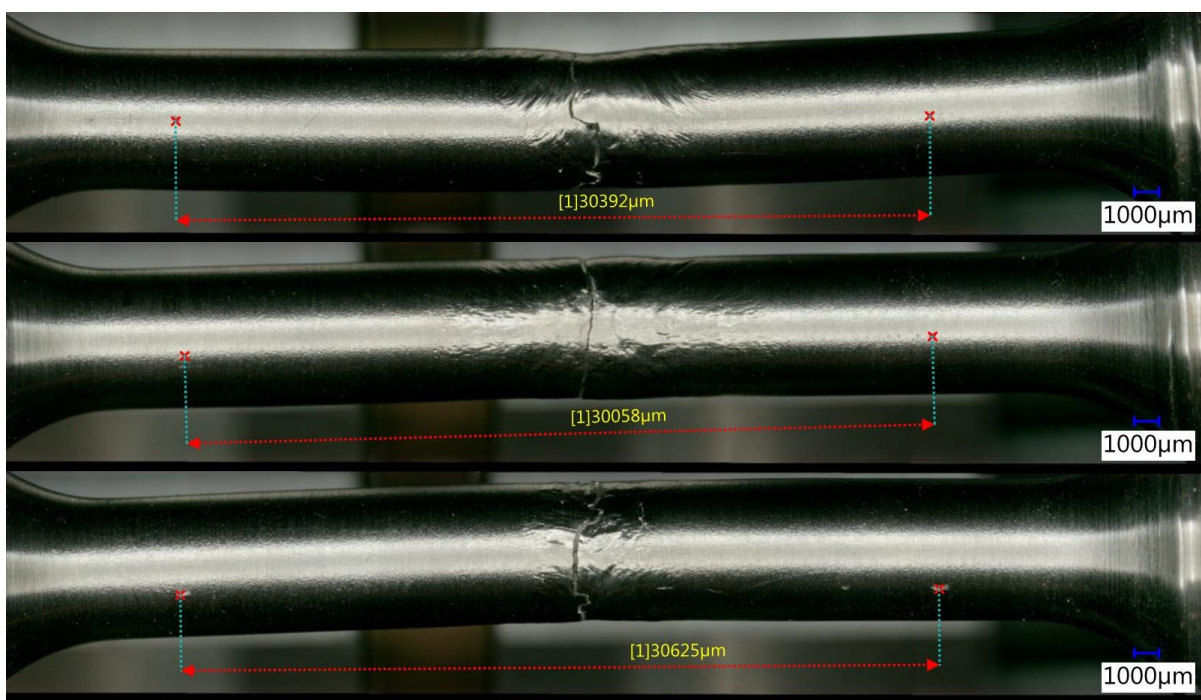
The gage length, or initial separation of the three sets of markings produced by the extensometer clamp, is 25.4 mm. Images were recorded of each marking pair (three per specimen) and measured (units are microns). For example, the first image of W1T1 shows a separation of 33,007 μm or 33.007 mm.



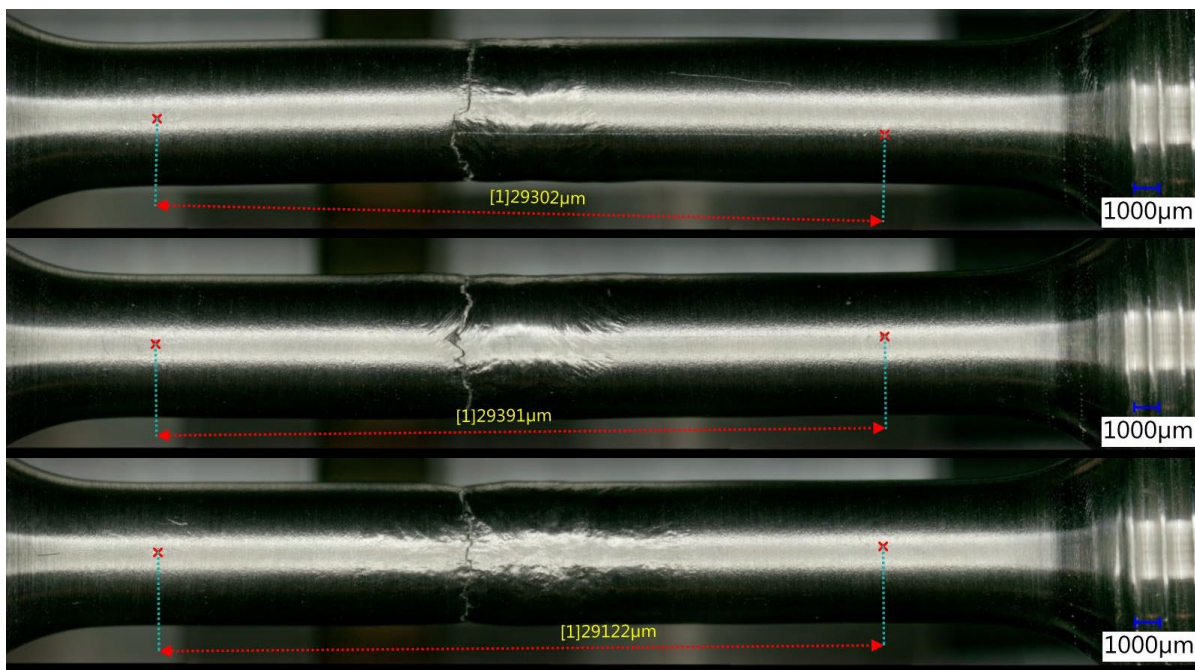
W1T1, tested at 77 K



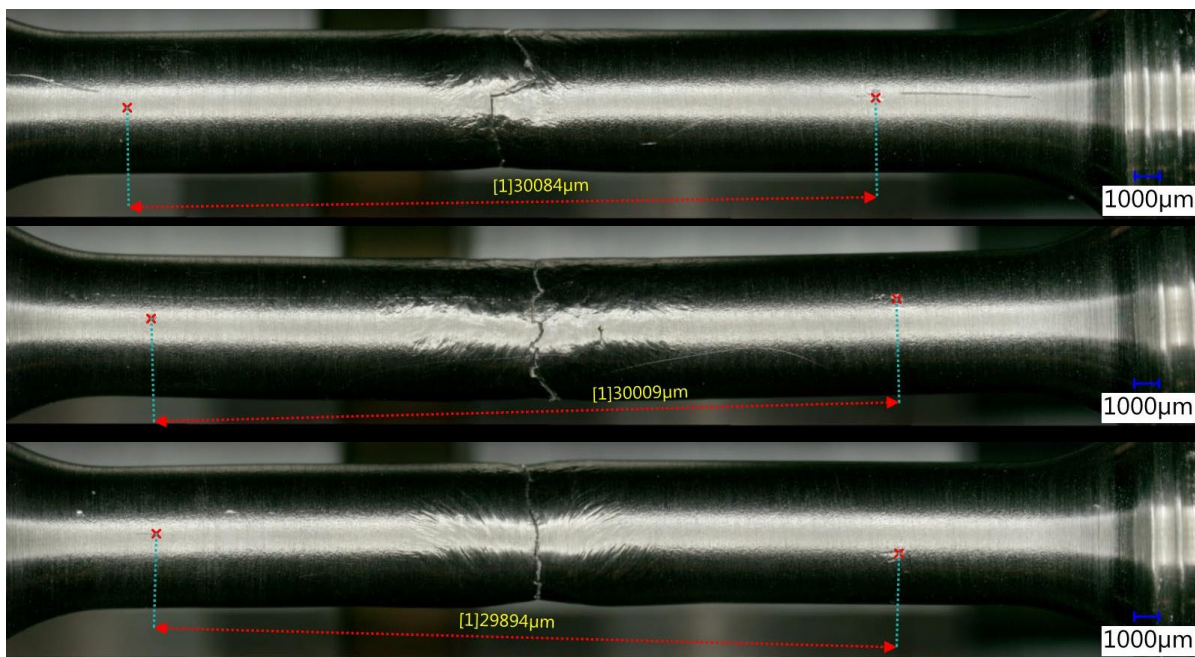
W1T2, tested at 77 K



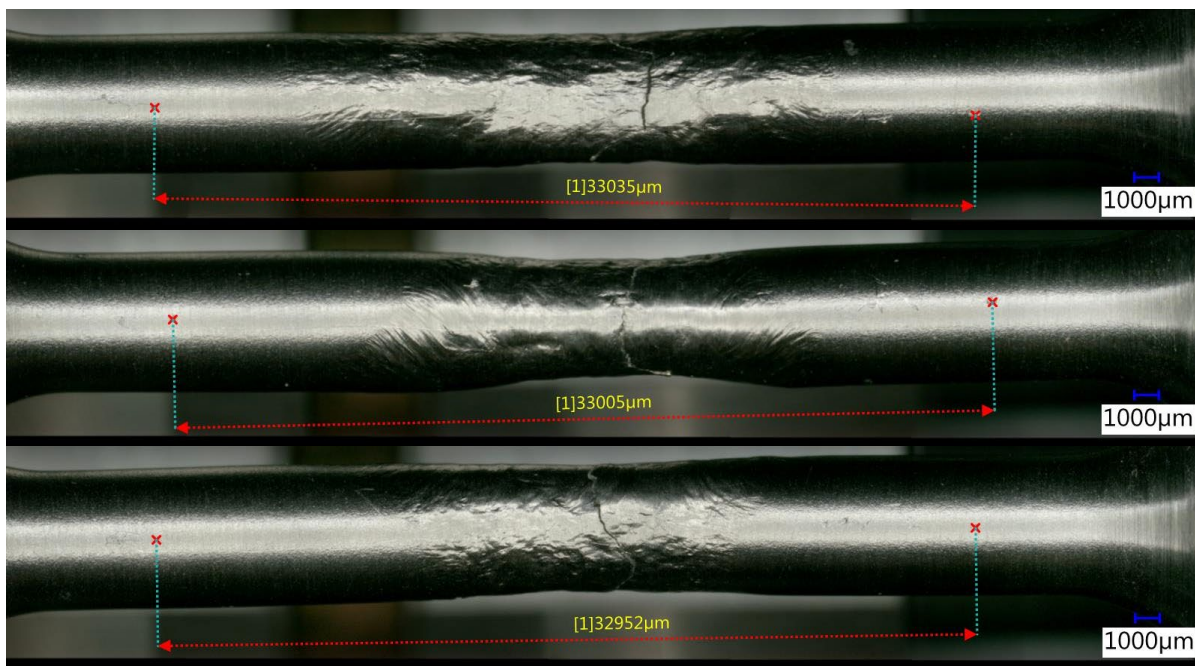
W1T3, tested at 77 K



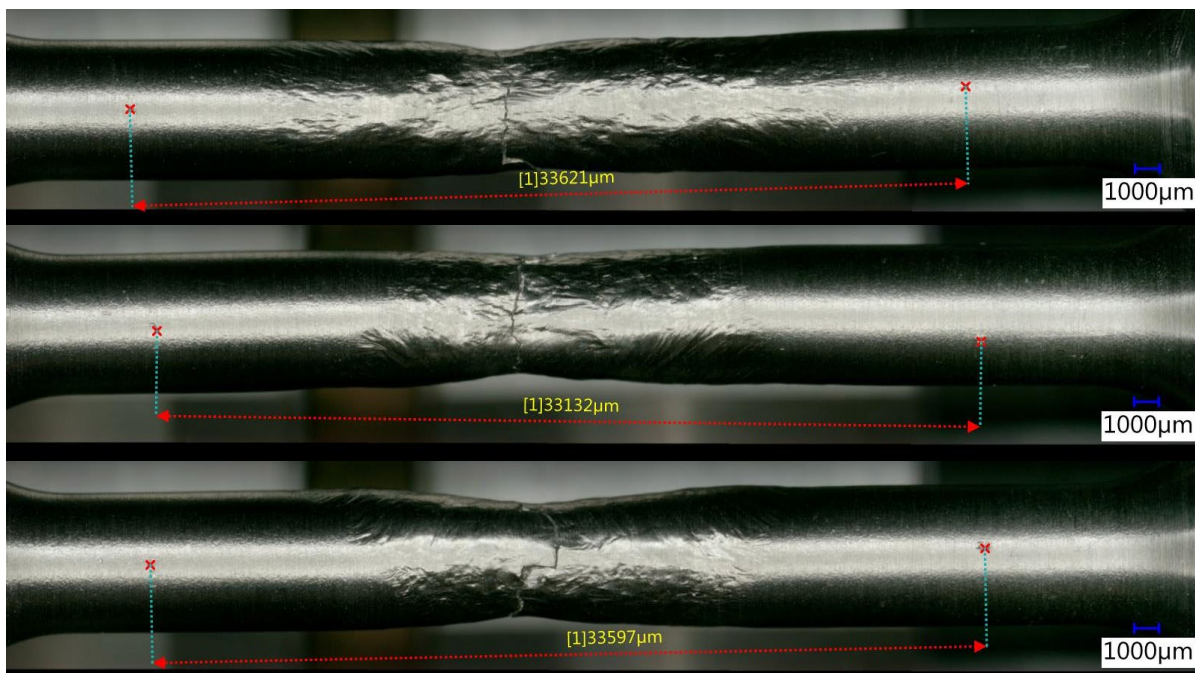
W1T5, tested at 4 K



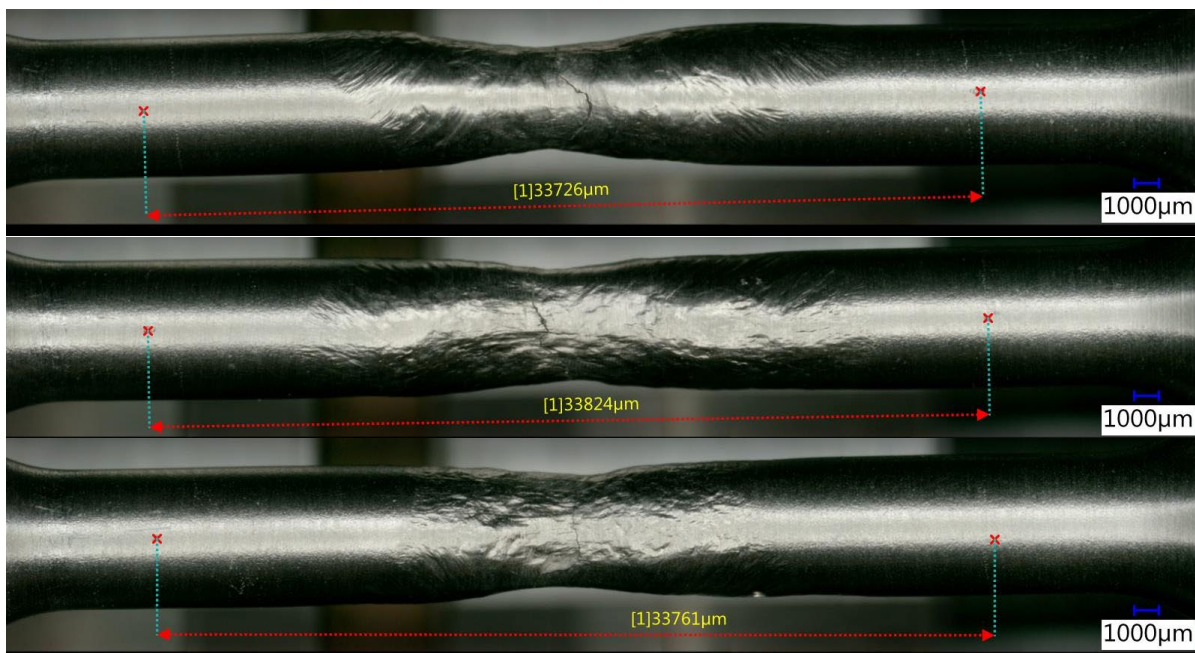
W1T6, tested at 4 K



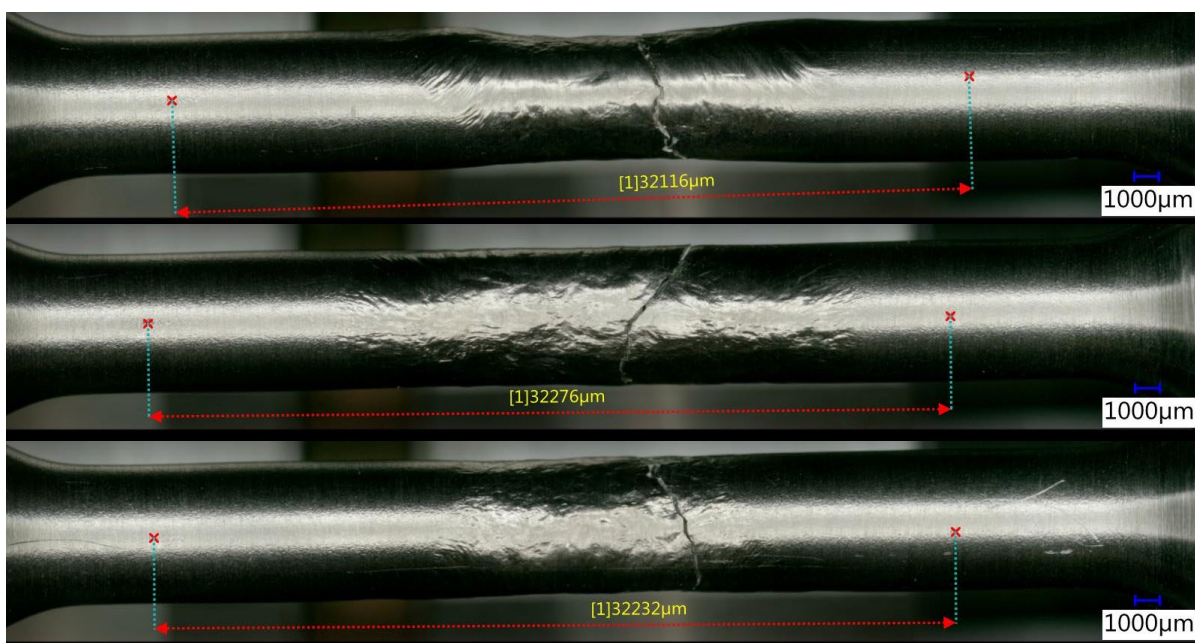
W2T1, tested at 77 K



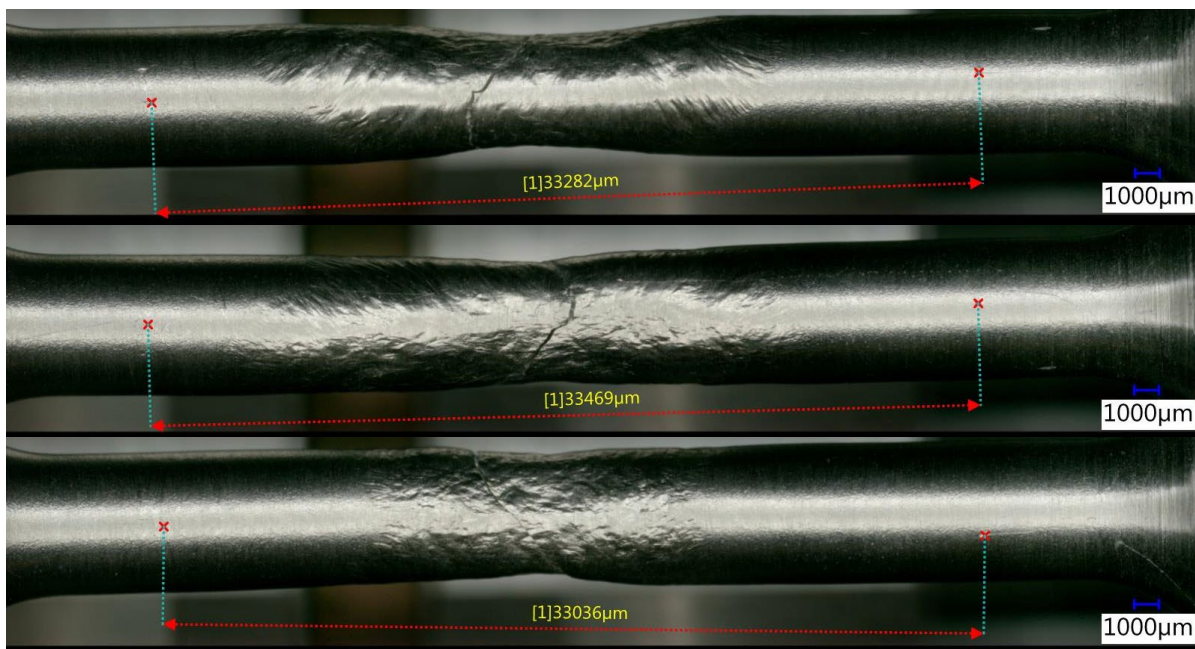
W2T2, tested at 77 K



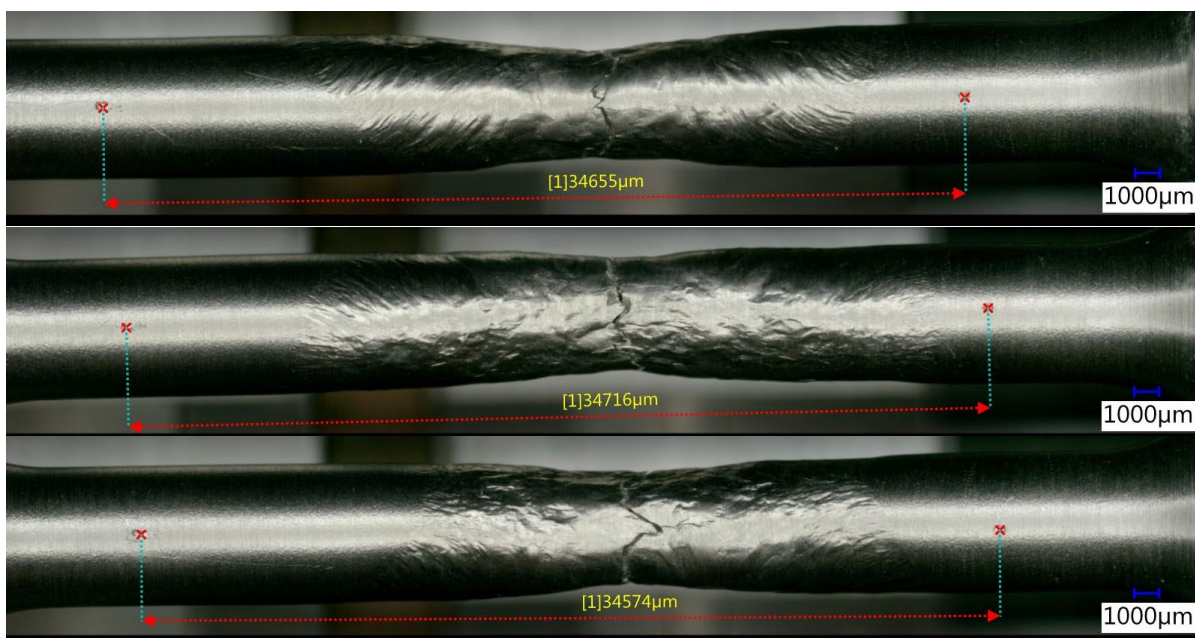
W2T3, tested at 77 K



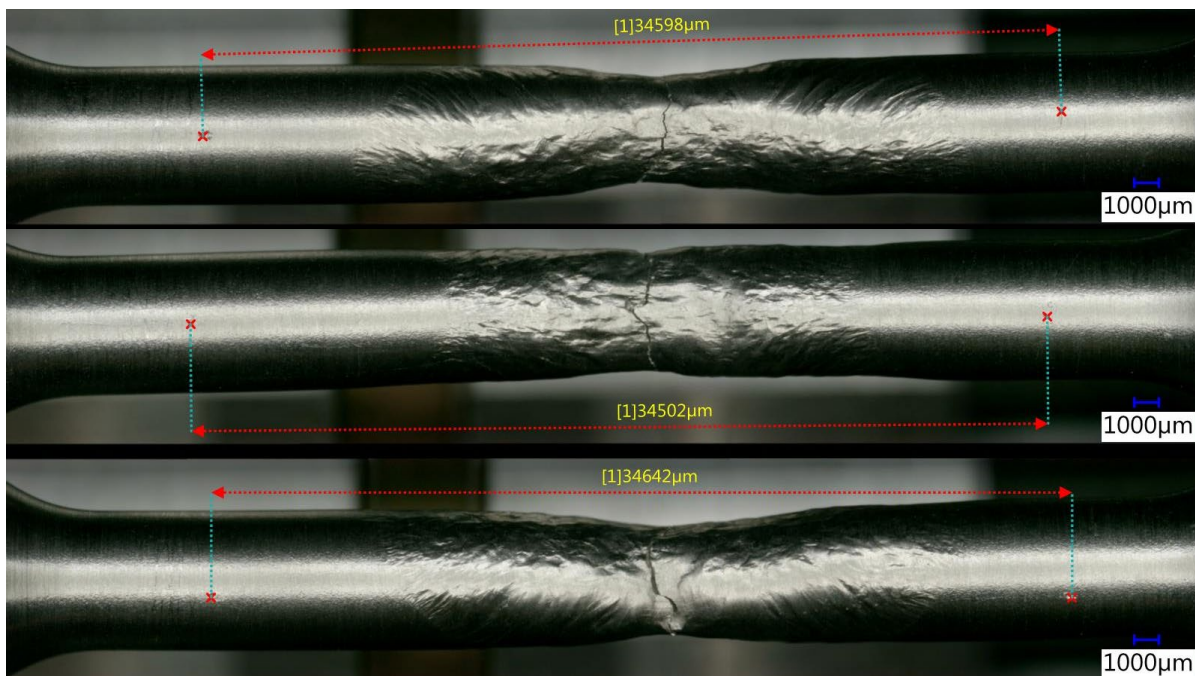
W2T4, tested at 4 K



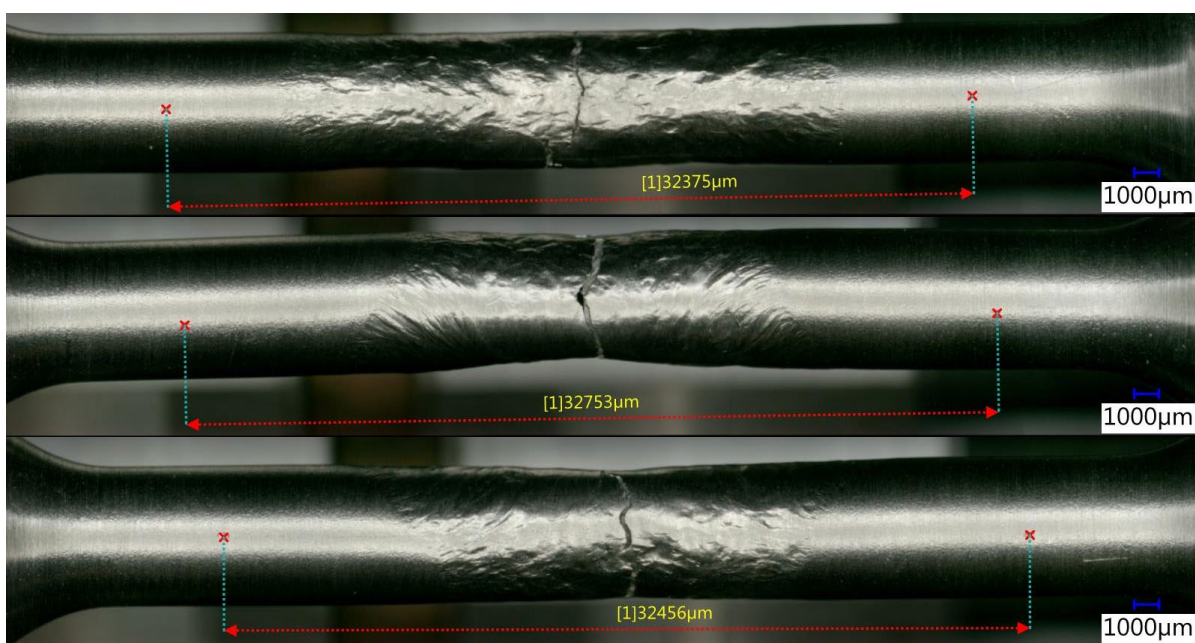
W2T5, tested at 4 K



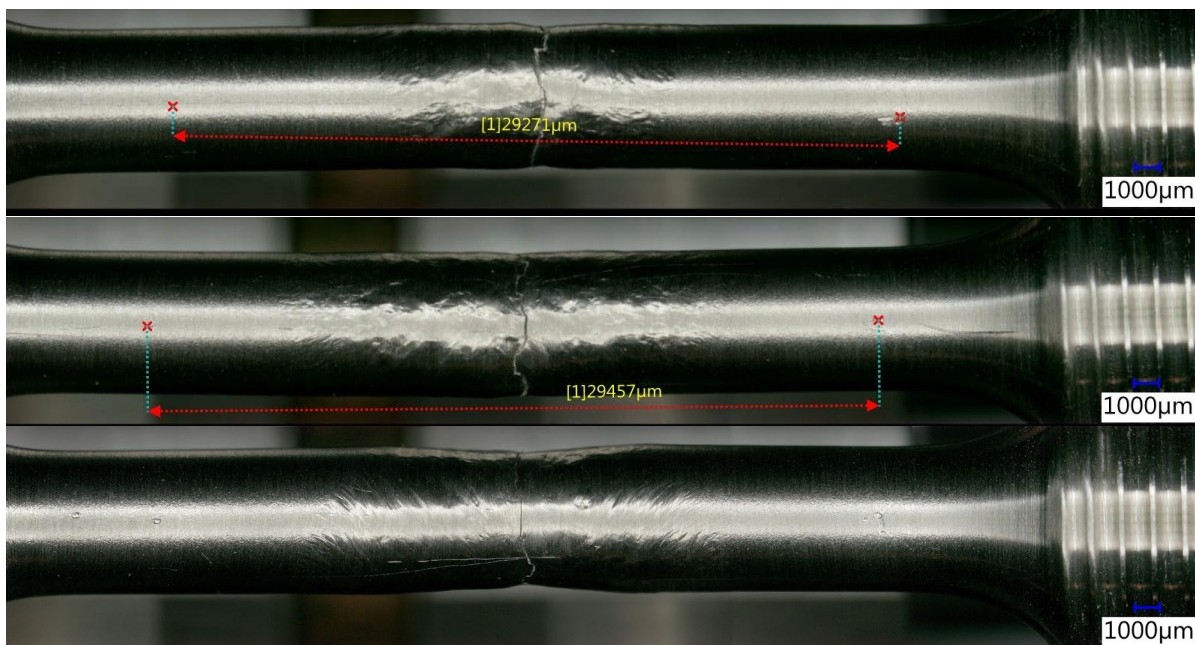
W3T1, tested at 77 K



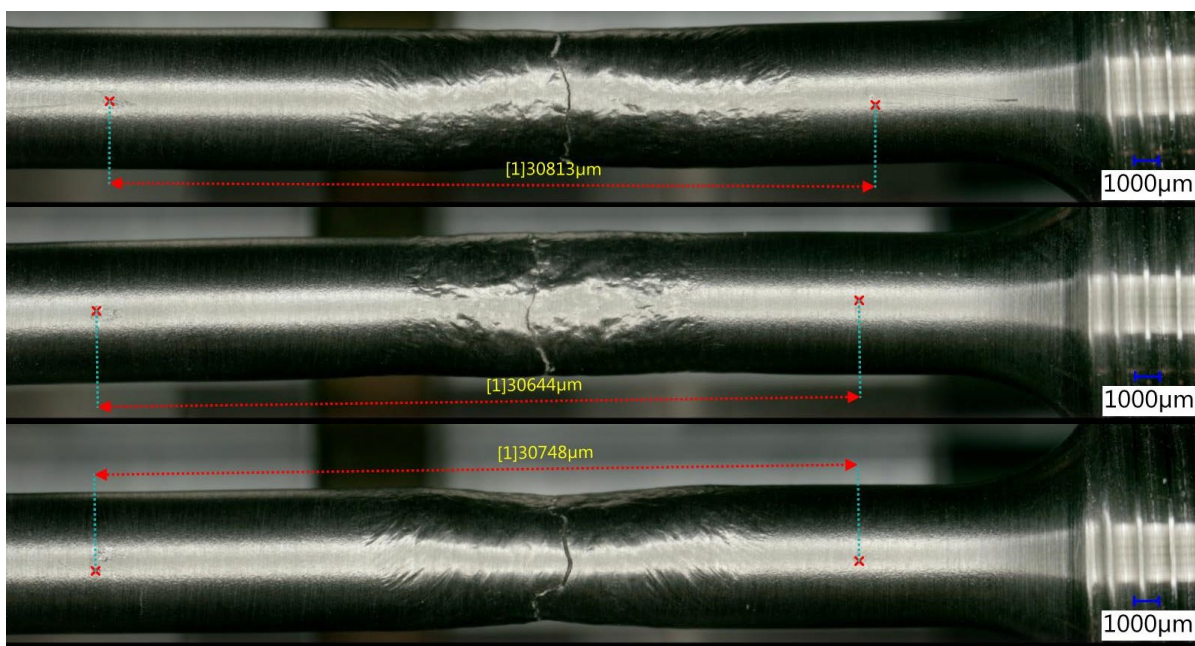
W3T2, tested at 77 K



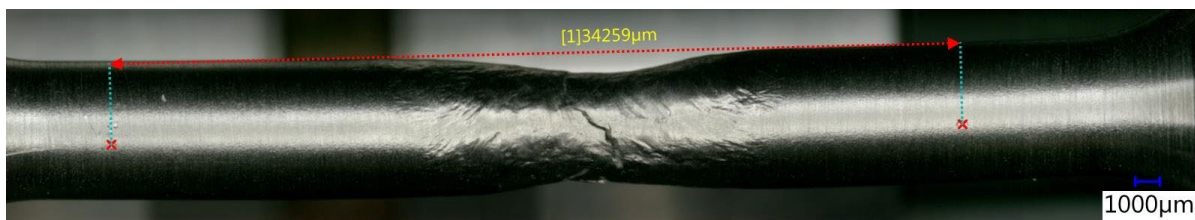
W3T3, tested at 77 K

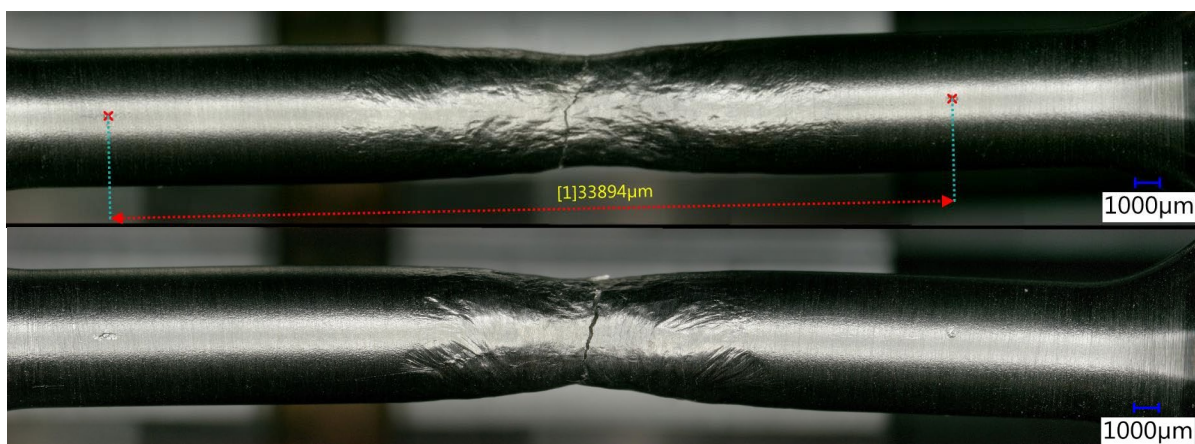


W3T4, tested at 4 K

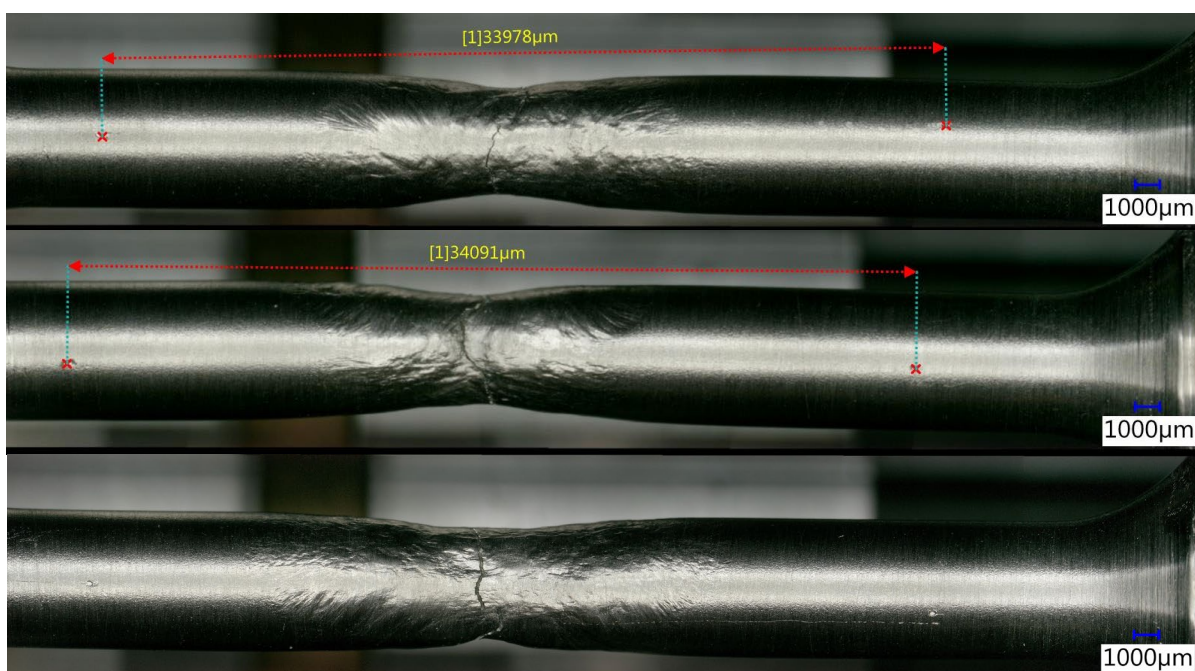


W3T5, tested at 4 K

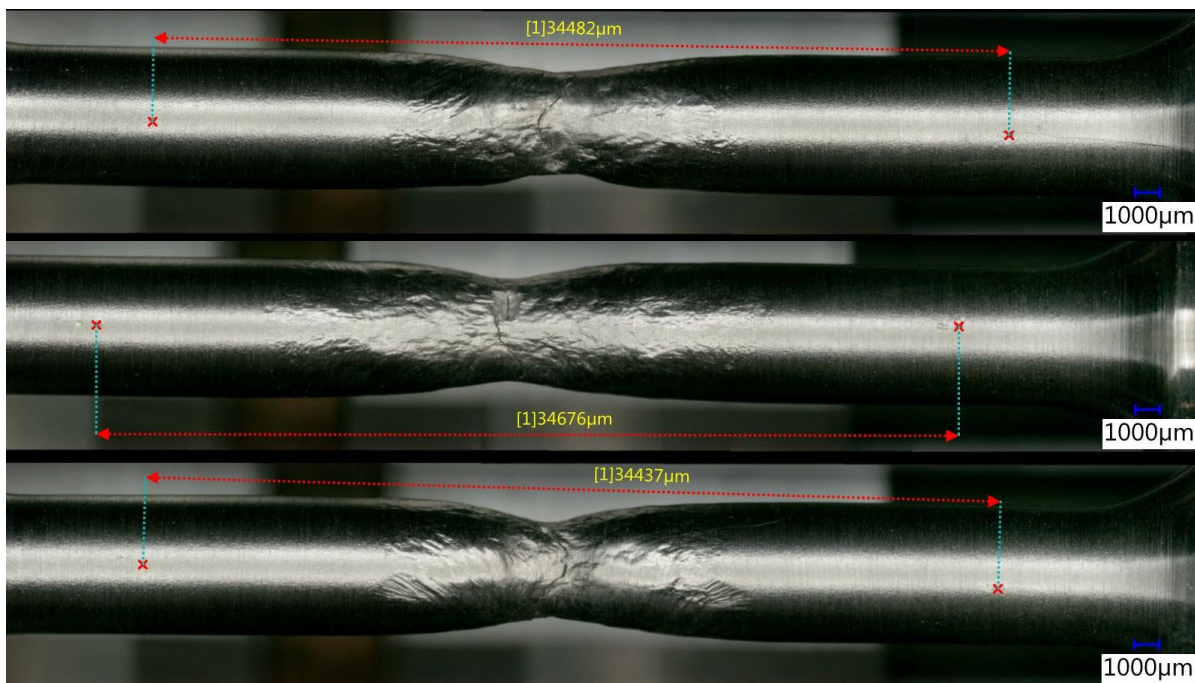




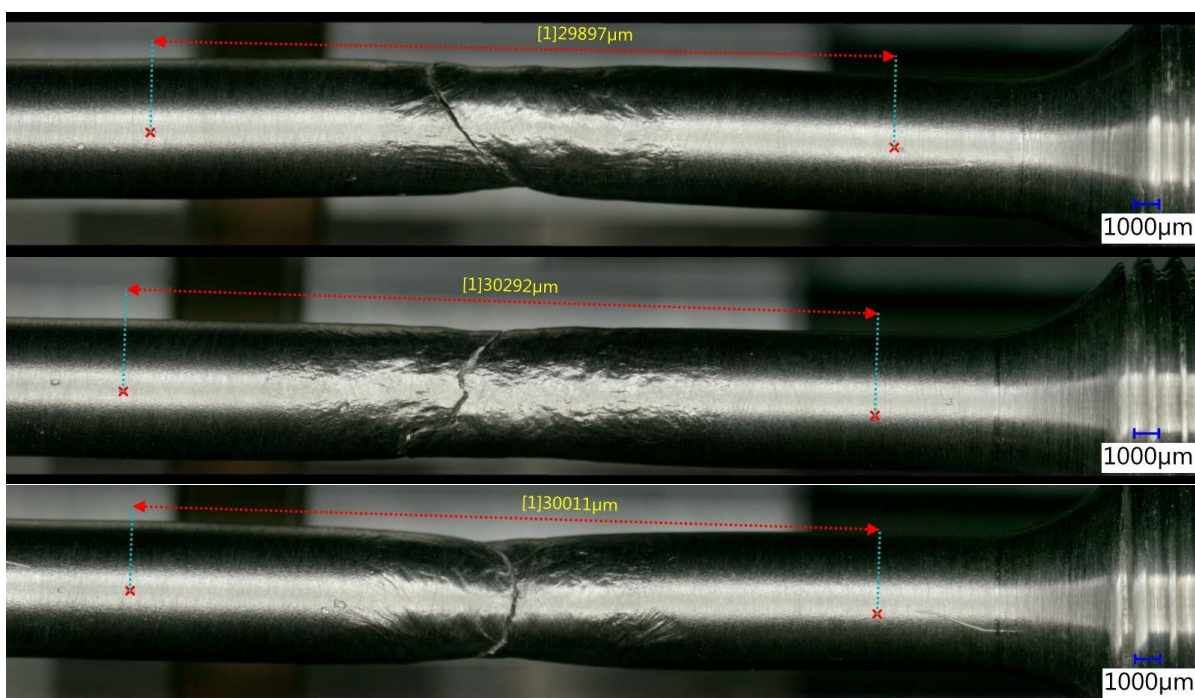
W4T1, tested at 77 K



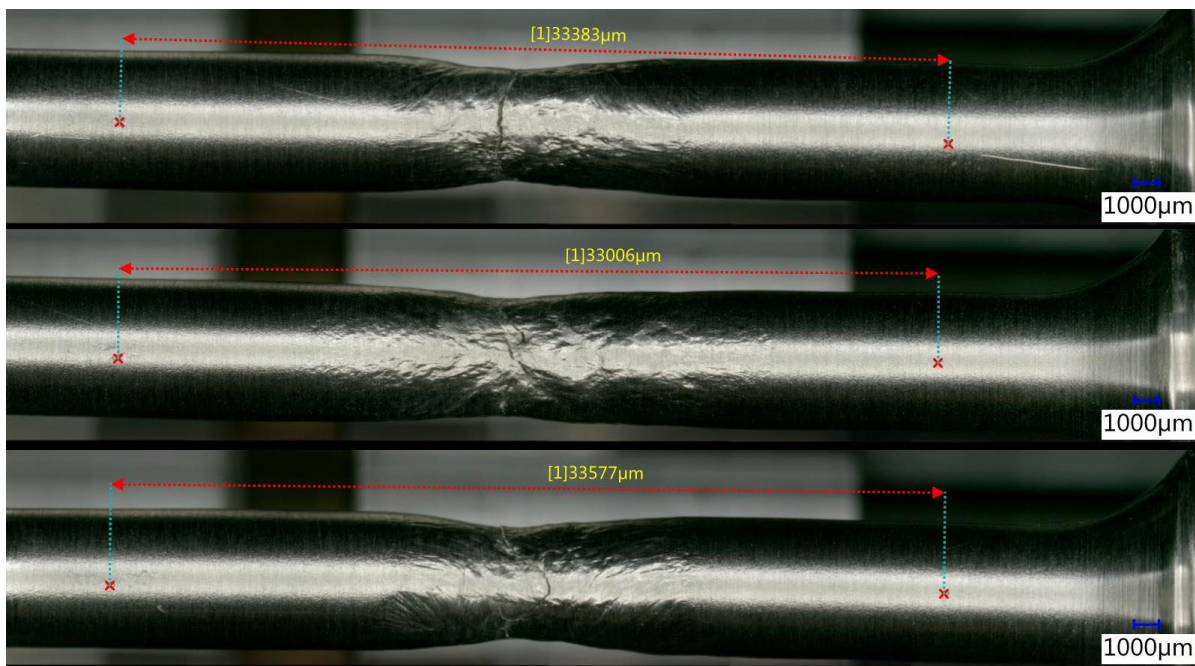
W4T2, tested at 77 K



W4T3, tested at 77 K



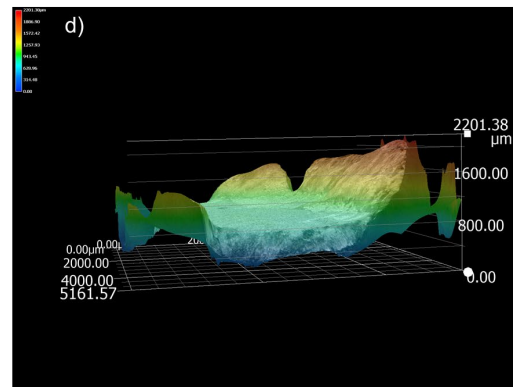
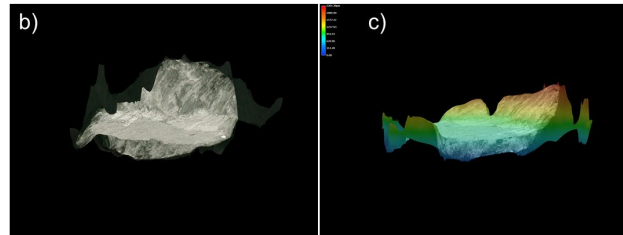
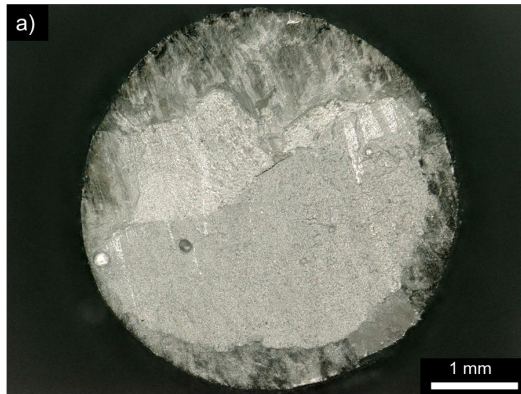
W4T4, tested at 4 K



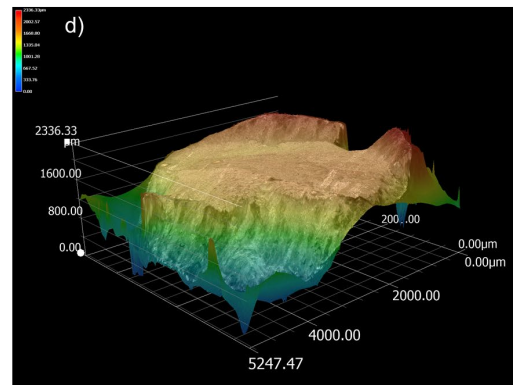
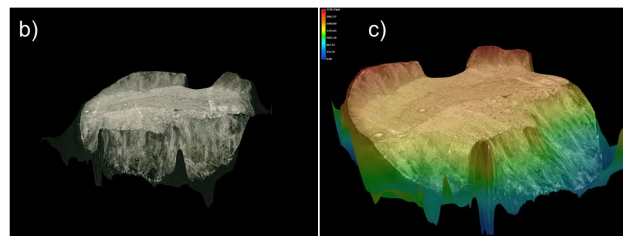
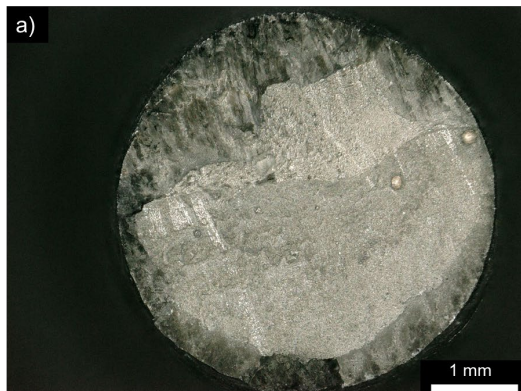
W4T5, tested at 4 K

Appendix E: Additional fractography: Optical images

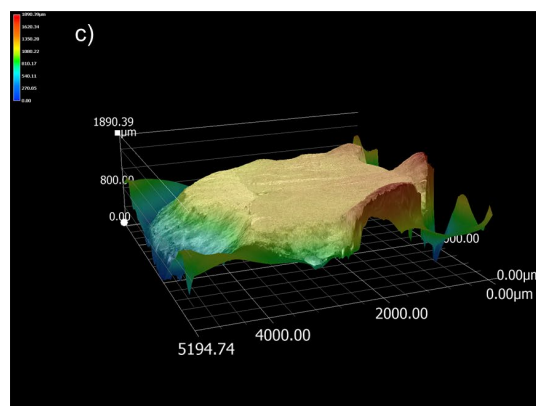
Weld 1 | T1 | 77K



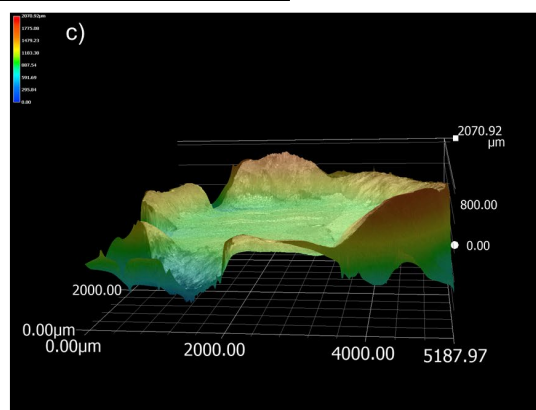
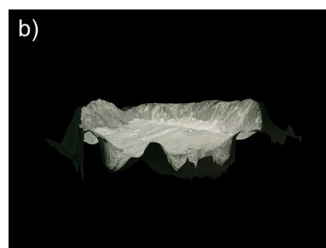
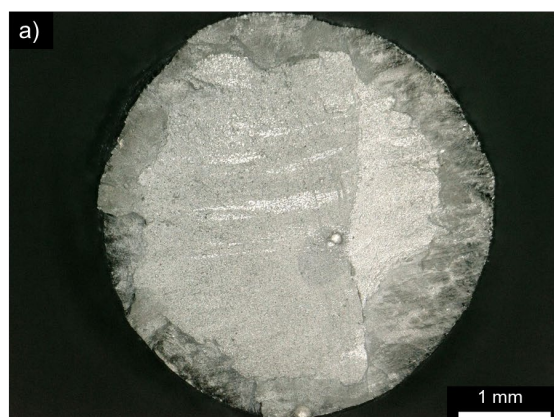
Weld 1 | T1 | 77K | Dot



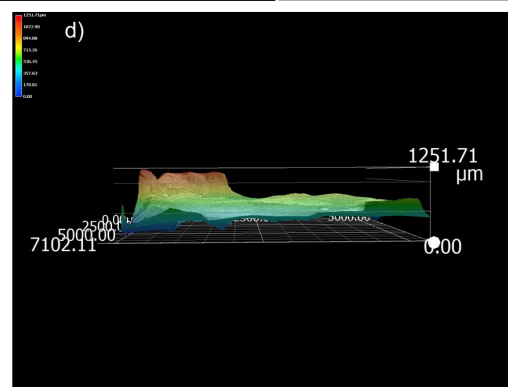
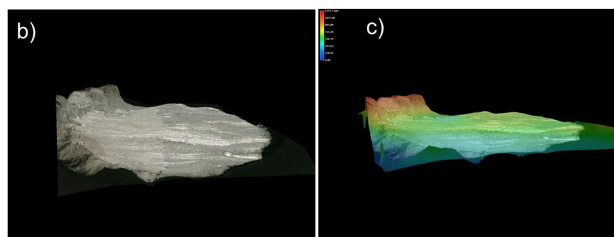
Weld 1 | T2 | 77 K



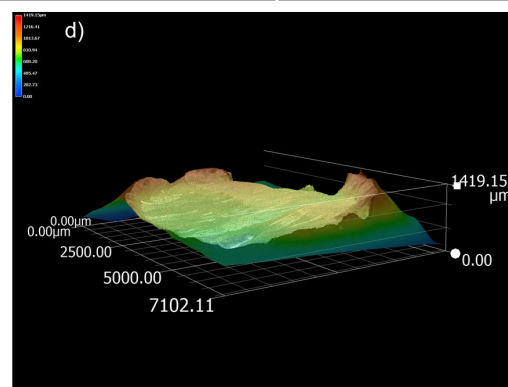
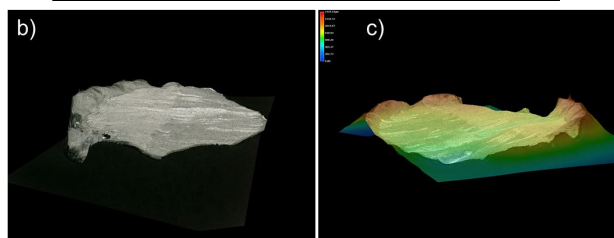
Weld 1 | T2 | 77 K | Dot



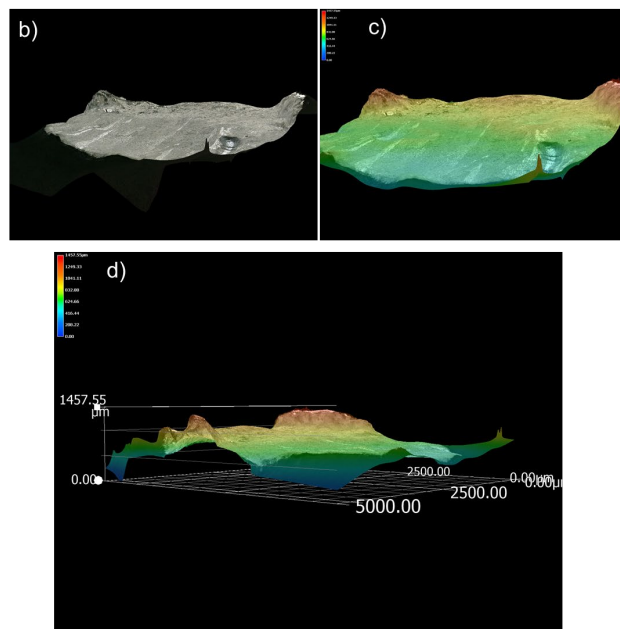
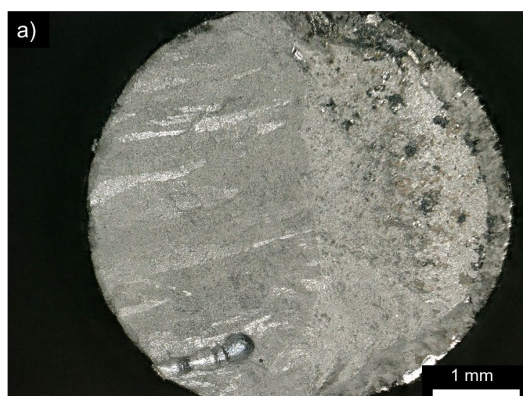
Weld 1 | T3 | 77 K



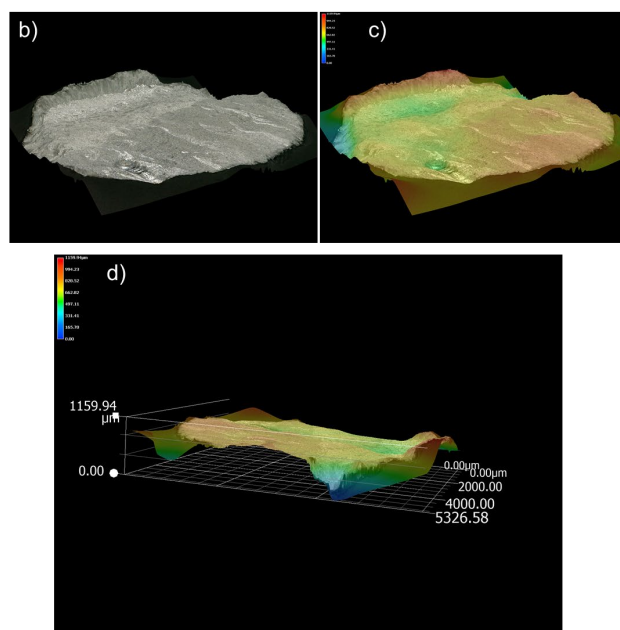
Weld 1 | T3 | 77 K | Dot



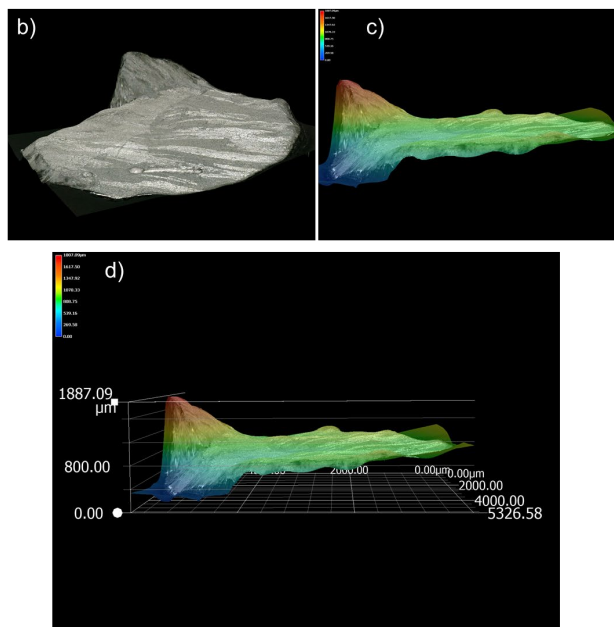
Weld 1 | T5 | 4 K



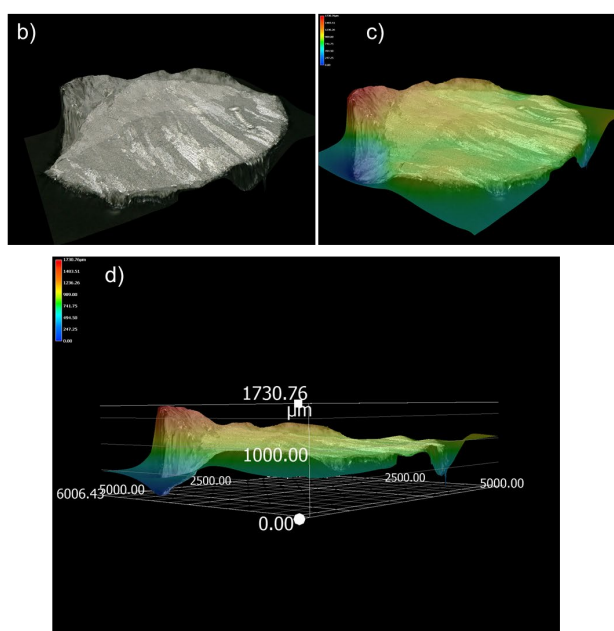
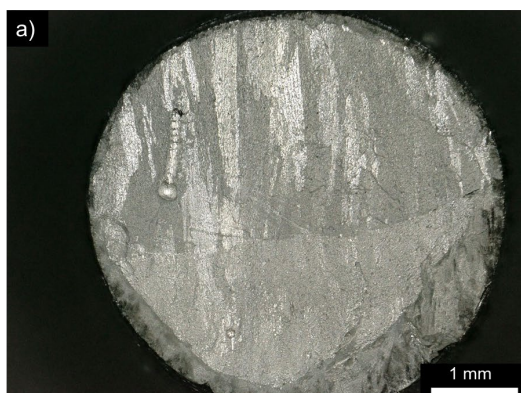
Weld 1 | T5 | 4 K | Dot



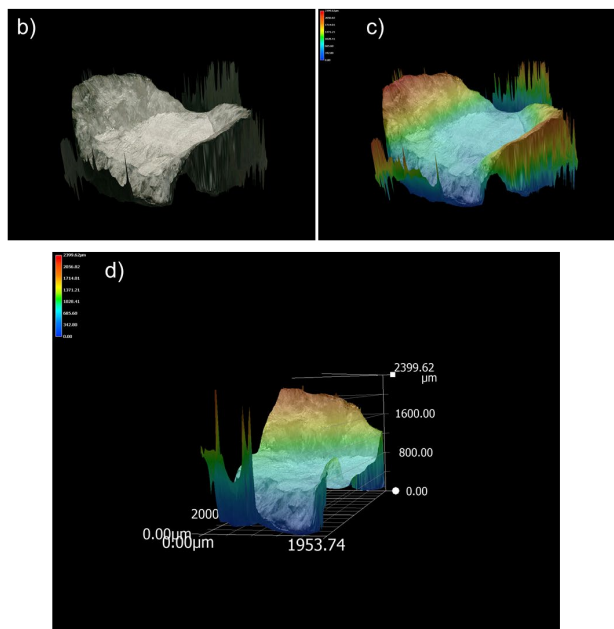
Weld 1 | T6 | 4 K



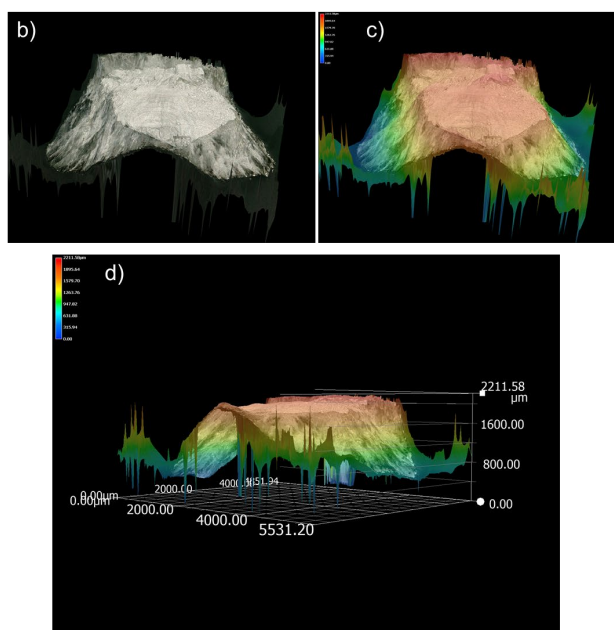
Weld 1 | T6 | 4 K | Dot



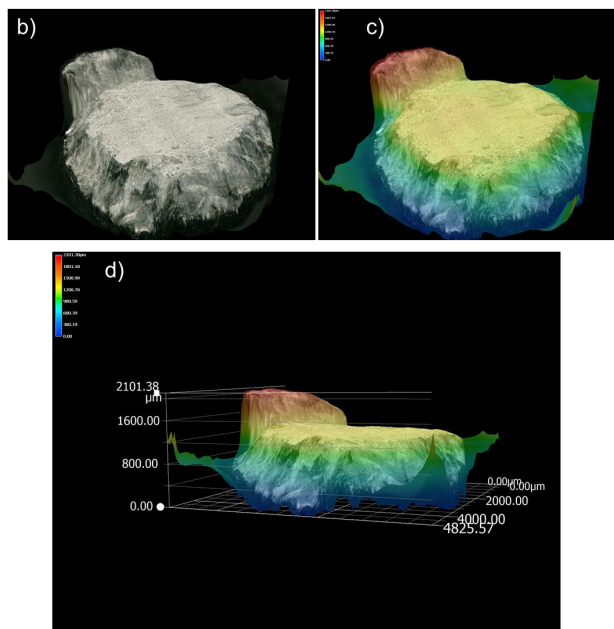
Weld 2 | T1 | 77 K



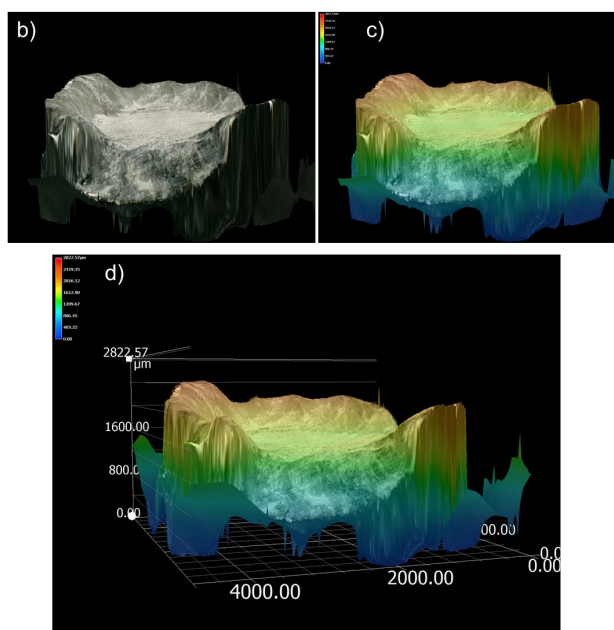
Weld 2 | T1 | 77 K | Dot



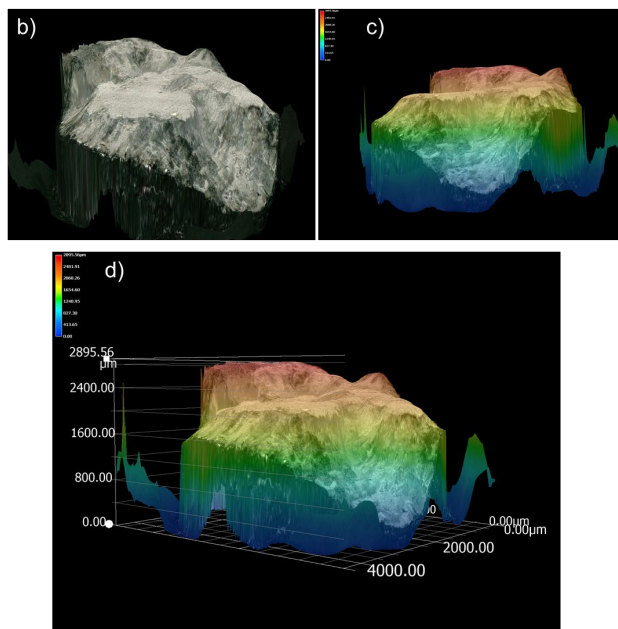
Weld 2 | T2 | 77 K



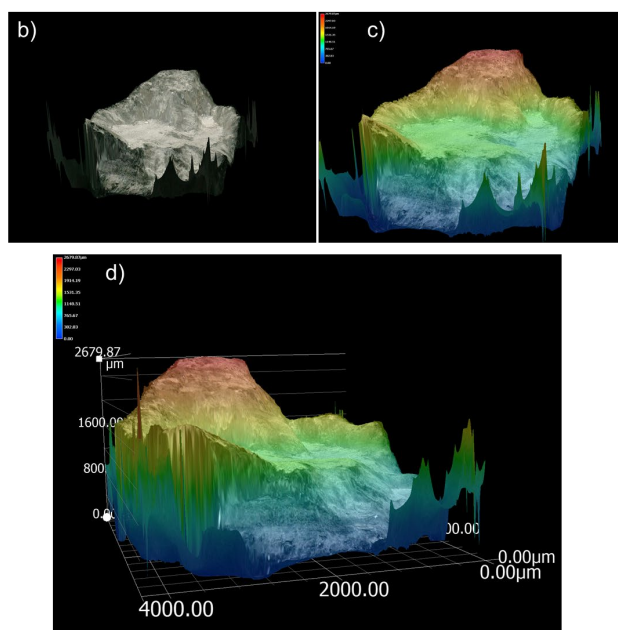
Weld 2 | T2 | 77 K | Dot



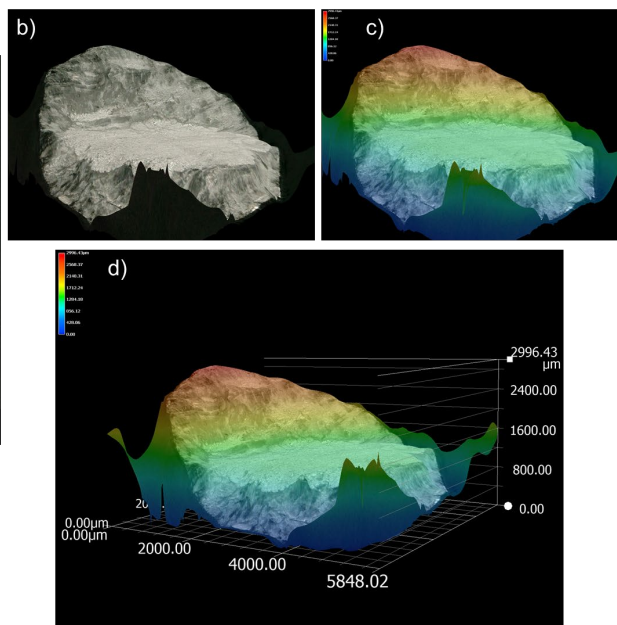
Weld 2 | T3 | 77 K



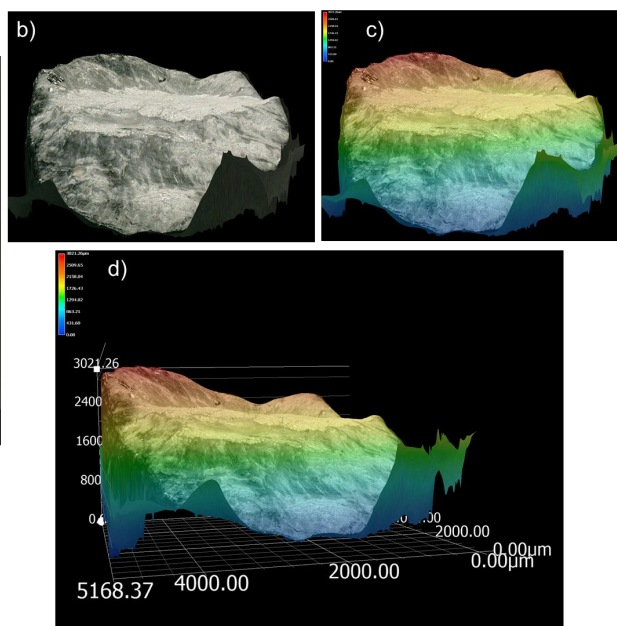
Weld 2 | T3 | 77 K | Dot



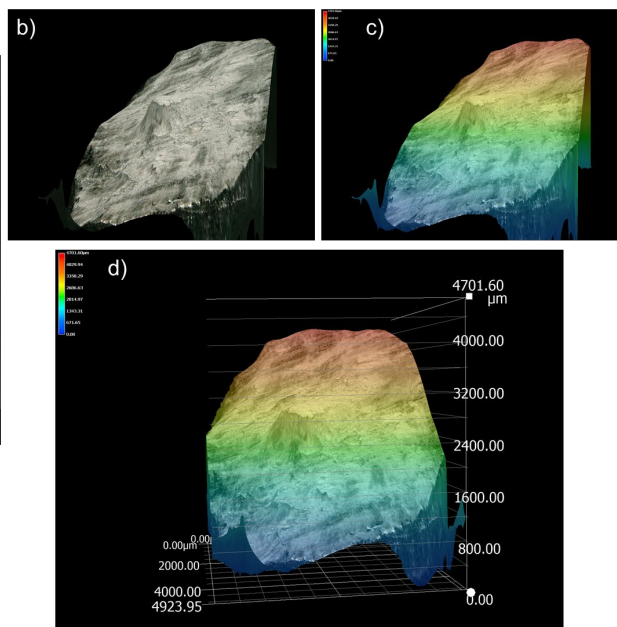
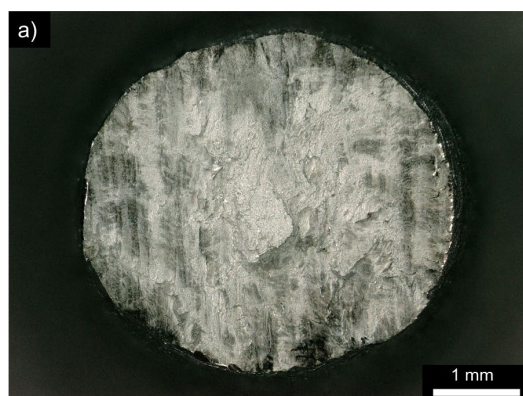
Weld 2 | T4 | 4 K



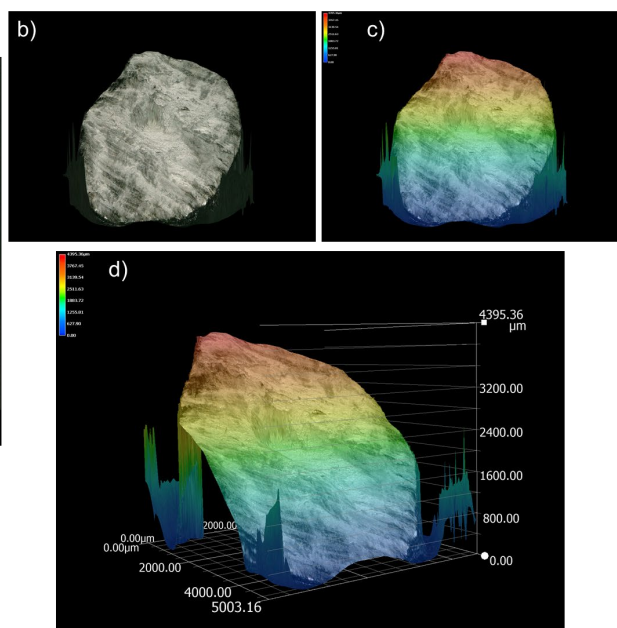
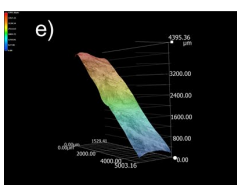
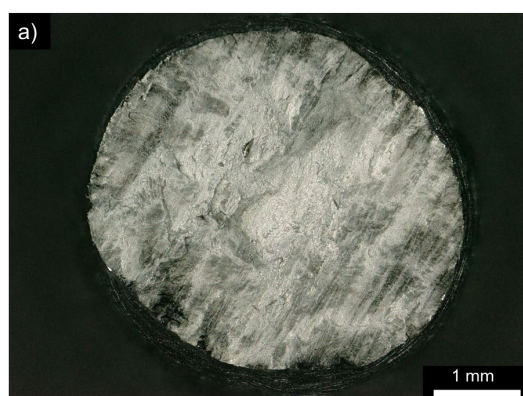
Weld 2 | T4 | 4 K | Dot



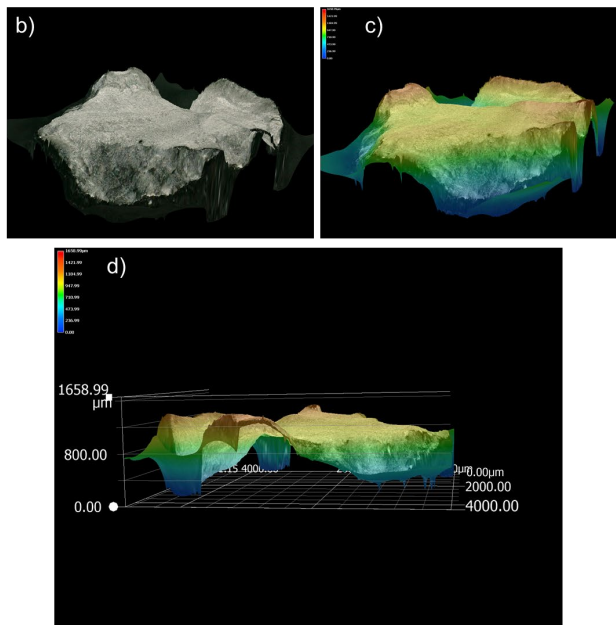
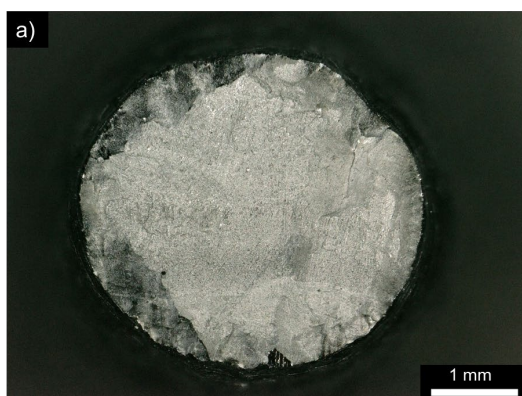
Weld 2 | T5 | 4 K



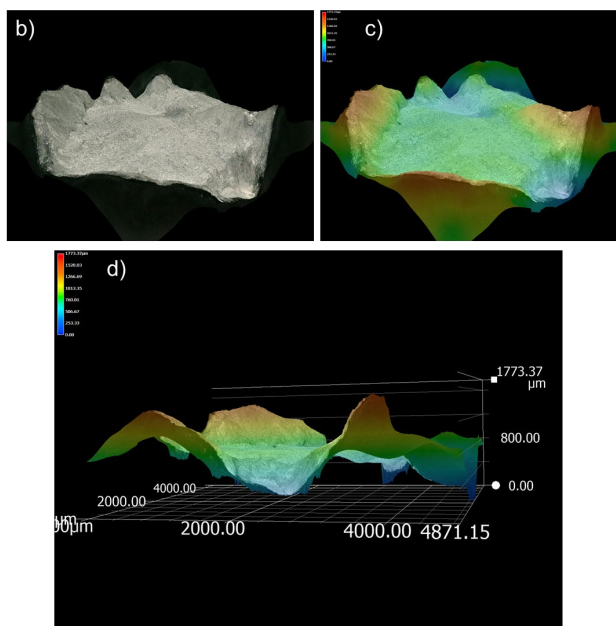
Weld 2 | T5 | 4 K | Dot



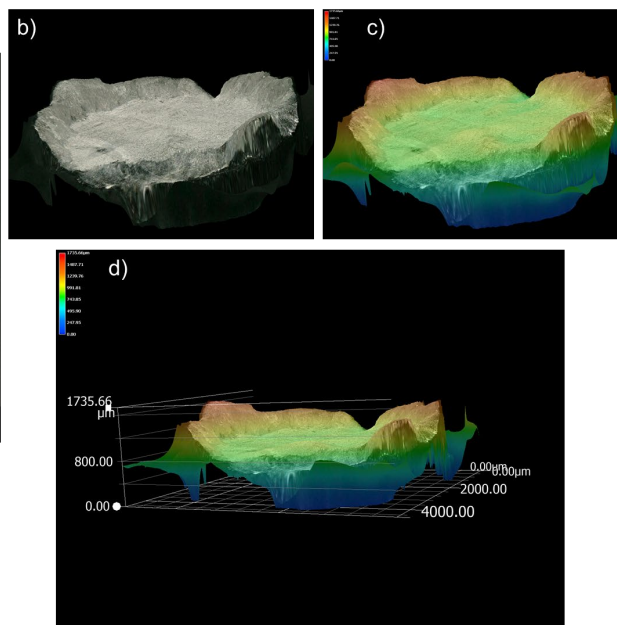
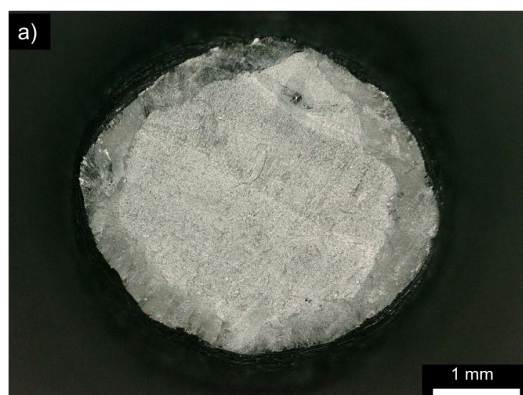
Weld 3 | T1 | 77 K



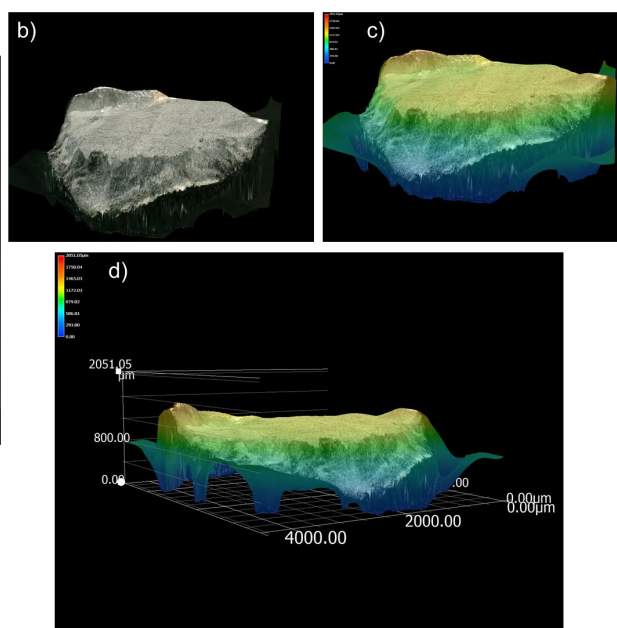
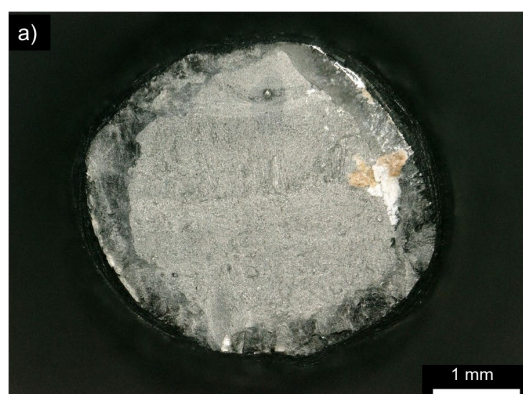
Weld 3 | T1 | 77 K | Dot



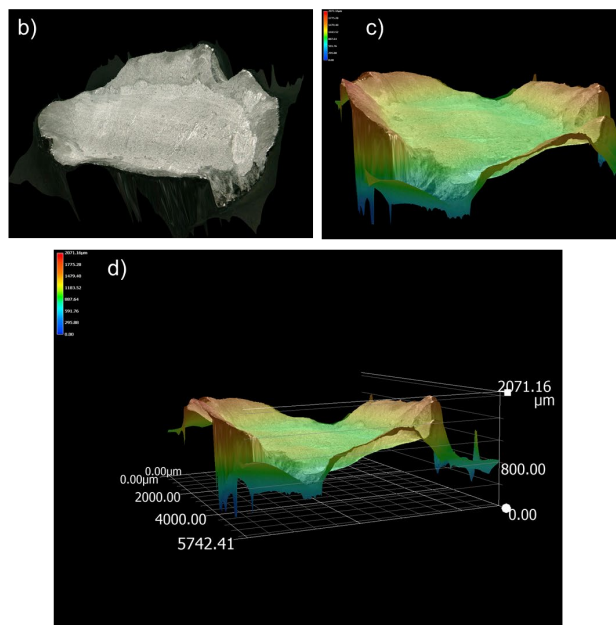
Weld 3 | T2 | 77 K



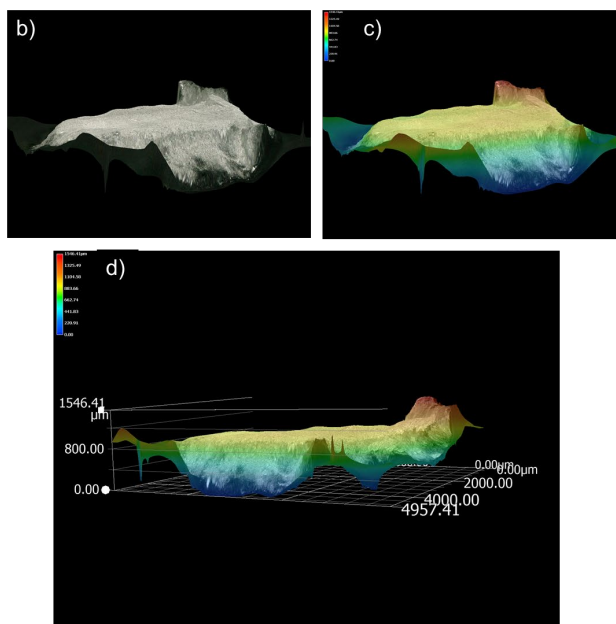
Weld 3 | T2 | 77 K | Dot



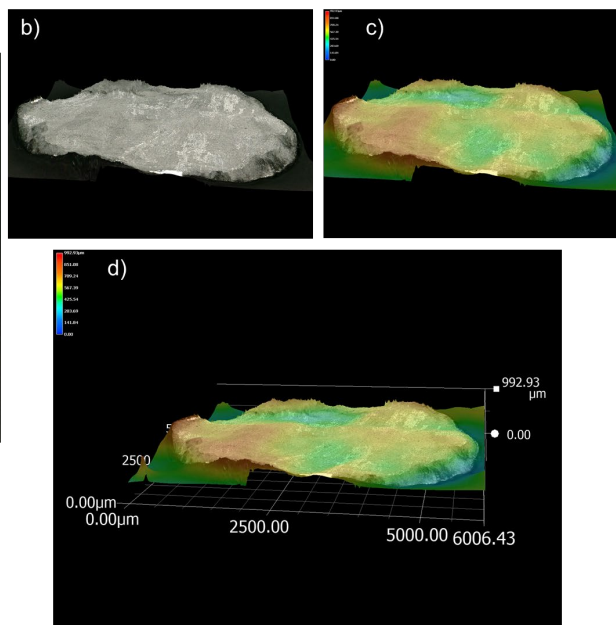
Weld 3 | T3 | 77 K



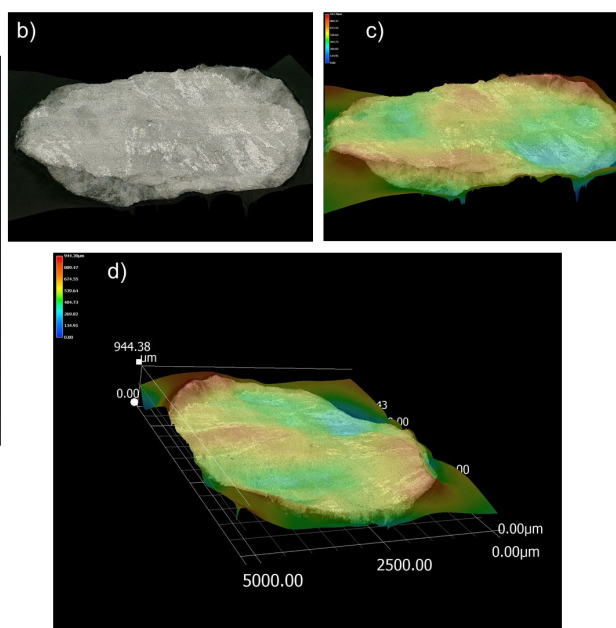
Weld 3 | T3 | 77 K | Dot



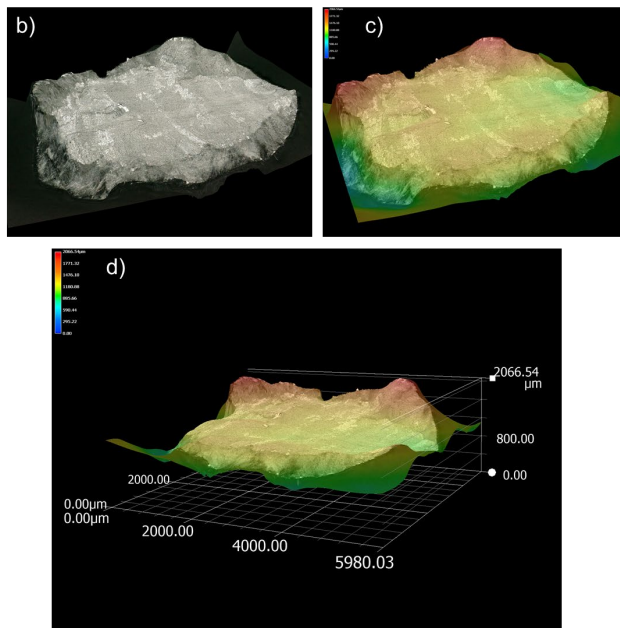
Weld 3 | T4 | 4 K



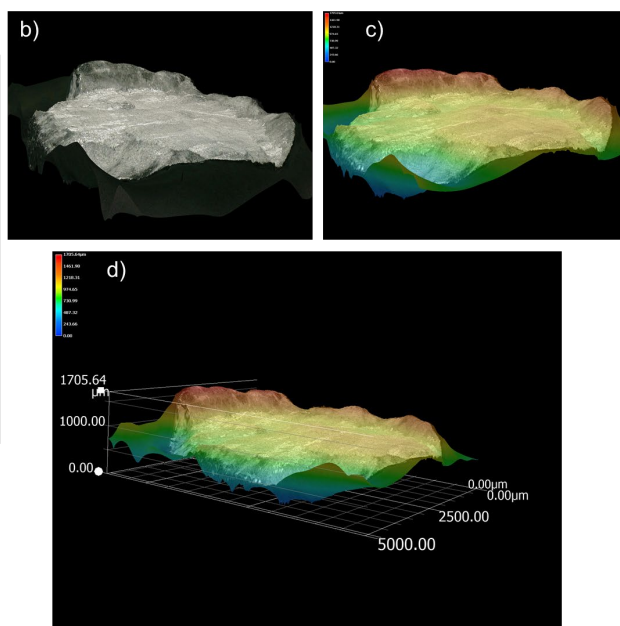
Weld 3 | T4 | 4 K | Dot



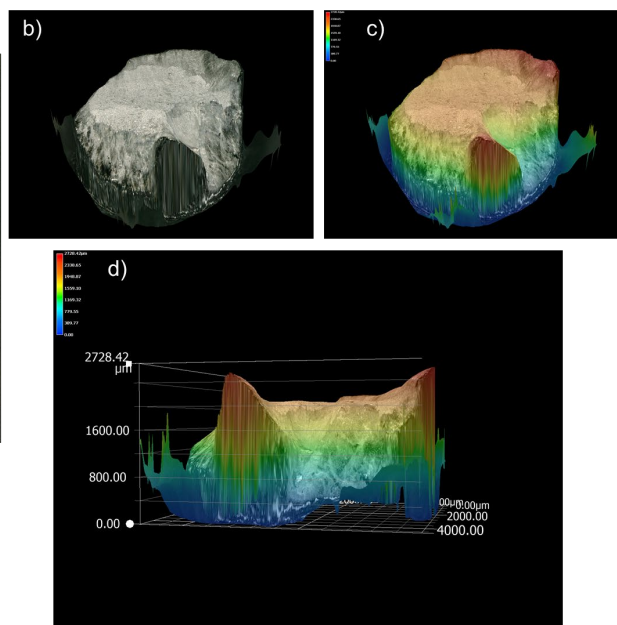
Weld 3 | T5 | 4 K



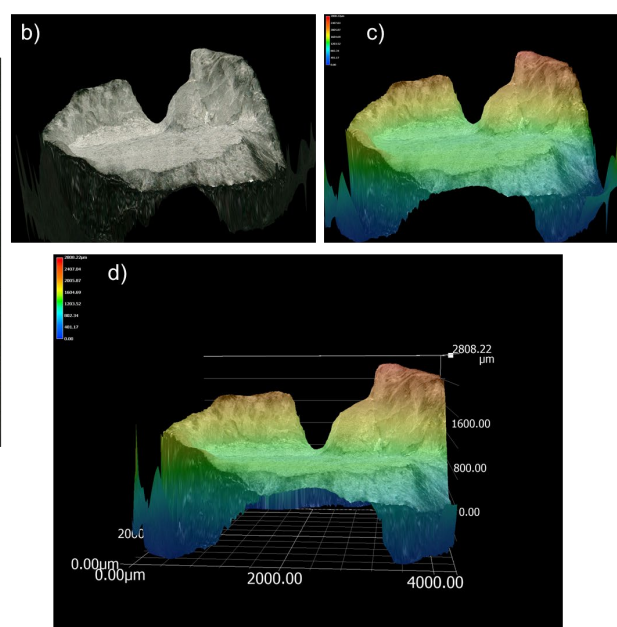
Weld 3 | T5 | 4 K | Dot



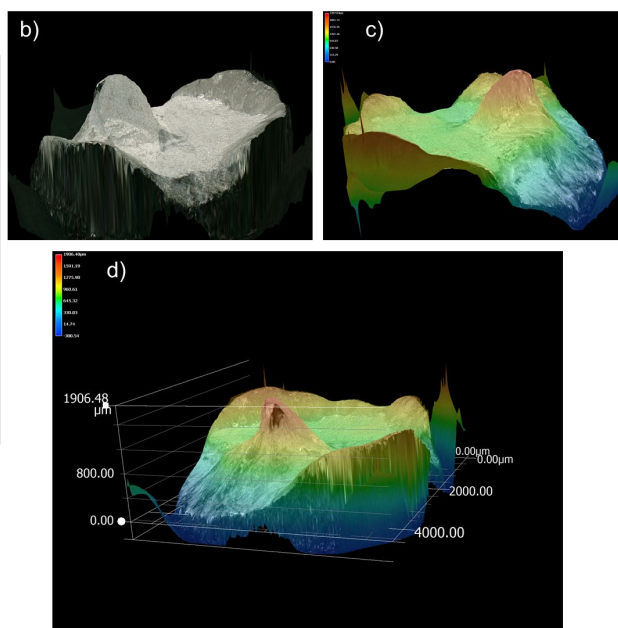
Weld 4 | T1 | 77 K



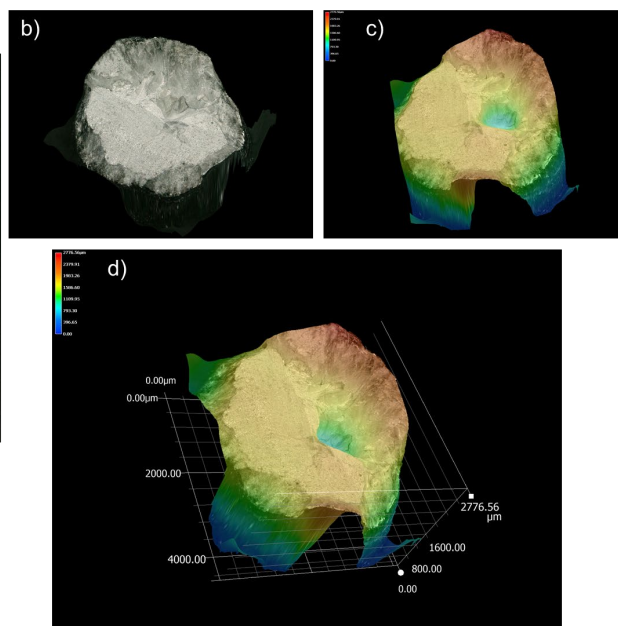
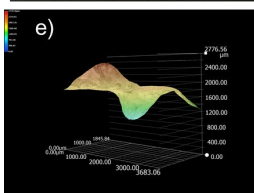
Weld 4 | T1 | 77 K | Dot



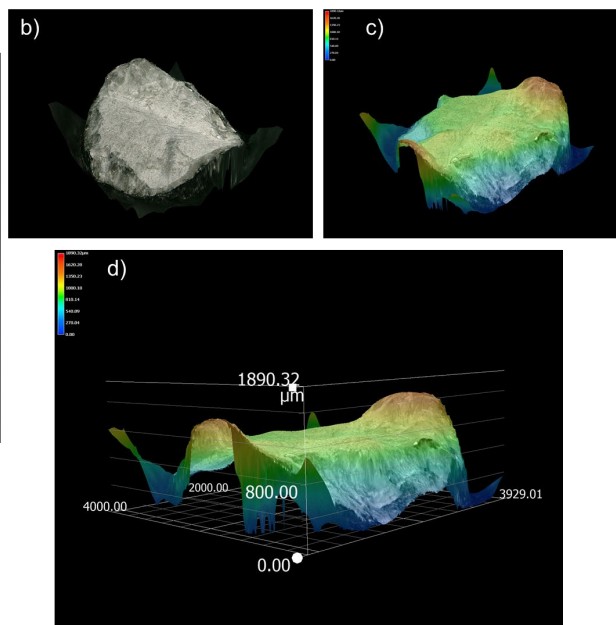
Weld 4 | T2 | 77 K



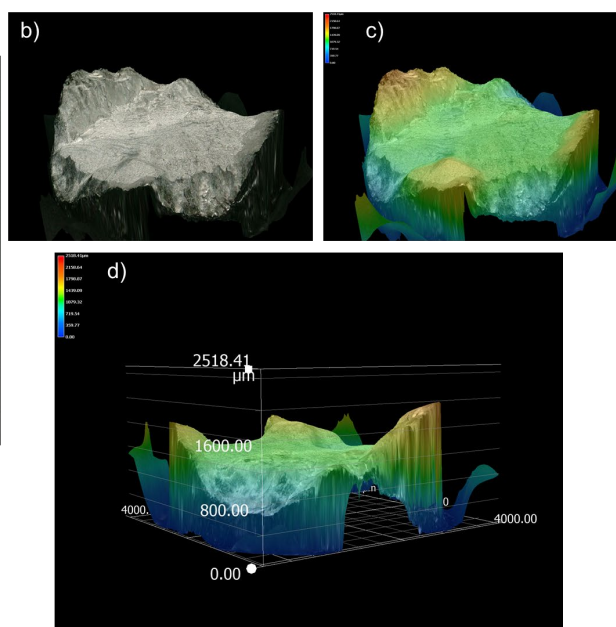
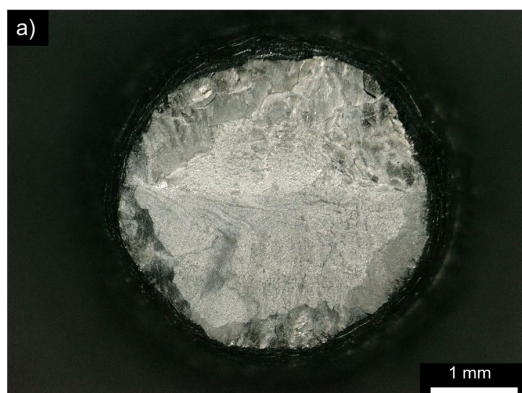
Weld 4 | T2 | 77 K | Dot



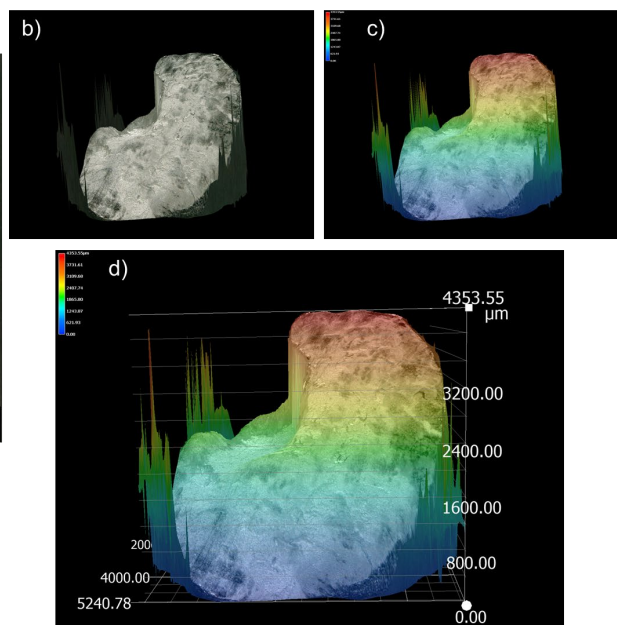
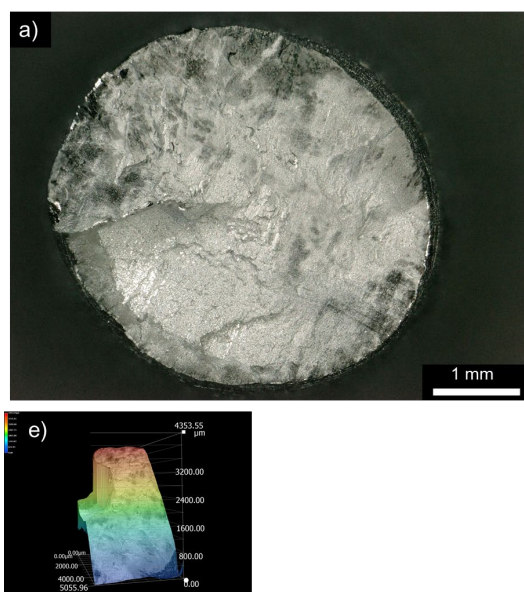
Weld 4 | T3 | 77 K



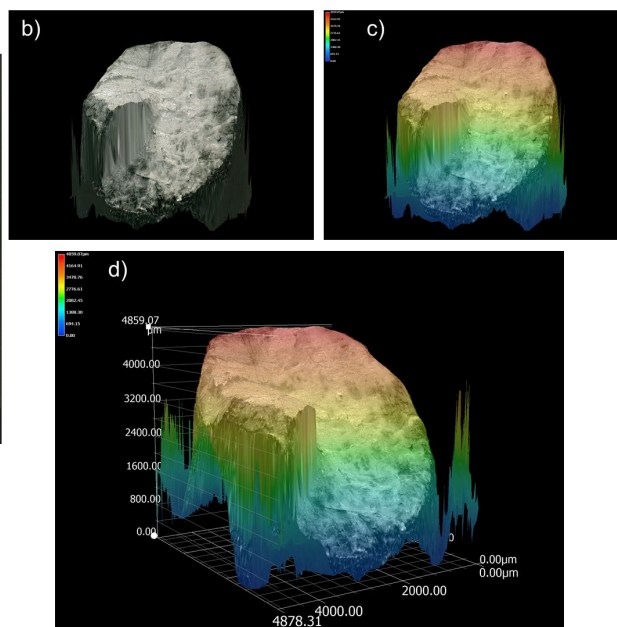
Weld 4 | T3 | 77 K | Dot



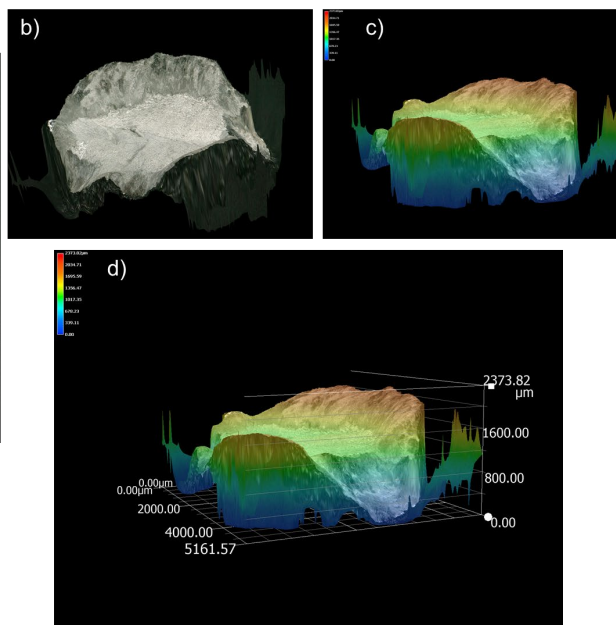
Weld 4 | T4 | 4 K |



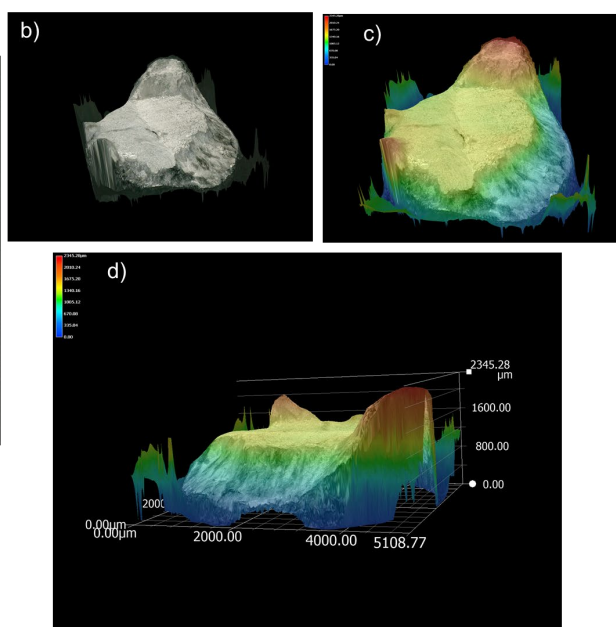
Weld 4 | T4 | 4 K | Dot



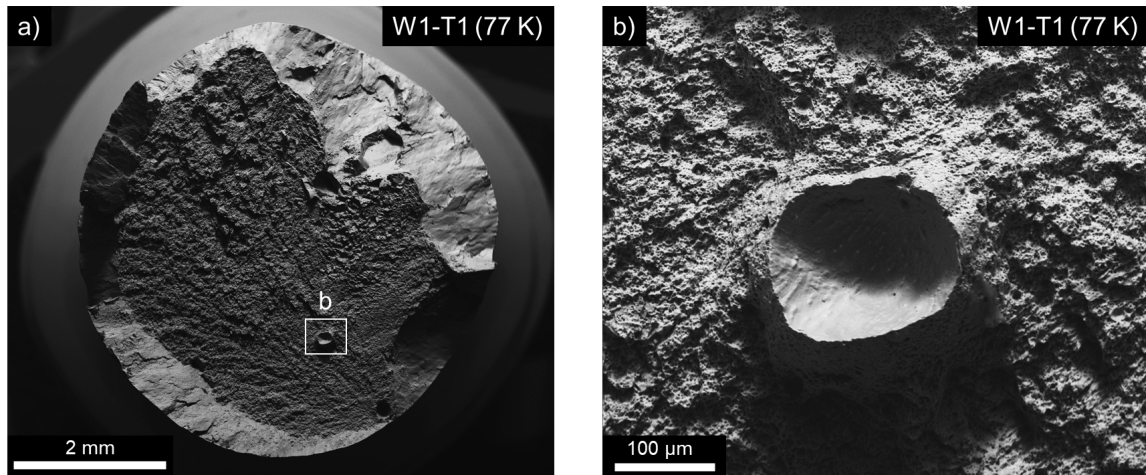
Weld 4 | T5 | 4 K



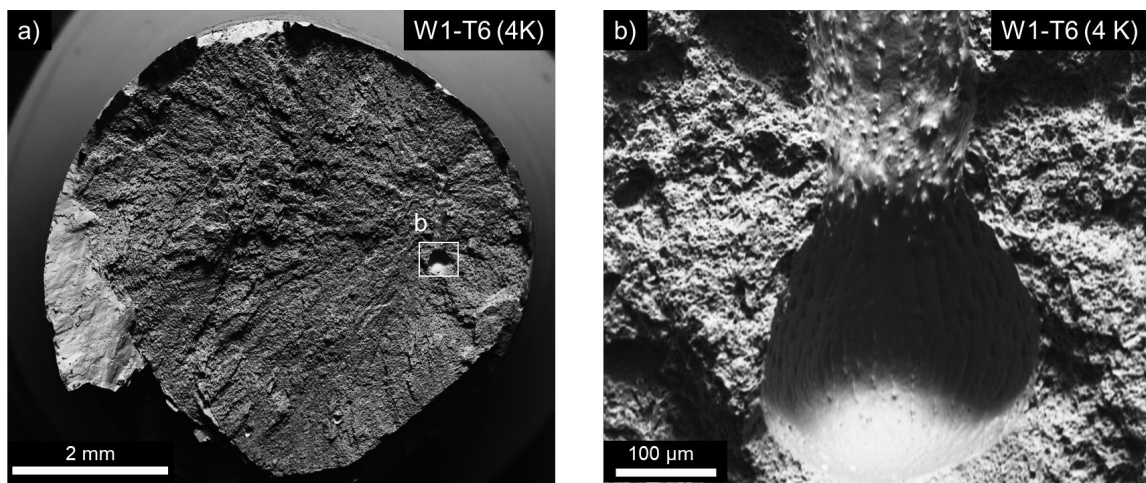
Weld 4 | T5 | 4 K | Dot



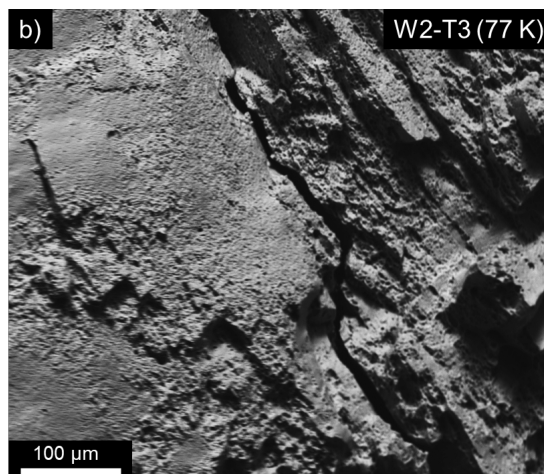
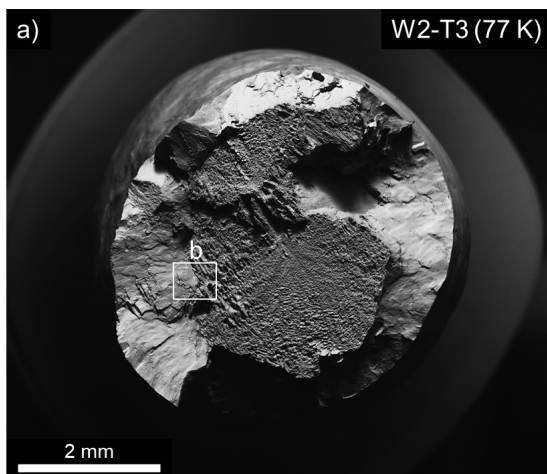
Appendix F: Additional fractography: SEM images



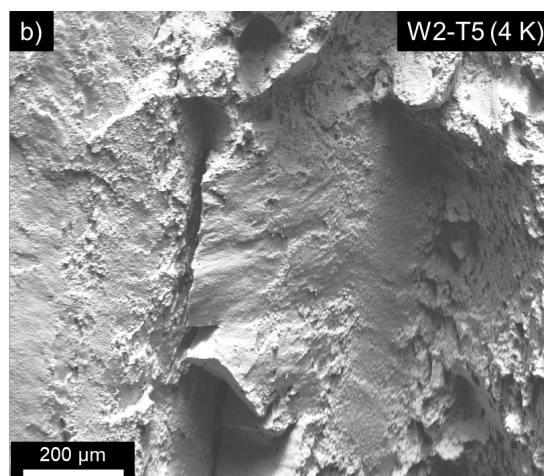
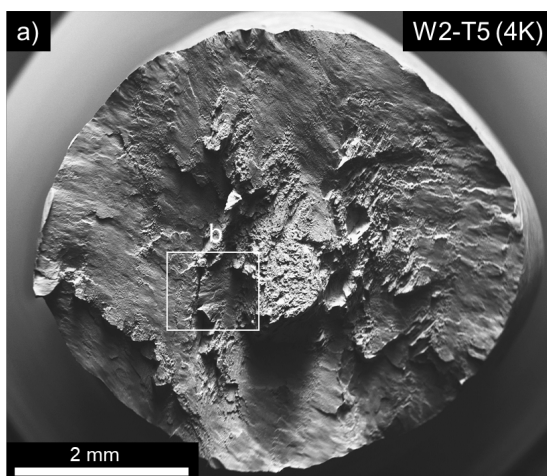
a) Full field of view of cup and cone fracture surface, b) partial wormhole pore.



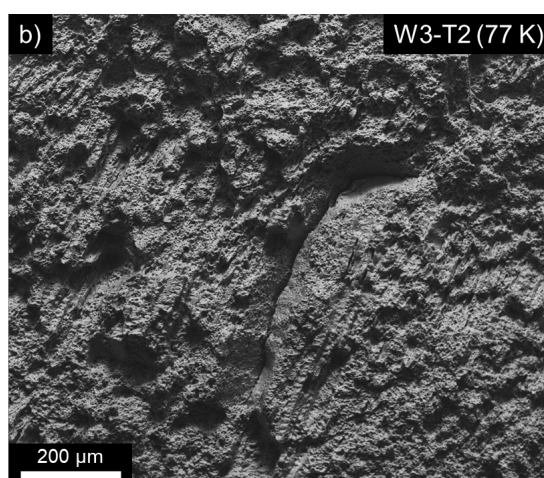
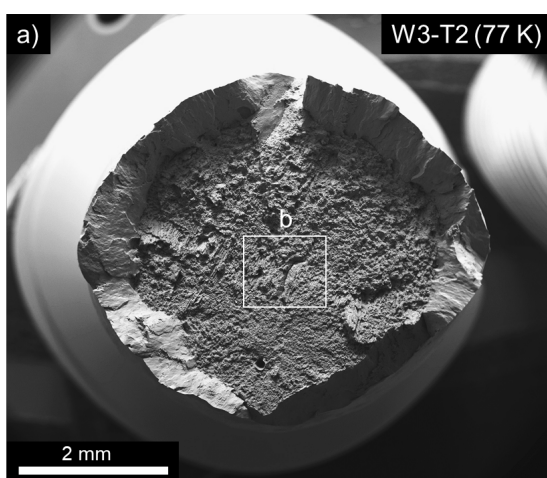
a) Full FOV of high angle shear b) wormhole pore.



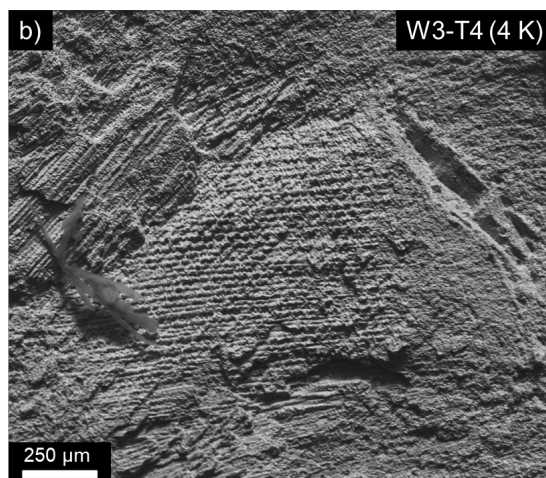
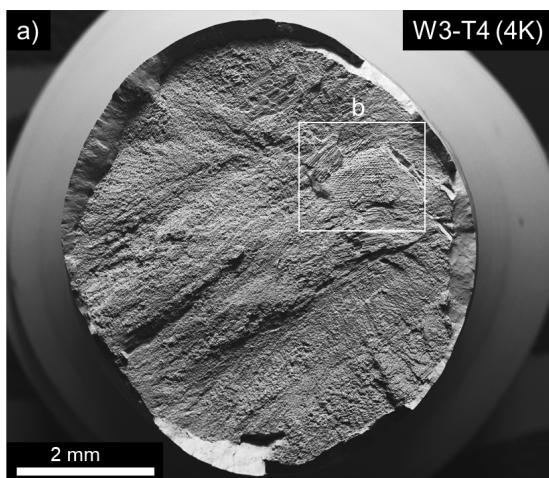
a) Full FOV of cup and cone morphology, b) crack near cup morphology.



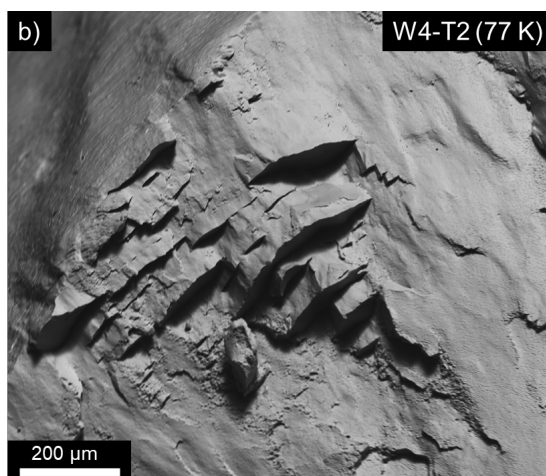
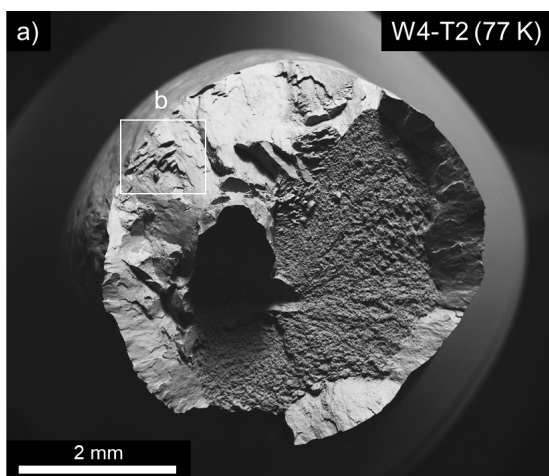
Full FOV of high angle shear, b) crack near cleavage morphology.



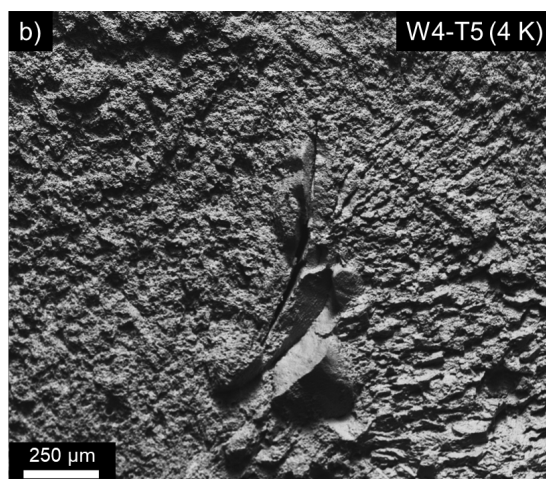
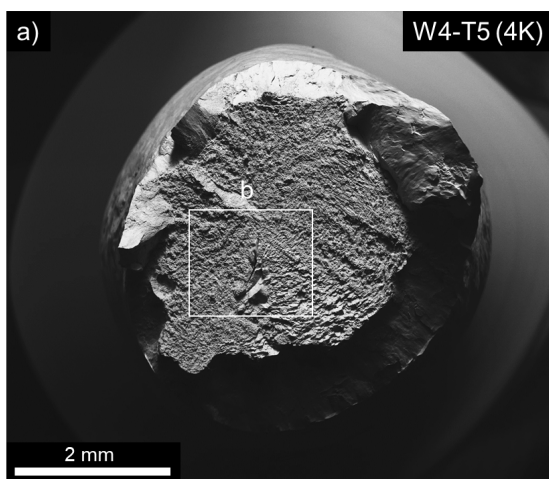
a) Full FOV showing cup morphology b) crack near MVC.



a) Flat shear, b) indications of brittle fracture.



a) Partial cup morphology and partial high angle shear, b) large cleavage features near the edge of the shear



a) Full FOV of cup morphology, b) crack on the surface near cleavage-like features.